Order Number 9413973

Strengthening of continuous-span composite bridges using post-tensioning and superimposed trusses

El-Arabaty, Hisham Ahmed, Ph.D.

Iowa State University, 1993

U·M·I
300 N. Zeeb Rd.
Ann Arbor, MI 48106

Strengthening of continuous-span composite bridges using post-tensioning and superimposed trusses

by

Hisham Ahmed El-Arabaty

A Dissertation Submitted to the
Graduate Faculty in Partial Fulfillment of the
Requirements for the Degree of
DOCTOR OF PHILOSOPHY

Department: Civil and Construction Engineering
Major: Civil Engineering (Structural Engineering)

Approved:

Signature was redacted for privacy.

In Charge of Major Work

Signature was redacted for privacy.

For the Major Department

Signature was redacted for privacy.

For the Graduate College

Members of the Committee:

Signature was redacted for privacy.

Iowa State University
Ames, Iowa

1993

To

My Father

TABLE OF CONTENTS

Page

LIST OF FIGURES vi

LIST OF TABLES ix

ABSTRACT x

1. INTRODUCTION 1
   1.1. General background 1
   1.2. Objectives 1
   1.3. Research program 4
      1.3.1. Development of a design manual 5
      1.3.2. Field tests 6
   1.4. Literature review 7

2. BEHAVIOR OF POST-TENSIONED CONTINUOUS-SPAN STEEL-STRINGER COMPOSITE BRIDGES 12
   2.1. Development of the finite element model 13
      2.1.1. Preprocessing and postprocessing programs 13
      2.1.2. ANSYS finite element model 14
   2.2. Verification of the finite element model . . . 19
   2.3. Flexural Strength Model 21

3. STRENGTHENING OF THREE-SPAN BRIDGE IN CERRO GORDO COUNTY, IOWA 27
   3.1. Bridge description 27
   3.2. Design of strengthening system 30
      3.2.1. Design of shear connectors 31
      3.2.2. Design of post-tensioning and superimposed trusses 31
   3.3. Field results 46

4. DEVELOPMENT OF A STRENGTHENING DESIGN METHODOLOGY . . 59
   4.1. Computation of axial forces and moments on the total bridge section 61
   4.2. Computation of axial forces and moments on the individual bridge stringers 63
      4.2.1. Definition of force and moment fractions 63
      4.2.2. Development of force and moment fraction formulas 68
   4.3. Accounting for approximations errors and post-tensioning losses 81
   4.4. Recommended design procedure 82

4.5. Recommendations for design 85
4.5.1. Selection of the strengthening scheme 85
4.5.2. Selection of the bracket locations . . 86
4.5.3. Design considerations for the post- tensioning tendons and superimposed trusses 88
4.6. Application of the design methodology to actual bridges 89
4.6.1. Strengthening system 1 91
4.6.2. Strengthening system 2 91
4.6.3. Comparison between the different strengthening systems 93

5. DESIGN EXAMPLE 96
5.1. Using the spreadsheet 97
5.1.1. Retrieving the spreadsheet into LOTUS 1-2-3 99
5.1.2. Getting acquainted with the spreadsheet 100
5.2. Computation of section properties: 101
5.2.1. Section properties of the exterior stringers 101
5.2.2. Section properties of the interior stringers 104
5.2.3. Section properties of the entire bridge cross-section 105
5.3. Computation of vertical loads on the bridge stringers 107
5.3.1. Dead loads 107
5.3.2. Long-term dead loads 108
5.3.3. Live loads 108

5.4. Computation of maximum moments due to vertical loads 110
5.5. Computation of stresses on the bridge stringers due to vertical loads 114
5.6. Input of bridge parameters and computation of force and moment fractions 115
5.7. Computation of overstresses to be removed by strengthening 118
5.7.1. Allowable stresses 119
5.7.2. Stresses due to vertical loads at the critical sections 121
5.7.3. Computation of overstresses at the critical sections 122

5.8. Design of the required strengthening system 126
5.8.1. Choice of strengthening scheme . . . 126
5.8.2. Computation of strengthening forces 130
5.8.3. Final design forces 133
5.9. Check of stresses 135
5.9.1. Stresses in the bottom flanges of the steel stringers 135
5.9.2. Stresses in the top flanges of the steel stringers 144
5.9.3. Stresses in the concrete deck 146
5.10. Accounting for post-tensioning losses and approximations in the design methodology . . 146

6. SUMMARY AND CONCLUSIONS 148
6.1. Summary 148
6.2. Conclusions 151

7. RECOMMENDED FURTHER RESEARCH. 154

REFERENCES. 156

ACKNOWLEDGEMENTS 160

APPENDIX A: FORMULAS FOR FORCE AND MOMENT FRACTIONS 161

APPENDIX B: DESIGN METHODOLOGY SPREADSHEET TABLES . . 178

APPENDIX C: AXLE LOADS FOR 1980 IOWA DOT RATING TRUCKS 183

LIST OF FIGURES

		Page
Figure 1.1.	Strengthening methods	3
Figure 2.1.	Finite element model of continuous-span composite bridge	15
Figure 2.2.	Details of angle-plus-bar shear connector	16
Figure 2.3.	Modeling of shear connectors and post-tensioning brackets	18
Figure 2.4.	Bottom flange strains for model bridge. (Post-tensioning all spans of the exterior stringers)	20
Figure 2.5.	Bottom flange strains for bridge tested in Pocahontas County, 1990. (Post-tensioning all spans of both stringers)	22
Figure 2.6.	Idealization of bridge stringer at ultimate load	26
Figure 3.1.	Framing plan of Mason City bridge	28
Figure 3.2.	Photographs of Mason City bridge	29
Figure 3.3.	New bolt shear connector layout	32
Figure 3.4.	Reference sections along half bridge length	34
Figure 3.5.	Stringer stress envelopes due to vertical loads	37
Figure 3.6.	Finite element model cases	38
Figure 3.7.	Stringer stresses due to post-tensioning	41
Figure 3.8.	Stringer stresses due to superimposed trusses	42
Figure 3.9.	Stringer stress envelopes due to vertical loads and strengthening system	43
Figure 3.10.	Post-tensioning layout	44
Figure 3.11.	Photographs of strengthening system in place	45
Figure 3.12.	Superimposed truss system	47
Figure 3.13.	Order strengthening system was applied to bridge	48
Figure 3.14.	Theoretical strengthening force (kips) required per stage	49
Figure 3.15.	Actual force (kips) applied per stage	50
Figure 3.16.	Bottom-flange stringer strains: Stage 2 strengthening	51
Figure 3.17.	Bottom-flange stringer strains: Stage 4 strengthening	52
Figure 3.18.	Bottom-flange stringer strains: Stage 6 strengthening	53
Figure 3.19.	Bottom-flange stringer strains: Stage 7 strengthening	54

Figure 3.20. Bottom-flange stringer strains: Stage 8 strengthening 55
Figure 4.1. Various locations of post-tensioning and superimposed trusses 60
Figure 4.2. Total moment on the bridge section: Strengthening scheme [C] 62
Figure 4.3. Idealization of axial force and moment diagrams on the stringers due to strengthening system: Strengthening scheme [A] 64
Figure 4.4. Locations of distribution fractions: Strengthening scheme [A] 67
Figure 4.5. Regression formula variables 79
Figure 4.6. Design procedure for strengthening system 83
Figure 4.7. Bottom flange stresses for V14 standard Iowa DOT bridge (length = 250 ft.) due to vertical loads 90
Figure 4.8. Bottom flange stresses for V14 standard Iowa DOT bridge (length = 250 ft.) due to vertical loads and strengthening system. (All spans of both stringers post-tensioned) 92
Figure 4.9. Bottom flange stresses for V14 standard Iowa DOT bridge (length = 250 ft.) due to vertical loads and strengthening system. (All spans of exterior stringers post-tensioned) 94
Figure 5.1. Idealized transverse section of composite bridge 98
Figure 5.2. Locations of various moments of inertia along stringers 112
Figure 5.3. Stress envelopes due to vertical loads . . 116
Figure 5.4. Critical stress locations 123
Figure 5.5. Various locations of post-tensioning and superimposed trusses 127
Figure 5.6. Strengthening system selected for use in example problem 128
Figure 5.7. Stress envelopes due to vertical loads and strengthening system 145
Figure A.1. Locations of distribution fractions for strengthening scheme [A] 164
Figure A.2. Locations of distribution fractions for strengthening scheme [B] 167
Figure A.3. Locations of distribution fractions for strengthening scheme [C] 170
Figure A.4. Locations of distribution fractions for strengthening scheme [D] 173

Figure A.5. Locations of distribution fractions for strengthening scheme [E] 176
Figure C.1. Iowa Department of Transportation legal dual axle truck loads 184

LIST OF TABLES

		Page
Table 3.1.	Description and location of reference sections	34
Table 3.2.	Bridge load-behavior assumptions	36
Table 4.1.	Iowa DOT standard bridge models included in regression analysis for distribution fractions	69
Table 4.2.	Non-standard bridge models (Developed by changing some of the dimensions of the Iowa DOT standard bridges)	70
Table 4.3.	Finite element analysis results: V12-2 standard Iowa DOT bridge.	71
Table 4.4.	Computation of force and moment fractions V12-2 standard Iowa DOT bridge.	72
Table 4.5.	Input data for the regression analysis: Strengthening scheme [A], Force Fraction at section 1.	74
Table 4.6.	Regression analysis output: Strengthening scheme [A], Force Fraction at section 1.	75
Table 4.7.	Effect of variable X_I on the accuracy of the developed regression formulas	78
Table 5.1.	Section properties used for analysis and stress computations in stringers under vertical loads	113
Table A.1.	Force Fractions for strengthening scheme [A]	165
Table A.2.	Moment Fractions for strengthening scheme [A]	166
Table A.3.	Force Fractions for strengthening scheme [B]	168
Table A.4.	Moment Fractions for strengthening scheme [B]	169
Table A.5.	Force Fractions for strengthening scheme [C]	171
Table A.6.	Moment Fractions for strengthening scheme [C]	172
Table A.7.	Force Fractions for strengthening scheme [D]	174
Table A.8.	Moment Fractions for strengthening scheme [D]	175
Table A.9.	Moment Fractions for strengthening scheme [E]	177

ABSTRACT

The need for upgrading understrength bridges in the United States has been well documented in the literature. In this thesis, two methods of strengthening are presented: post-tensioning of the positive moment regions of the bridge stringers and the addition of superimposed trusses at the piers. The use of these two systems is an efficient method of reducing flexural overstresses in undercapacity bridges. The objective of the research described in this thesis was to develop a design methodology to assist bridge engineers with designing a strengthening system to obtain the desired stress reductions. In addition, one such strengthening system was designed for use on a three-span continuous steel stringer bridge in the field.

A design methodology was developed to simplify the design process for the strengthening system on a typical continuous-span composite bridge. As a result of the longitudinal and transverse force distribution, the design methodology presented in this thesis for continuous-span composite bridges is extremely complex. To simplify the procedure, a spreadsheet has been developed for use by practicing engineers. The force and moment distribution fraction formulas developed in this study are primarily for the Iowa DOT V12 and V14 three-span four-stringer bridges. These formulas may be used on other bridges if they are within the limits stated in this study. Use of the distribution fraction formulas for bridges not within the stated limits is not recommended.

The bridge selected for strengthening was in Cerro Gordo County near Mason City, Iowa on County Road B65. A strengthening system composed of post-tensioning and superimposed trusses was designed to remove overstresses that occurred when the bridge was subjected to Iowa legal

loads. The strengthening system was installed in the summer of 1992. Instrumentation was installed in the summers of 1992 and 1993. In the summer of 1993, the bridge was load tested before and after the strengthening system was activated. The load test results indicate that the strengthening system was effective in reducing the overstress in both the positive and negative moment regions of the stringers.

1. INTRODUCTION

1.1. General background

Based on current bridge rating standards, a considerable number of continuous-span composite bridges in the state of Iowa are classified as deficient and in need of rehabilitation or replacement. The change in the AASHTO Specifications [1] concerning the wheel-load-distribution fractions in 1957, has increased the wheel-load-distribution fractions for exterior stringers. In 1980, the Iowa state legislature passed legislation which significantly increased the legal loads in the state. This increase in legal loads widened the gap between the rated strength of the older composite bridges with small exterior stringers and current rating standards. To help alleviate these problems, strengthening can often be used as a cost-effective alternative to replacement or posting.

Most Iowa bridges designed prior to 1957 are understrength due to excessive flexural stresses in the steel stringers. However, shear connectors and other parts of the bridge may also be inadequate. In the flexurally overstressed bridges, the exterior stringers are smaller than the interior stringers and thus the overstress is larger in the exterior stringers. For bridges with flexural overstresses, it is logical to strengthen the overstressed stringers to avoid embargoes or costly early replacement of the bridges.

1.2. Objectives

The primary objective of this study was the development of a design methodology for designing strengthening systems for overstressed continuous span bridges. A secondary

objective of the research program was to design, install, and test a strengthening system for both the positive and negative moment regions of a given continuous span bridge.

In this study, two methods for strengthening continuous-span composite bridges are utilized. The first method involves post-tensioning the positive moment regions of the bridge stringers. In the second method, superimposed trusses are provided at the piers of the exterior stringers to supplement the post-tensioning system. In some cases, it is possible to strengthen the bridge without the addition of the superimposed trusses. A general layout of the strengthening system is illustrated in Fig. 1.1.

The post-tensioning system is composed of high-strength steel tendons on both sides of the stringer web. Tendons are connected to the stringers utilizing brackets that are bolted to the stringers using high strength bolts. The use of bolts avoids the problems associated with field welding which are magnified when the bridge's steel welding characteristics are unknown. In most instances, tendons are positioned above the bottom flanges of the stringers to protect the system from being struck by high loads when the bridge is over a roadway or by floating debris when the bridge is over a flooded stream.

The superimposed truss strengthening system is composed of two steel tubes (the inclined members of the trusses) connected to the stringer web and bottom flange at the pier through brackets. One truss is provided on each side of the web of the exterior stringers. The top ends of the tubes of these trusses bear against the top flange of the stringer through a roller bearing. A high strength steel tendon is used to connect the top ends of the tubes to form a truss. By applying tension to the truss tendon, the top ends of the tubes bear against the stringer at the bearing locations.

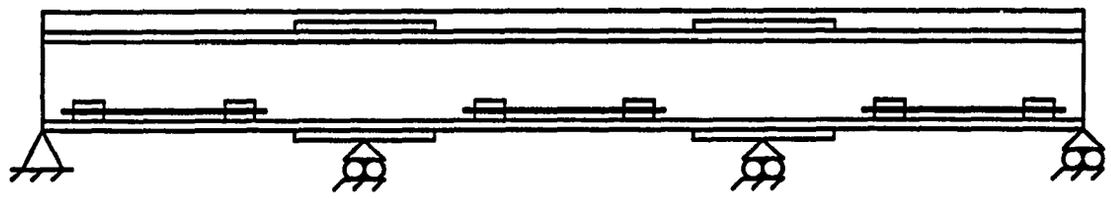

a. POST-TENSIONING

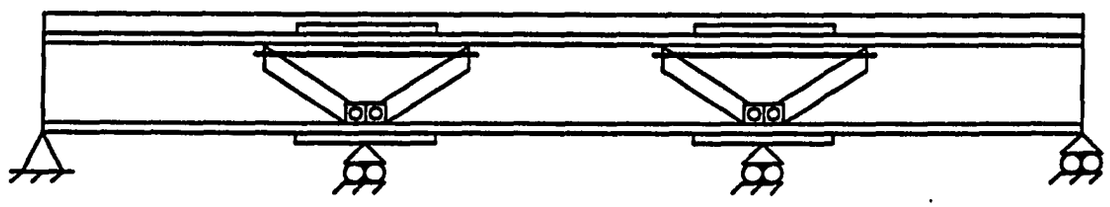

b. SUPERIMPOSED TRUSSES

Fig. 1.1. Strengthening methods.

The vertical uplift exerted by the truss on the bridge is proportional to the tendon force.

It is recommended to only post-tension the positive moment regions of the stringers whenever possible, due to the lower cost and ease of installation of the post-tensioning system. However, in some instances such post-tensioning does not reduce the overstresses at the piers the desired amount. In such cases, it is necessary to use superimposed trusses in combination with post-tensioning the positive moment regions.

Since the exterior stringers are smaller than the interior stringers, they usually have higher overstresses in the negative moment regions at the piers. Thus, superimposed trusses are employed on exterior stringers only. As the result of lateral distribution, the superimposed trusses reduce negative moment region overstresses in the interior stringers also. Although they were not employed on the Cerro Gordo County bridge [2], in the author's opinion it would be extremely difficult to install superimposed trusses on interior stringers.

Depending upon the magnitude of post-tensioning forces employed, there may be stresses of sufficient magnitude to induce cracking in the curbs and bridge deck. The possibility of cracks occurring increases when the post-tensioning forces are high. The use of superimposed trusses reduces the possibility of cracking since smaller post-tensioning forces are required. In this case, the change in the overall stress profile along the stringer is relatively small and therefore there is less potential for cracking.

1.3. Research program

The research program consisted of two parts: Part 1 - Development of a Design Manual, Part 2 - Field Tests. Parts

1 and 2 will be discussed separately in the following subsections. In conjunction with the two main parts of the research program, several additional tasks were also performed.

A comprehensive literature review pertaining to the strengthening of bridges was performed. Section 1.4 of this report refers to the previous literature reviews along with literature reviews of current research. Because the previous literature reviews are readily available, they have not been duplicated here.

The supplemental literature review is presented in Sec. 1.4. Chapter 2 describes the development and verification of the finite element model used for the analysis of continuous-span bridges in this study. The design of a system for strengthening a three-span bridge in Cerro Gordo County, Iowa is described in Chp 3. Chapter 4 presents the development of the strengthening design methodology. In Chapter 5, a design example is given to illustrate the use of the spreadsheet in designing a strengthening system for a typical steel-stringer, concrete-deck, composite, continuous-span bridge. The summary and conclusions are presented in Chp. 6 and recommended further research is presented in Chp. 7.

1.3.1. Development of a design manual

The development of a design manual [3] involved the development of a practical procedure for determining the magnitude and location of post-tensioning and truss forces required to strengthen a given bridge. Finite element analysis and experimental results from previous projects HR-308,HR-287 [4,5] were used in the formulation and calibration of the developed design methodology. A sensitivity study was conducted to determine the effects of

the various bridge parameters on the distribution of the axial forces and moments due to the strengthening system. Factors such as number of spans, span lengths, angle-of-skew, stringer spacing, deck thickness, tendon lengths, etc. were considered. From this analysis, the most significant parameters affecting the distribution of forces and moments due to the strengthening system through the bridge were determined. These parameters were used to develop a number of regression equations which can be used to compute distribution fractions for the forces and moments at various locations. The design methodology is similar to the one developed for simple span bridges, HR-238 Part III [6] which involved force and moment fractions. However, because of the longitudinal distribution of force exhibited by continuous bridges, the resulting design methodology for continuous span bridges is considerably more complex.

A spreadsheet was developed to facilitate the calculation of the required strengthening forces. This will enable the practicing engineer to design the strengthening system while avoiding the use of a more complex analysis such as finite element analysis.

1.3.2. Field tests

The field tests involved the implementation of a strengthening system for application to a three-span continuous, steel-girder, concrete-deck bridge. Vertical load testing of the bridge was performed prior to and after the strengthening system was implemented to investigate the effectiveness of the strengthening system.

A 3-span composite bridge was selected for strengthening in this study. The overstresses in the bridge stringers due to vertical loads were determined and the strengthening system was designed to eliminate these

overstresses. A two part strengthening system was used involving post-tensioning as utilized in 1988 (HR-308) [4] and a superimposed truss system to further reduce negative moment overstresses at the pier supports.

The strengthening system was installed on the bridge in the summer of 1992. Instrumentation of the bridge was accomplished in the summers of 1992 and 1993. The bridge was then load tested both prior to and subsequent to the strengthening system being activated. Some of the field-test results are given in Chp. 3. Details of the instrumentation, test procedure, and field results are given in Ref. 2.

1.4. Literature Review

The literature review presented here is not intended to be a complete examination of existing strengthening techniques but rather to be a supplement to the previous literature reviews performed for the Iowa DOT. The previous literature reviews are available in the following references:

- post-tensioning of simple span bridges [6,7,8,9]
- post-tensioning of continuous span bridges [4]
- strengthening of highway bridges [10,11,12]

The articles summarized in this section deal with recent strengthening methods for simple and continuous span bridges which are not in the literature reviews previously noted. Several related experimental studies have been documented in the literature. Some of these studies have included developing analytical models to confirm the experimental results.

A flexural design and analysis methodology for prestressed composite beams was proposed by Saadatmanesh et al. [13]. The methodology incorporates both working stress

design and load factor design principles. Its application is limited to the following construction sequences. For positive moment regions, the steel stringer must be prestressed prior to the concrete deck being cast. For negative moment regions, the steel stringer should be prestressed, then compositely connected to a precast, prestressed concrete deck.

Five prestressed, composite, welded girders were tested to failure under negative bending moment by Ayyub et al. [14]. The test setup approximated the support region between the inflection points of a continuous girder. The steel girders had varying proportions with some elements being non-compact in an attempt to determine the effect of compactness on prestressed composite girders. In addition, the study involved comparing the structural behavior of the prestressed composite girders under several different deck prestressing conditions and prestressing sequences for the deck and girders.

In a companion paper to the preceding article, Ayyub et al. [15] reported on an analytical study of two of the prestressed composite girders mentioned in Ref. 13. An incremental deformation technique was used in the analysis. A detailed comparison of experimental and analytical results was included in the study.

In another investigation by Ayyub et al. [16], three composite steel-concrete beams with varying tendon types and profiles were tested to failure under positive bending moment. Analytical models of the beams were developed in an attempt to predict stresses in the tendons, concrete deck, and steel beams. The investigators also attempted to predict deflections with their models which were developed using the strain compatibility method. The theoretical stresses and deflections determined with the model agreed quite well with the experimental results. Comparisons

between tendon types (bar vs. strand) and tendon profiles (straight vs. draped) were also made.

The results indicated that strands are the preferable tendon type because of savings in the steel weight. It was also shown that straight tendons were better than draped tendons because of the higher yield load experienced and their lower construction cost.

The elastic behavior of continuous prestressed beams was investigated by Tong and Saadatmanesh [17]. The investigators presented two methods of analysis for the beams. For straight discontinuous tendons, the stiffness method was used. A combination of stiffness and flexibility methods was used for draped continuous tendon profiles.

Two girders were modeled using these methods. The first model was a two-span, continuous, prestressed, composite girder. With this model, the effect of prestress force, eccentricity, tendon profile, and tendon length were investigated.

A three-span, continuous, prestressed, composite girder model was also developed. The effect that different tendon profiles had on the model's behavior was examined. Also, pattern loading of both models was investigated to determine its effect on the change in tendon force in each span.

Mancarti [18] has presented design criteria and strengthening methods for short span bridges. These criteria are currently being used by the California Department of Transportation (CalTrans).

The State of California has designated specific routes for permit vehicles. Many of the bridges on these routes, however, were deficient with respect to moment capacity for the permit vehicles. Caltrans has used post-tensioning to strengthen many of these bridges. They have had success post-tensioning both steel girder and concrete girder bridges.

Albrecht and Li [19] investigated the fatigue strength of prestressed composite beams in 1989. The beams tested were prestressed prior to the deck being cast and had the following fatigue prone details: prestressing strands, shear studs, and coverplates. The prestressed composite beams were stress cycled until a fatigue crack developed at the end of the coverplates. The beam was repaired using the first of three repair methods investigated and was stress cycled again. When the first repair failed, the beam was repaired using a second method. The beam was stress cycled a third time until fatigue failure once again occurred. The final repair method investigated increased the initial prestressing force until the bottom flange was no longer experiencing tensile stresses during the cyclic loading. Increasing the prestressing force changed the stress cycle in the bottom flange from tension-compression to low compression-high compression. The third repair procedure was found to be a very effective means of repairing fatigue cracked beams.

The remaining articles in this literature review pertain to strengthening techniques used in strengthening reinforced concrete members. A strengthening method for reinforced concrete beams was examined in the papers authored by Saadatmanesh and Ehsani [20] and by An and Saadatmanesh [21]. The strengthening technique employed involved the use of fiber composite plates. Fiber composite plates were epoxy-bonded to the exterior of the reinforced concrete beams. The use of fiber composites as a method of strengthening bridge beams has several advantages. Among them are the high strength-to-weight ratio of fiber composites and their resistance to corrosion.

In the paper by Saadatmanesh and Ehsani [20], six simply supported beams were tested to failure under two concentrated loads near midspan. Deflections were measured

in addition to strains in the reinforced steel, concrete beam, and fiber reinforced plate. For each beam, plots of deflection and strain vs. load were made up to failure. In the companion paper by An and Saadatmanesh [21], analytical methods were developed to predict the behavior of the externally reinforced beams. With these analytical models, the researchers were able to make comparisons between experimental and predicted values. The investigators also calculated values for beams that were not externally reinforced with fiber composite plates. The results of this study showed that the yield and ultimate loads of the reinforced steel could be increased by 33% and 65%, respectively.

Seible et al. [22] investigated strengthening techniques on a test specimen taken from a cast in place 25 year old reinforced concrete T-beam bridge. Three different strengthening techniques were utilized on the test section. Substantial flexural cracking existed in the positive moment regions of the section. These cracks were repaired using an epoxy injection technique. Subsequent testing revealed that epoxy injection of the flexural cracks increased the longitudinal stiffness of the member. The remaining two strengthening techniques had to be investigated in conjunction with the epoxy injection because it was not possible to remove the epoxy after the first test was performed. Test results showed that external post-tensioning of the epoxy injected bridge section did not increase the longitudinal or transverse flexural stiffness characteristics of the section. However, longitudinal and transverse stiffnesses were increased with the use of a concrete bottom soffit panel attached to the T-beam stems in conjunction with the epoxy injection.

2. BEHAVIOR OF POST-TENSIONED CONTINUOUS-SPAN STEEL-STRINGER COMPOSITE BRIDGES

The analysis of continuous-span bridges due to the effect of vertical loads is addressed in the AASHTO Standard Specifications for Highway Bridges [23]. Wheel load fractions are provided to aid the designer in determining the percentage of the vertical loads distributed to each of the bridge stringers.

The analysis of continuous-span bridges strengthened using post-tensioning and superimposed trusses presents a significantly more involved analysis problem. The forces acting on the bridge in this case, include axial forces and concentrated moments induced by the tendons at the various bracket locations, as well as vertical forces induced at the bearing points of the superimposed trusses. The lateral stiffness of the deck and the diaphragms causes the transfer of a significant portion of the axial forces and moments from the strengthened stringer to other stringers. The longitudinal continuity of the stringers and the deck results in force and moment transfer from one span to the others. To date, no data are available for computing the previously described strengthening system force and moment distribution fractions throughout a given continuous-span bridge.

This chapter describes the development and verification of the finite element model used for the analysis of continuous-span, steel-stringer, concrete-deck bridges. This model is a general model applicable to a wide variety of continuous-span bridges. In Chapter 3, this finite element model is used to analyze a 3-span composite bridge in Cerro Gordo County, Iowa, due to the effect of post-tensioning of the bridge's steel stringers in the positive moment regions, as well as the addition of superimposed

trusses to the exterior stringers at the piers. The analysis results are used to design a strengthening system for the bridge.

In Chapter 4, the finite element model is applied to a large number of continuous-span bridges and the analysis results are used to develop a design methodology for strengthening continuous-span composite bridges.

2.1. Development of the finite element model

The author utilized the finite element method for the development of the proposed design methodology. Several finite element packages were available at ISU, for instance, ABAQUS, ANSYS, NASTRAN and SAP. The ANSYS program was selected for use in this investigation, primarily because of its very convenient preprocessing (i.e., input data generation) and postprocessing (i.e., retrieving results). The program contains over 90 different types of finite elements that can be used to analyze different structures. Running ANSYS on workstations had the advantage of a large memory storage capacity and a high speed of execution, thus permitting the development of a rather large and sophisticated model.

2.1.1. Preprocessing and postprocessing programs

One of the main advantages of the ANSYS programs is the integration of the three phases of finite element analysis - preprocessing, solution , and postprocessing. However, to expedite generation of the finite element meshes and to retrieve particular results, the authors found it necessary to develop additional preprocessing and postprocessing programs. These programs were developed in "PC TURBO PASCAL".

The function of the preprocessing program was to read a minimal input of the basic bridge parameters and use this input to create a command file which is subsequently used by ANSYS to create the finite element mesh. This preprocessor made it possible to create models of several bridges in a minimum amount of time.

The postprocessor developed was used to sort through the ANSYS results to retrieve the nodal forces and moments at a number of nodes and use these force and moment values to compute the total axial forces and moments on the composite sections of the stringers. These resultants were used later in determining the distribution fractions which describe the distribution of axial forces and moments throughout the bridge.

2.1.2. ANSYS finite element model

The basic finite element model used in this work is shown in Fig. 2.1. The model is applicable to a wide variety of continuous-span composite bridges.

The model consisted of plate elements idealizing the bridge deck, bridge curbs and post-tensioning brackets while 3-D beam elements were used to model the stringers and the diaphragms. A quarter symmetry model was used to model right-angle bridges while a full-scale model was used to model skewed bridges.

The shear connection between the steel stringers and the concrete deck is achieved through angle-plus-bar shear connectors (see Fig. 2.2). In practice, the angle-plus-bar shear connectors allow no vertical movement between the concrete and the steel surfaces, as well as provide restraint in the longitudinal direction. The rotations are essentially the same in the concrete and the steel surfaces along the stringers. Only a small horizontal movement

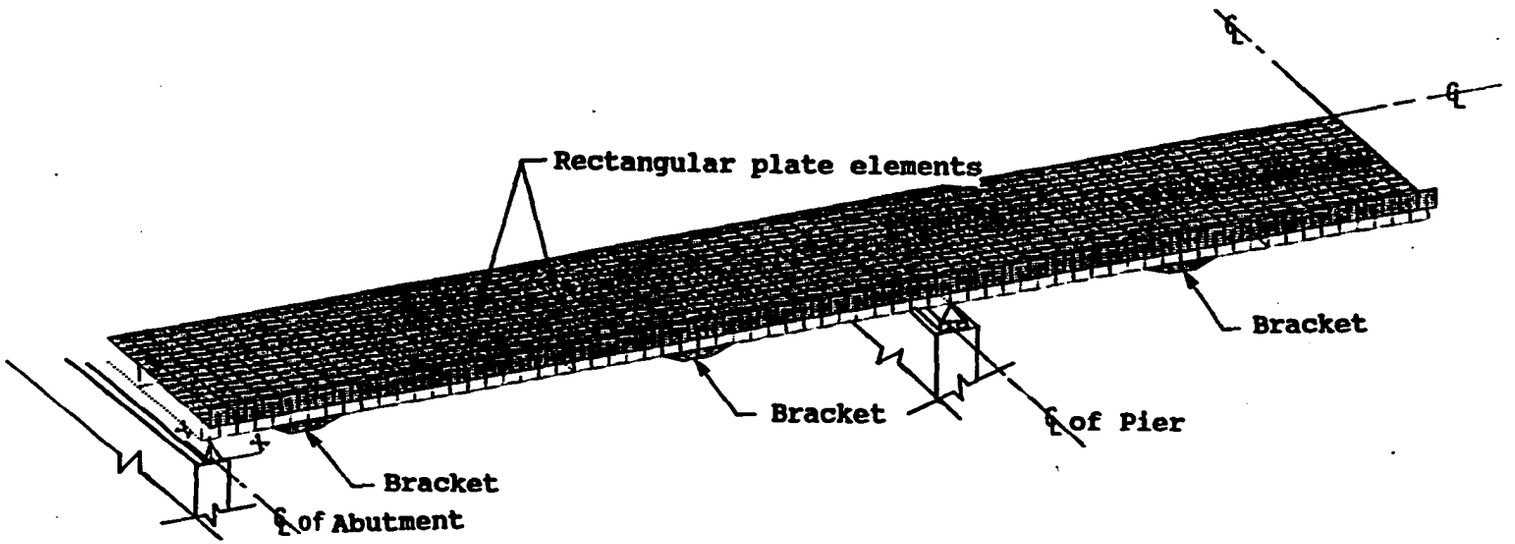

Fig. 2.1. Finite element model of continuous-span composite bridge.

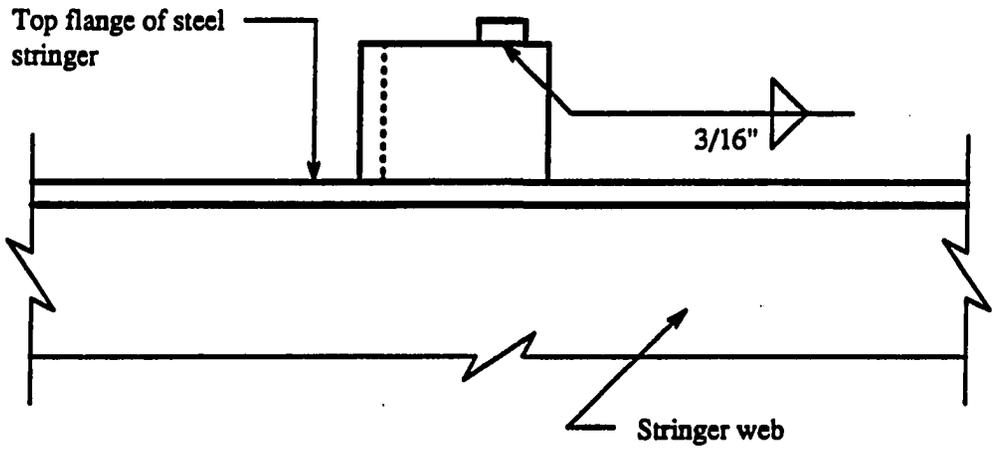

a. ELEVATION

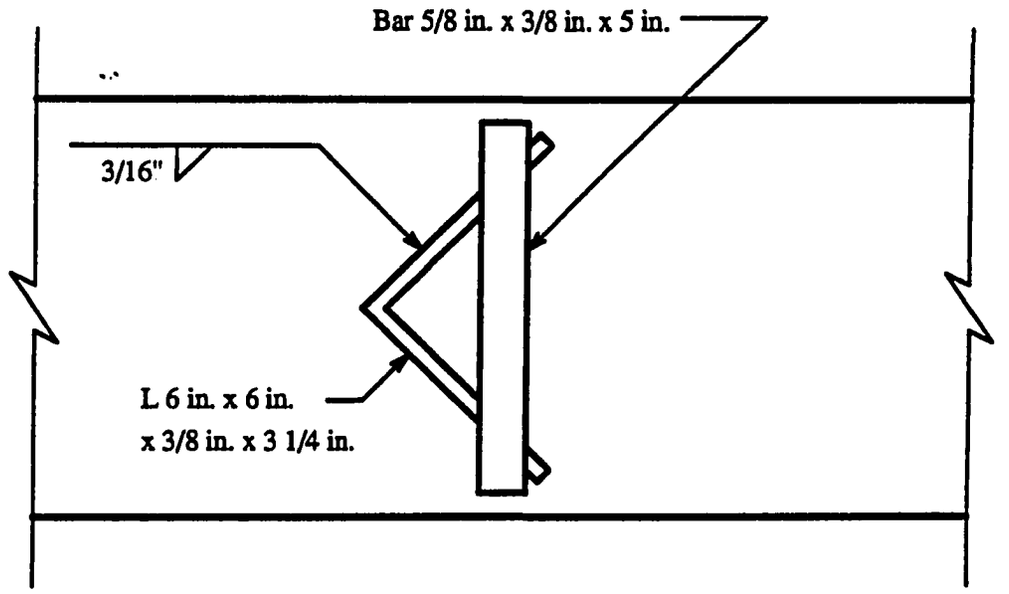

b. PLAN

Fig. 2.2. Details of angle-plus-bar shear connector.

occurs between the concrete and the steel at the shear connector position, depending on the stiffness of the shear connector. The stiffness of the shear connectors has been established through shear tests in the laboratory; force-displacement relationships for the full-scale angle-plus-bar shear connectors are presented in Ref. 24.

In order to model the shear connectors accurately, horizontal slip elements were used to model the link between the stringer nodes and the deck nodes. Constraint equations were utilized to couple the rotations and the vertical displacement of the deck and the stringers. Beam elements were used to connect the two nodes and their stiffnesses were computed to give a stiffness equivalent to that of the actual shear connectors (see Fig. 2.3).

The diaphragms connecting the bridge stringers were modeled using 3-D beam elements. Due to the difference between the vertical level of the diaphragm center-lines and the steel stringer center-lines, rigid links were used to connect the diaphragm nodes to the steel stringer nodes.

Two models were investigated to determine the most suitable idealization for the connection between the post-tensioning forces and the stringers. In the first attempt, each tendon force was modeled as a concentrated force together with a concentrated moment acting at one node on the stringer. This model produced a stress concentration at the bracket locations. To eliminate this problem, plate elements were used to model the brackets thus distributing the force and moment along the actual bracket length (see Fig. 2.3). This removed the stress concentration, and made it possible to obtain the desired stress reduction at the critical sections without obtaining overstresses at the bracket locations.

Two alternatives were investigated to model the deck slab in the negative moment regions. First, all plate

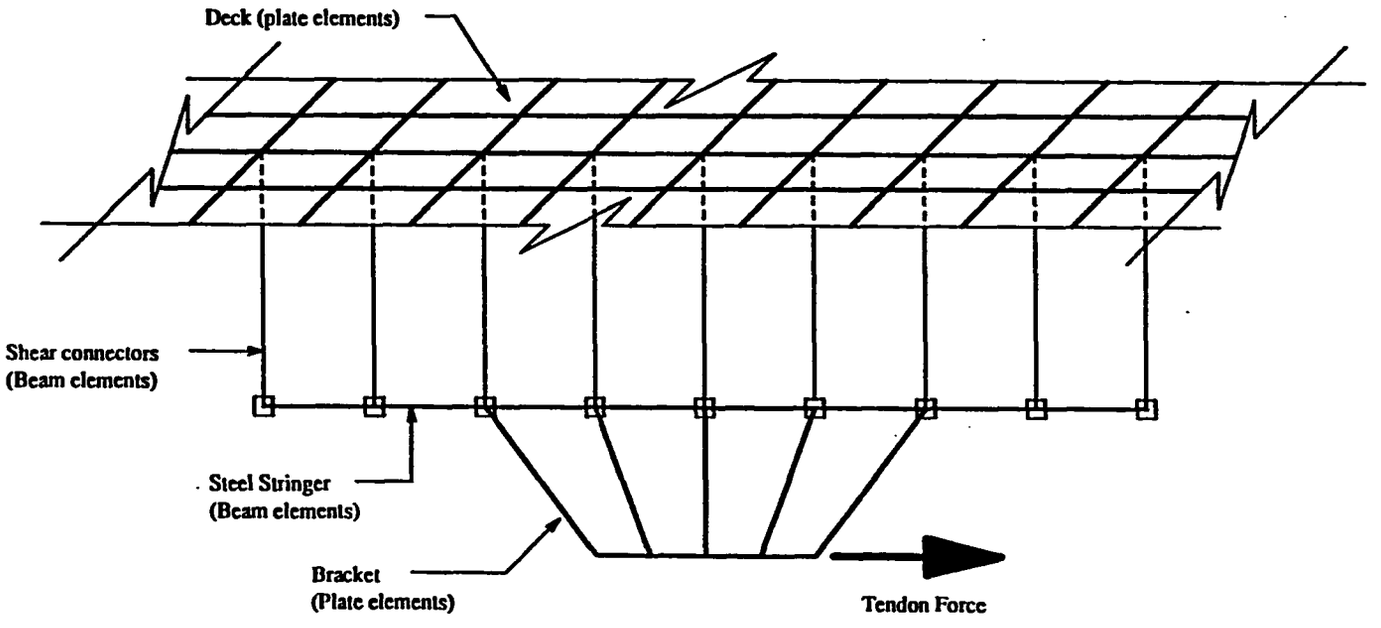

Fig. 2.3. Modeling of shear connectors and post-tensioning brackets.

elements representing the bridge deck in these regions were removed from the finite element model. In the second idealization, all plate elements modeling the entire deck were assumed to be uncracked. The results of using these alternatives were compared to field data. The comparison showed that the second idealization yielded results close to the experimental results. Therefore, no cracking was considered throughout the finite element analysis. This can be explained by the fact that although the deck is cracked, it can still transfer longitudinal forces transversely. Moreover, the existence of reinforcing steel helps the lateral transfer of forces through the deck. Deck cracking was therefore ignored throughout the finite element analysis.

2.2. Verification of the finite element model

To verify the suitability of the finite element model developed in Sec. 2.1, use was made of available experimental data obtained from previous projects done at Iowa State University.

Klaiber et al. [5] investigated the effect of post-tensioning the various spans of different stringers of a one-third scale continuous composite bridge model at Iowa State University Structural Research Laboratory. The model bridge was designed to simulate actual Iowa composite bridges. The test procedure and the experimental results are described in Ref. 5.

The finite element model developed for the current study was used to analyze the one-third scale model bridge under similar loading conditions as those applied to the model bridge in the lab (i.e., 20 kips post-tensioning force in each span of the exterior stringers). Fig. 2.4 shows the bottom flange strains predicted using the finite element

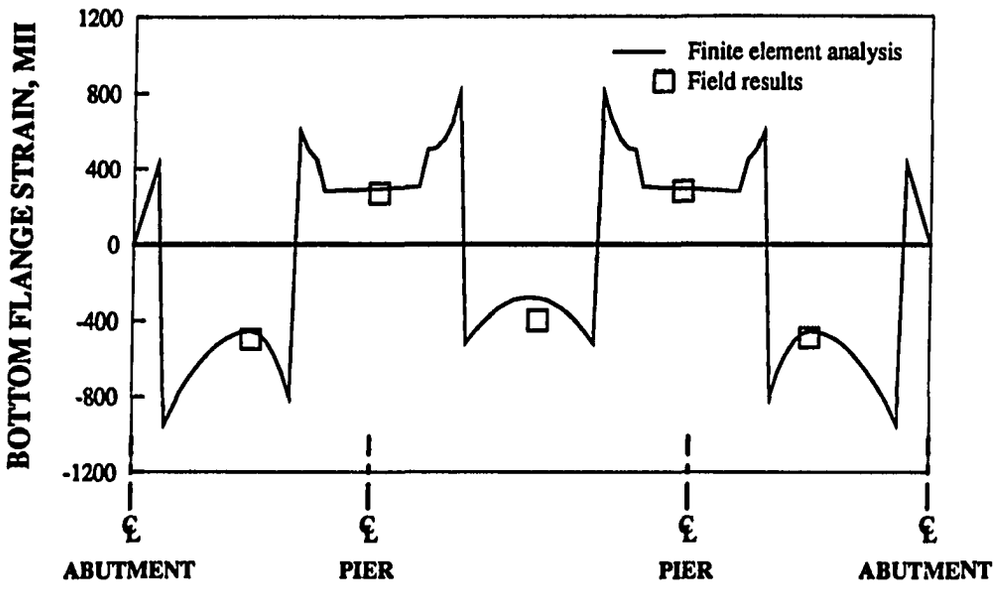

a. EXTERIOR STRINGER

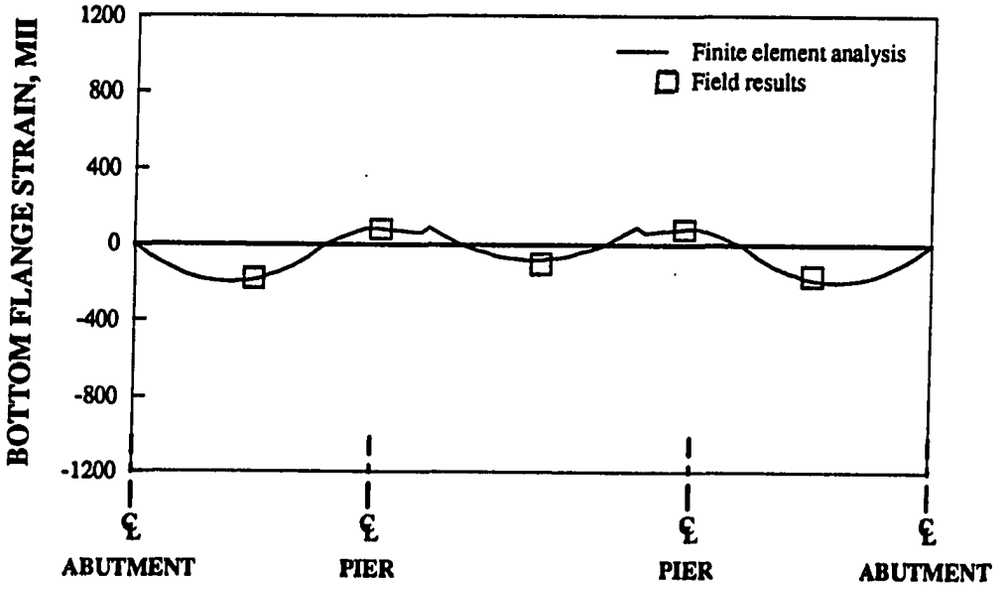

b. INTERIOR STRINGER

Fig. 2.4. Bottom flange strains for model bridge. (Post-tensioning all spans of the exterior stringers)

model plotted versus the experimentally measured strains. It can be seen from the figure that the finite element results show good agreement with the experimental results.

Klaiber et al. [4] also strengthened and field-tested one continuous-span bridge in Pocahontas County, Iowa by post-tensioning the positive moment regions of all stringers. This bridge was tested two consecutive summers to obtain data on the loss of prestress with time. This bridge was analyzed using the ANSYS finite element model. The strengthening forces applied to the bridge were applied to the finite element model and the analysis was performed (The force values are given in Fig. 3.10.f of Ref. 4). Fig. 2.5 shows the bottom flange strains predicted by the finite element model together with the bottom flange strains measured in the field.

The finite element results generally show good agreement with the field results. The most notable difference between the predicted and measured strains occurs at the midpoint of the center-span. As mentioned in Ref. 4, a possible cause for this discrepancy is that the guardrails carry part of the forces on the bridge section.

2.3. Flexural Strength Model

The finite element model developed is suitable for the analysis of bridges in the elastic range. The model obviously can not be used to predict the behavior of the bridge at ultimate load.

Several laboratory tests have been conducted to investigate the behavior of post-tensioned bridge stringers at failure. A review of this work, conducted in the Iowa State University Structural Research Laboratory, is described in Sec. 5.4 of Ref. 8.

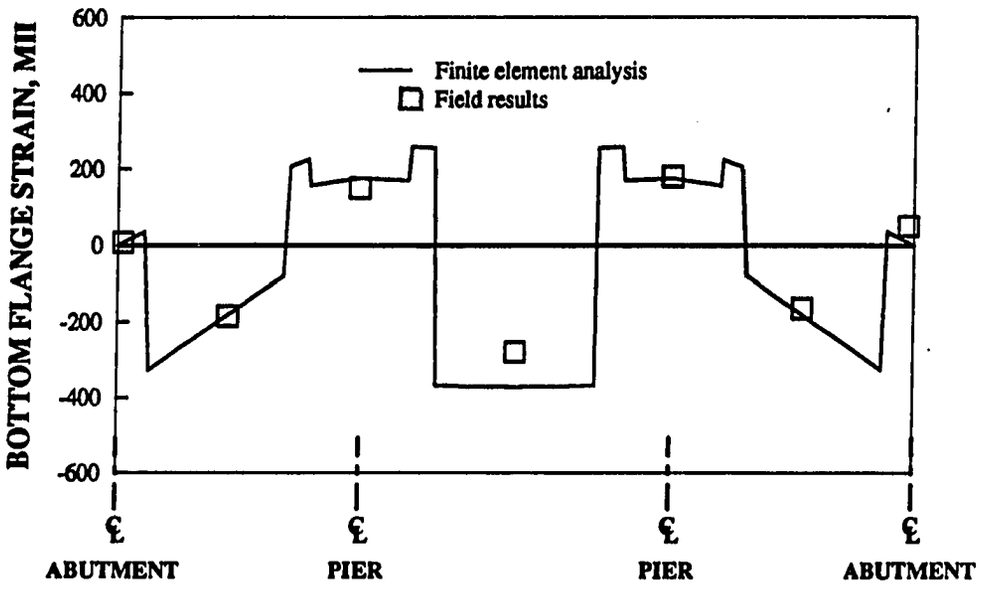

a. EXTERIOR STRINGER

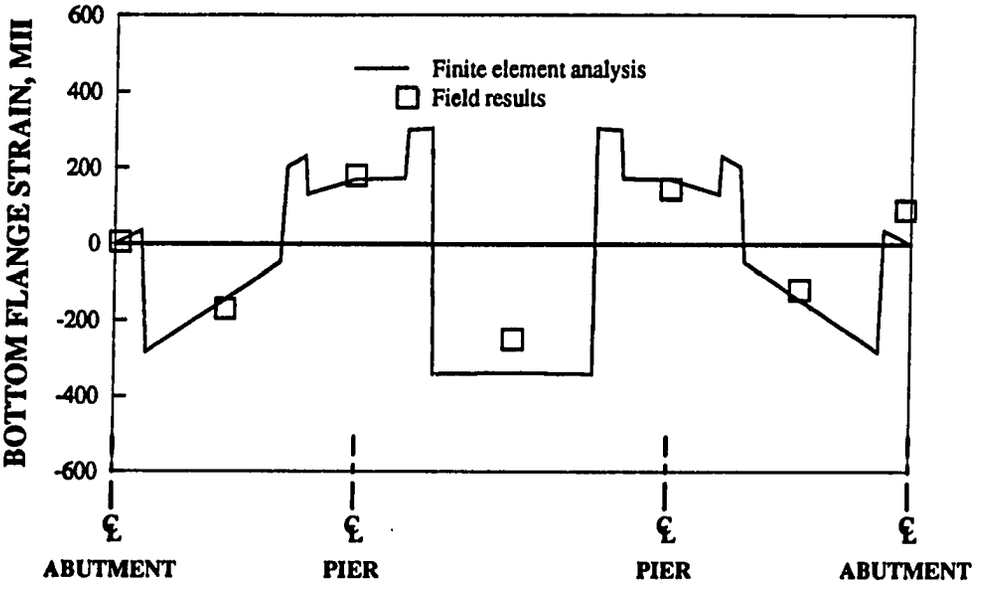

b. INTERIOR STRINGER

Fig. 2.5. Bottom flange strains for bridge tested in Pocahontas County, 1990. (Post-tensioning all spans of both stringers)

In this section, a procedure is suggested for predicting the ultimate strength of bridge stringers strengthened by post-tensioning and/or superimposed trusses.

A theoretical analysis was performed to investigate the effect of an increase in vertical live loads on the stresses in the bridge stringers as well as in the strengthening system (i.e., post-tensioning tendons and truss tubes and tendons). A typical Iowa DOT standard bridge of the V12 series was modeled using finite elements. The bridge was 150 ft long and was strengthened using a system composed of post-tensioning tendons on all stringer spans and superimposed trusses on the exterior stringers.

The strengthened bridge model was analyzed under the effect of vertical loads at various locations along the stringers and the increase in stringer stresses was compared to the increase in the strengthening (post-tensioning and trusses) system. The comparison showed that an increase in the vertical loads on the bridge causes a significantly larger percentage increase in the stresses in bridge stringers than in the post-tensioning tendons and superimposed trusses. This is mainly due to the relatively small stiffnesses of the post-tensioning tendons and the trusses compared to the stringers' stiffnesses. It is therefore hypothetical that failure would occur due to the formation of plastic hinges in the bridge stringers, rather than due to the collapse of the strengthening system.

The suggested pattern of failure is further validated by the experimental results described in Ref. 25. A system of superimposed trusses on a composite beam, supported to simulate the negative moment region in a continuous beam, was loaded to failure in the ISU Structural Research Laboratory. The results of this test showed that the beam failed before the superimposed trusses.

The following principles and assumptions are recommended for use in predicting the approximate flexural strength of the bridge stringers:

1. The failure pattern shown in Fig. 2.6a may be used. Plastic hinges are assumed to form at three locations:
   i. At the maximum positive moment location in the end span (assumed to be at a distance of 40% of the span length from the support).
   ii. At the maximum positive moment location in the center span (assumed to be at midspan).
   iii. At the maximum negative moment location (i.e., at the piers).
2. The deflection of the positive moment locations at which plastic hinges occur may be assumed to be (L/80), where L is the span length.
3. The effective flange width can be determined according to the AASHTO rules for load factor design [23, Sec. 10.38].
4. The compressive force in the slab can be determined according to AASHTO rules, which account for slab reinforcing (unlike service load design), relative capacity of concrete slab vs steel beam, and partial or full shear connection [23, Sec. 10.50].
5. The tendon strain can be obtained from the idealized stringer configuration shown in Fig.2.6a as follows:
   End-span tendon elongation = $\Delta LP1 + \Delta LP2$
   Center-span tendon elongation = $2 \times \Delta LP3$
6. The superimposed truss tendon strain can be obtained from the idealized truss configuration shown in Fig.2.6b as follows:
   $\Delta LT1 = \Delta V1 \times \tan(\theta 2)$
   $\Delta LT2 = \Delta V2 \times \tan(\theta 3)$
   Truss tendon elongation = $\Delta LT1 + \Delta LT2$.

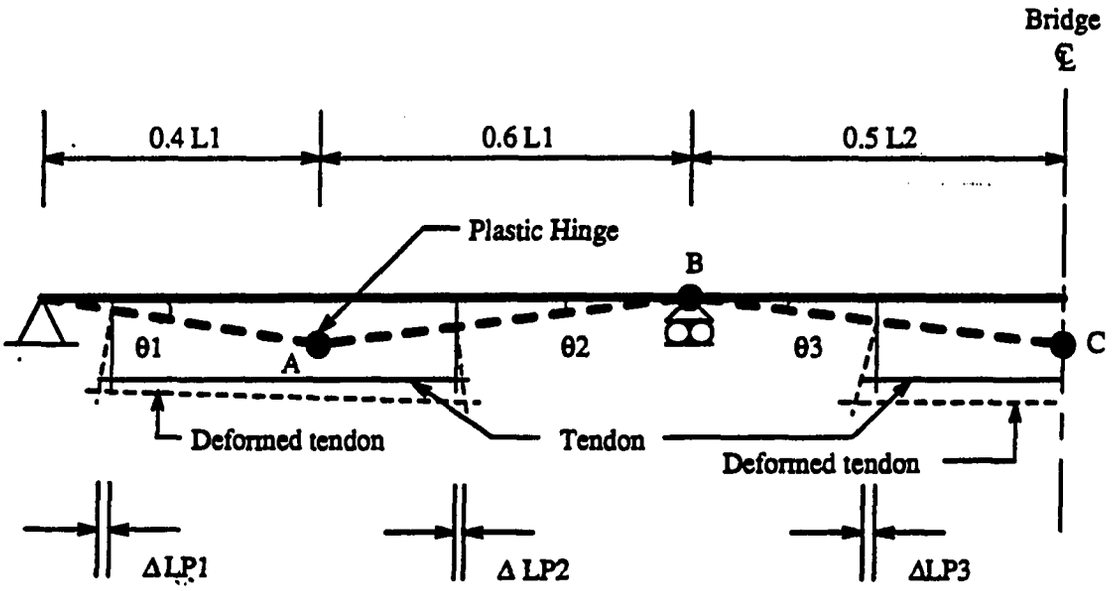

a. FAILURE PATTERN

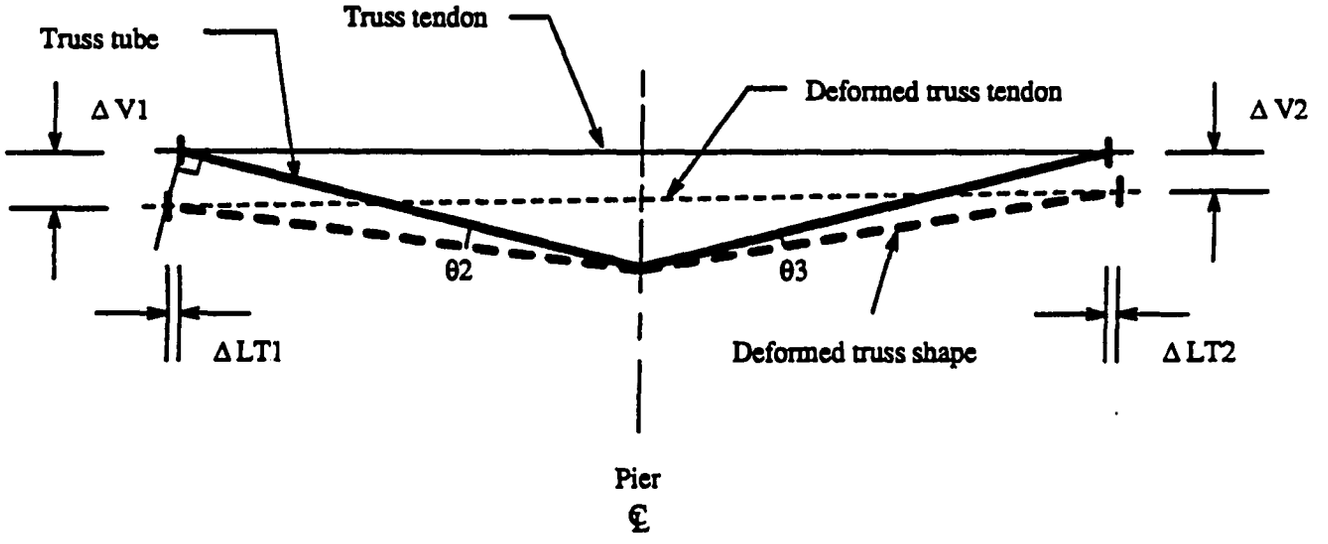

b. DEFORMATION OF SUPERIMPOSED TRUSS

Fig. 2.6. Idealization of bridge stringer at ultimate load.

7. Tendon force can be computed from an idealized stress-strain curve for the tendon steel.
8. The increase in the truss tendon force can be used to compute the increase in the truss vertical forces acting on the bridge exterior stringer.
9. Shear connector capacities can be computed from the formulas given in Sec.10.38 of Ref. 23. For angle-plus-bar shear connectors, the capacity can be based on a modified channel formula as noted in Ref. 7.
10. The distribution of forces in the bridge stringers at failure has not been addressed in this study. It is left for the designer either to obtain these distribution fractions by performing a finite element nonlinear analysis, or to use engineering judgement to make reasonable assumptions for the distribution fractions.

3. STRENGTHENING OF THREE-SPAN BRIDGE IN CERRO GORDO COUNTY, IOWA

3.1. Bridge description

With the help of the Office of Bridge Design at the Iowa DOT one continuous-span composite bridge was selected to be strengthened and field-tested. Ten three-span continuous bridges requiring posting were considered. Factors considered included: proximity to Iowa State University, height from ground to bridge at the midspans, and nearest available power source. The bridge selected is located in north central Iowa in Cerro Gordo county approximately 12 miles south of Mason City, Iowa and 7 miles east of Thornton, Iowa on County Road B65.

The bridge framing plan and cross section are shown in Figs. 3.1a and 3.1b. Photographs of the bridge side view and top view are shown in Figs. 3.2a and 3.2b, respectively. The bridge is a standard Iowa DOT bridge of the V12 series. The bridge is composed of three-spans with end spans of 45 ft 9 in. and a middle span of 58 ft 6 in. for a total length of 150 ft. The four bridge stringers are spliced at the nominal dead load inflection points in the center span. In addition, coverplates are located on both the top and bottom flanges of the stringers at the pier supports.

Steel wide-flange diaphragms are located at the one-third points of the middle span and at the midpoints of the end spans. Diaphragms consist of channel sections at the abutments and standard I-shapes at the piers.

The bridge section is 26 ft wide with a 24 ft roadway providing two 12 ft traffic lanes according to AASHTO [23]. The concrete deck has a variable thickness from 6 and 7/16 in. over the stringers to 6 and 3/4 in. between the stringers. A three-in. crown for positive drainage of the

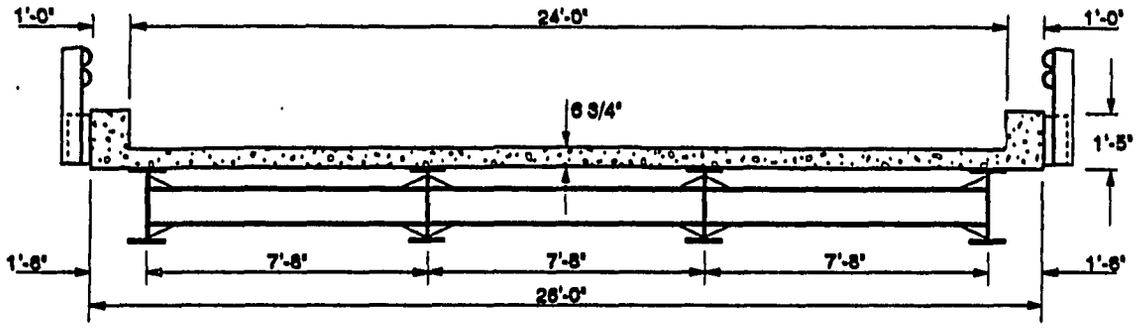

a. BRIDGE SECTION

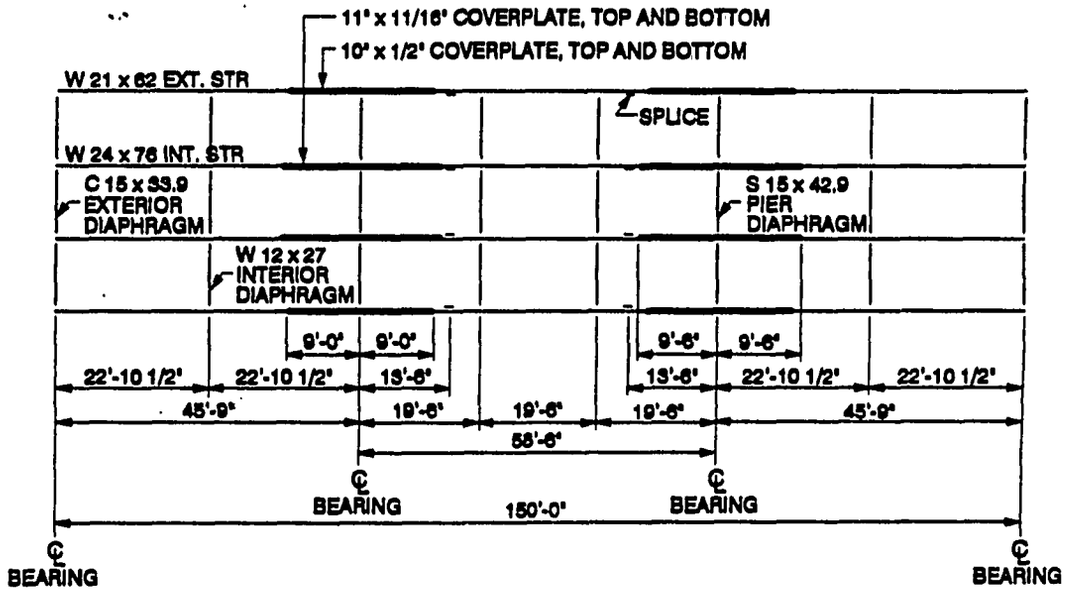

b. BRIDGE FRAMING PLAN

Fig. 3.1. Framing plan of Mason City bridge.

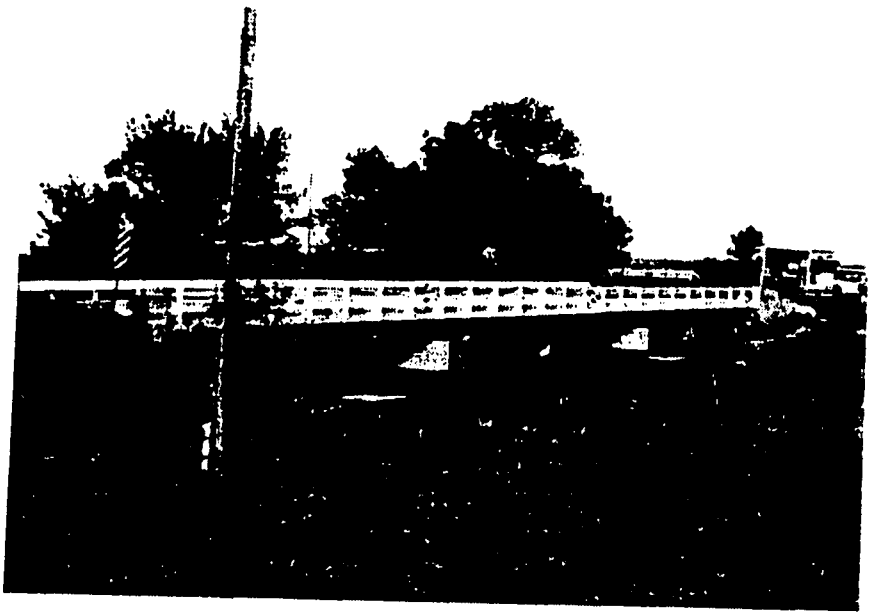

a. SIDE VIEW

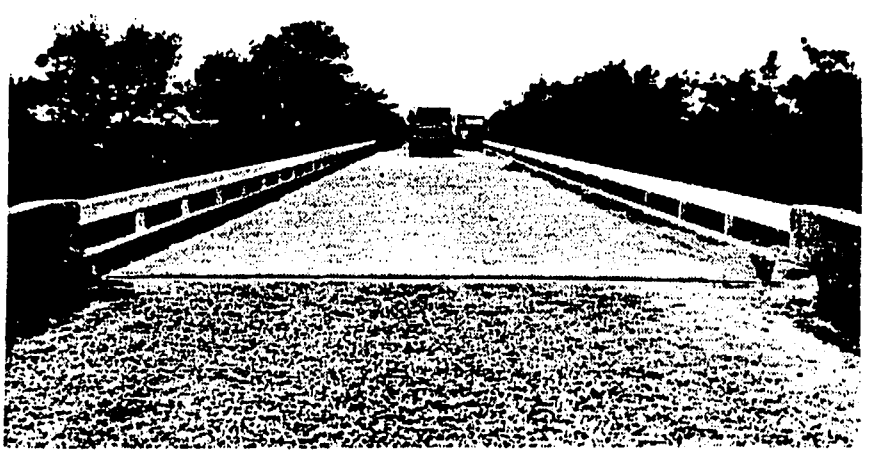

b. END VIEW

Fig. 3.2. Photographs of Mason City bridge.

roadway surface results from the difference in height of the interior and exterior stringers. A guardrail is bolted along each integral curb and consists of a 10-gauge formed steel beam rail bolted to L5x5-1/2x3/8 posts spaced at six ft. Continuity of the beam rail sections is provided at alternating angle posts by a bolted one ft overlap. The result of this construction technique is that the beam rail and stringer bottom flange simulate the top and bottom chords of a Vierendeel truss respectively.

Several concrete cores were tested to determine the concrete compressive strength of the deck. Cores had to be removed from the deck for the additional shear connectors required between the deck and stringers. The cores were equal in length to the deck thickness (approximately six in.) with a four in. diameter and were selected such that they did not contain deck reinforcement. Compressive strength tests on six cores were performed in accordance with ASTM Standards and yielded an average compressive strength of 5820 psi, which includes a correction factor for non-standard core dimensions.

3.2. Design of strengthening system

This section has been divided into two subsections. In Sec. 3.2.1 the need for and method of providing additional shear connection is presented. In Sec. 3.2.2 the design of the strengthening system is discussed.

3.2.1. Design of shear connectors

According to the current AASHTO design specifications [23] the Mason City bridge was not provided with the required shear connectors to develop full composite action between the concrete deck and the steel stringers. Thus,

additional shear connectors were required to satisfy the AASHTO requirements.

The original shear connectors used were the angle plus bar type. Typically, for the V12 series bridge, a three in. length of L5x5x3/8 is welded vertically to the top flange of the stringer. In addition, a small bar is welded across the top of the angle to prevent lift up of the concrete deck (see Fig. 2.2).

To provide additional shear capacity, one-inch diameter bolts were used. The number of additional shear connectors required was computed based on Sec. 10.38.5.1 of AASHTO [23]. Existing and new shear connector ultimate strength capacities were obtained from shear strength tests described in Ref. 25. The additional shear connectors were added at the locations shown in Fig. 3.3a on the exterior stringers and Fig. 3.3b on the interior stringers. A total of 220 new one in. diameter bolt shear connectors were added to the bridge: 52 on each of the exterior stringers and 58 on each of the interior stringers.

3.2.2. Design of post-tensioning and superimposed trusses

In order to compute the overstresses in the bridge stringers due to vertical loads, each of the bridge stringers was analyzed to obtain the maximum and minimum moment envelopes due to dead load, superimposed dead load, live load and impact. The computation of loads and of the wheel load distribution fractions was done according to AASHTO standard specifications [23]. Iowa legal truck loads were used for live load.

Figure 3.4 shows reference sections along the bridge length. Table 3.1 is a description of these reference sections. Only one half of the bridge has been included here because of the symmetry that exists.

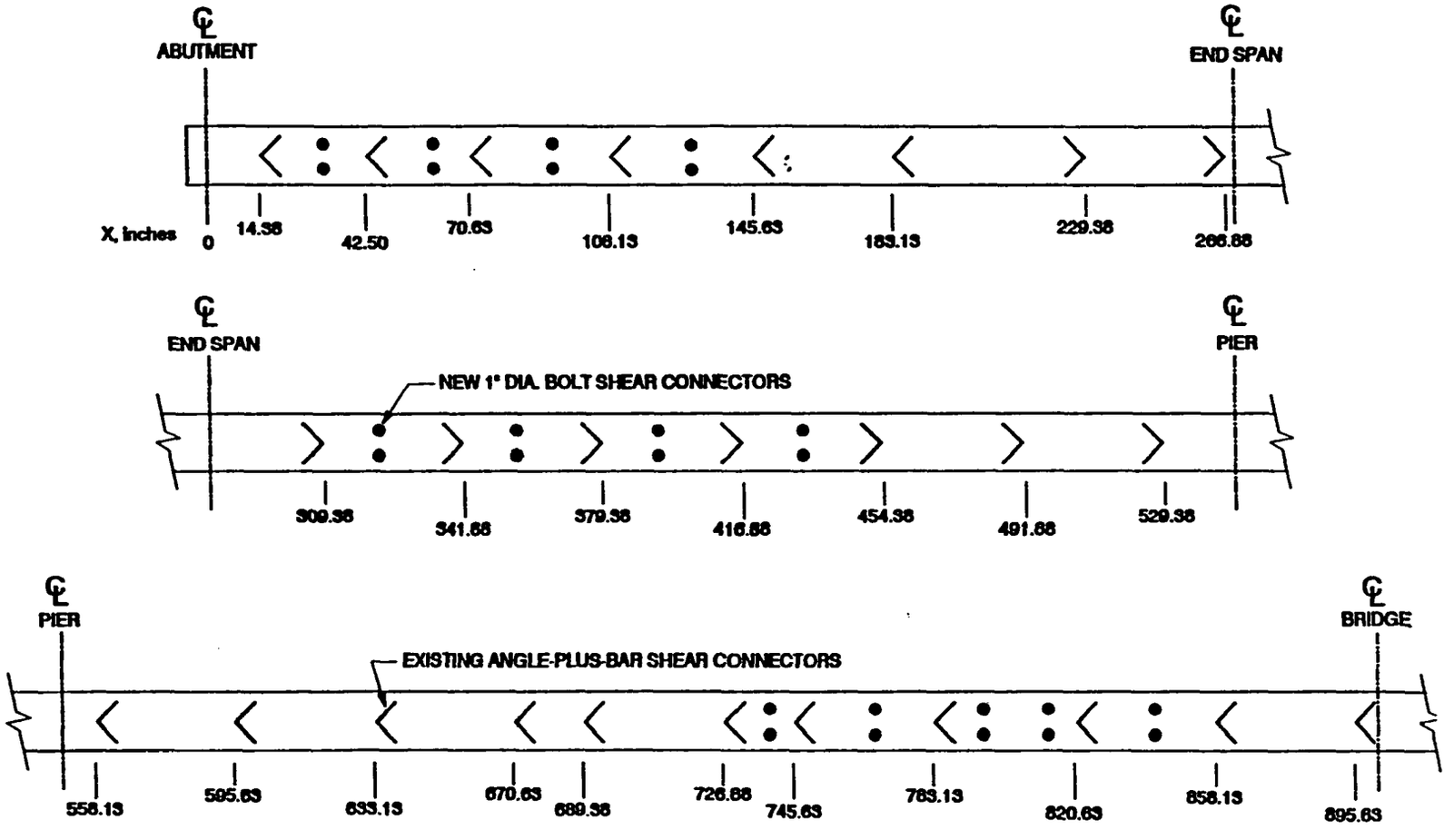

a. EXTERIOR STRINGER (52 bolts total)

Fig. 3.3. New bolt shear connector layout.

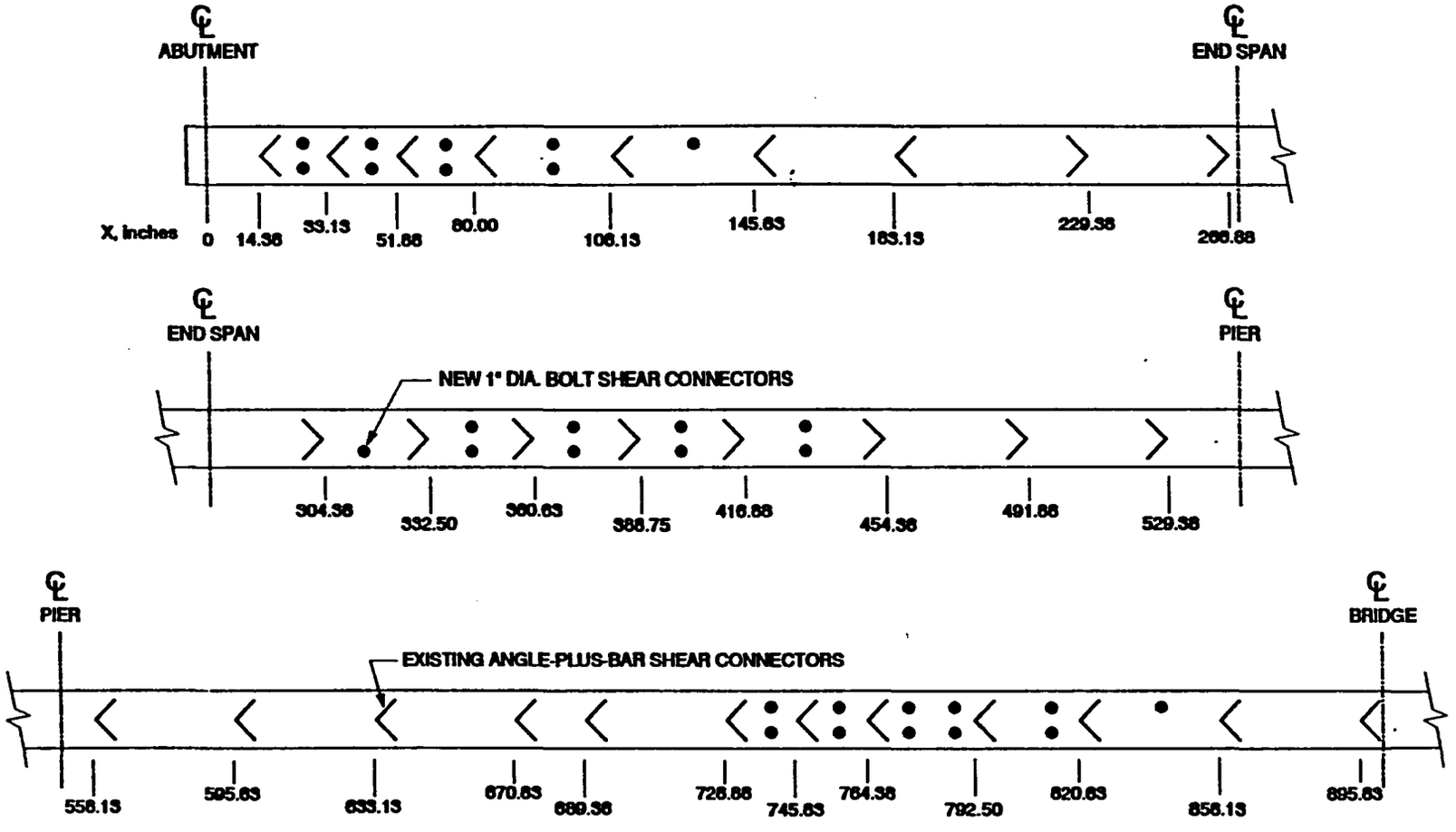

b. INTERIOR STRINGER (58 bolts total)

Fig. 3.3. Continued.

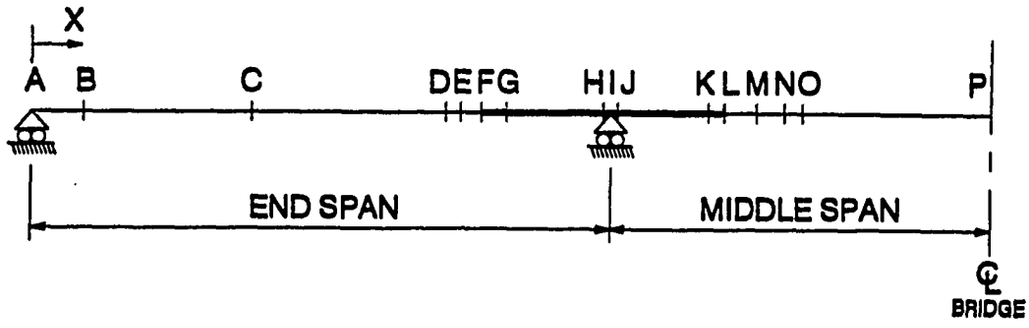

Fig. 3.4. Reference sections along half bridge length.

Table 3.1. Description and location of reference sections.

Section	Description	X, in.	
		Exterior Stringer	Interior Stringer
A	Abutment bearing	0	0
B	Tendon anchorage at Bracket A	66	66
C	Nominal maximum positive moment	220	220
D	Nominal dead-load inflection point and anchorage at Bracket A	400	400
E	Location of truss bearing	412	412
F	Actual coverplate end	431	435
G	Theoretical coverplate end	456	462
H	Pin anchorage at Bracket B	544	544
I	Pier bearing	549	549
J	Pin anchorage at Bracket B	554	554
K	Theoretical coverplate end	642	647
L	Actual coverplate end	657	663
M	Location of truss bearing	686	686
N	Splice and nominal dead-load inflection point	711	711
O	Tendon anchorage at Bracket A	727	727
P	Nominal maximum positive moment and center line of bridge	900	900

The moment envelopes obtained were used to compute the stresses in the stringers. Table 3.2 outlines the section properties assumed along the stringer length. The letters in the *Length* column correspond to the reference sections shown in Fig. 3.4. The bottom-flange stresses that resulted from these assumptions are shown in Fig. 3.5. From the figure, it can be seen that the maximum stresses exceed the allowable inventory stress level in the positive moment regions of all stringer spans and at the piers of the exterior stringers, hence it was necessary to provide a strengthening system to reduce these overstresses to the allowable values.

To design the strengthening system, finite element analyses were performed to calculate the required post-tensioning forces and truss forces.

The bridge was analyzed using the finite element model described in Sec. 2.1. For each of the five cases illustrated in Fig. 3.6, a unit force was applied to the post-tensioning or truss tendons. Parameters such as location of post-tensioning brackets and truss bearing points were varied several times within practical limits and the output from the finite element analysis was saved in files to be used later in design. The analysis provided axial forces and moments at different locations along the length of each stringer.

To calculate the required strengthening forces for the Mason City bridge, a computer program was developed. It should be noted that this program was prepared by the author for the purpose of designing a strengthening system for the Mason City bridge, and is not part of the design methodology developed for use by practicing engineers and described in Chapter 4.

Table 3.2. Bridge load-behavior assumptions.

Load	Length[1]	Assumed Effective Cross-Section
Dead (steel stringer and concrete deck)	A-G	wide-flange stringer
	G-K	coverplated wide-flange stringer
	K-P	wide-flange stringer
Long-Term Dead	A-D	composite deck and wide-flange stringer, n=27
	D-G	wide-flange stringer
	G-K	coverplated wide-flange stringer
	K-N	wide-flange stringer
	N-P	composite deck and wide-flange stringer, n=27
Live-positive moment envelope-(Iowa legal trucks and impact) and post-tensioning	A-G	composite deck (and curb for ext. stringer) and wide-flange stringer, n=9
	G-N	composite deck (and curb for ext. stringer) and coverplated wide-flange stringer, n=9
	N-P	composite deck (and curb for ext. stringer) and wide-flange stringer, n=9
Live-negative moment envelope-(Iowa legal trucks and impact) and post-tensioning	A-G	wide-flange stringer
	G-N	coverplated wide-flange stringer
	N-P	wide-flange stringer

[1] Lengths are defined by reference sections given in Fig. 2.3 and Table 2.1.

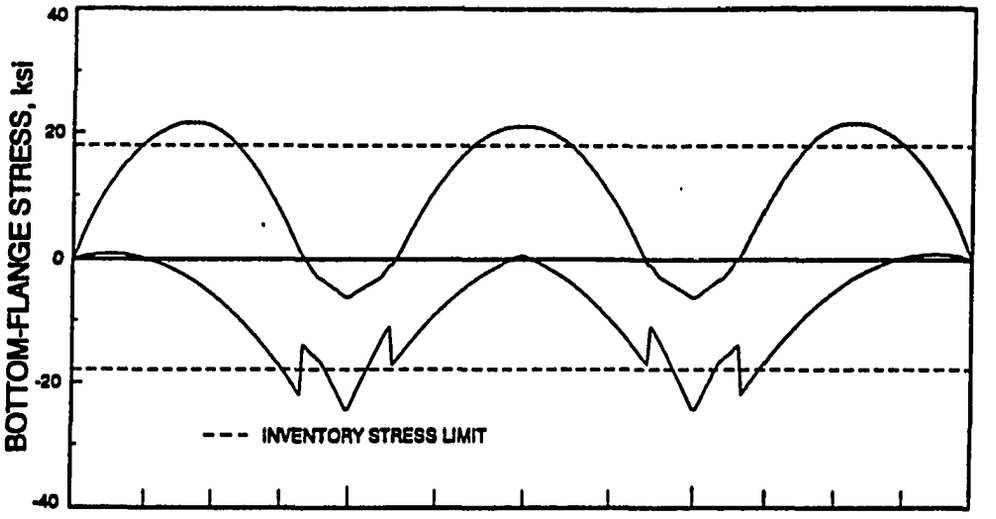

a. EXTERIOR STRINGER

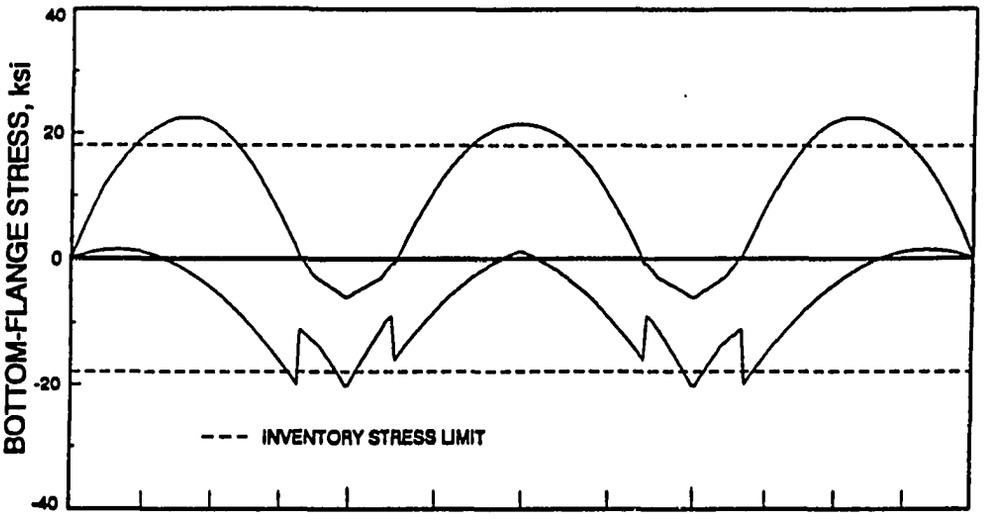

b. INTERIOR STRINGER

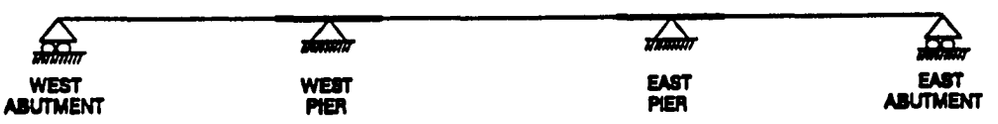

Fig. 3.5. Stringer Stress envelopes due to vertical loads.

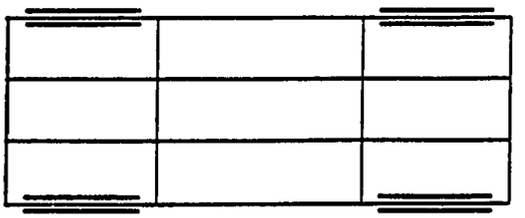

a. CASE 1

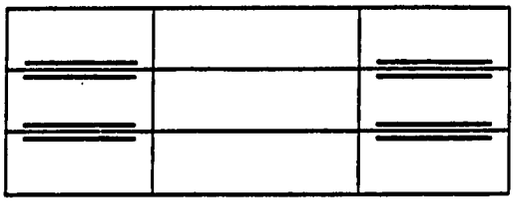

b. CASE 2

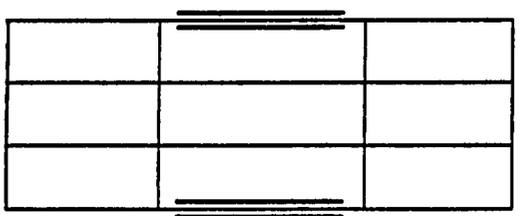

c. CASE 3

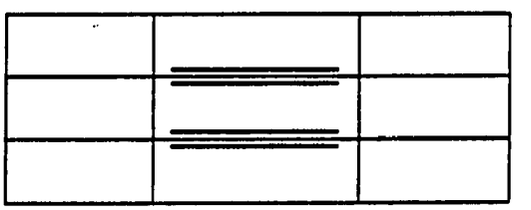

d. CASE 4

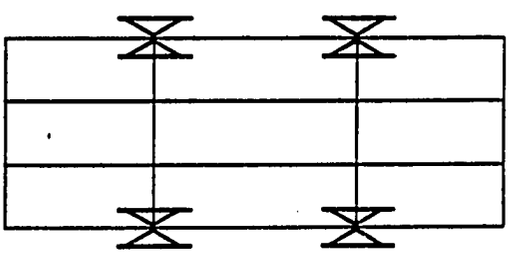

e. CASE 5

Fig. 3.6. Finite element model cases.

The program is comprised of several routines and performs the steps listed:

1. First, the designer selects the strengthening scheme to be used (any combination of the cases shown in Fig. 3.6). The user also makes preliminary assumptions for the bracket positions and values of the strengthening forces.
2. The designer analyses the bridge stringers under vertical loads (according to AASHTO) and forms a file containing the maximum moments in the bridge stringers due to vertical loads. The program reads the data in this file.
3. The designer provides files containing axial forces and moments on the stringers due to unit strengthening forces. These files are obtained from the finite element analyses as mentioned earlier. The program selects the correct input file according to the length of the post-tensioning and the superimposed truss tendons and reads the data in these files. This gives the designer the flexibility of changing the tendon lengths to arrive at an optimum design.
4. The program reads the section properties along the stringer length.
5. The program calculates the total moments induced in the stringers due to the vertical loads and the strengthening forces. To do that, the program magnifies the axial forces and moments induced by unit tendon forces using the specified strengthening force values and combines the magnified values with the vertical load moment envelopes. The final stresses are then computed and compared with the inventory stresses. The program provides screen plots of the final stress envelopes along the bridge stringers to aid the

designer in determining if the desired stress reduction in the entire bridge structure was achieved.

6. The designer changes the specified force values and tendon lengths as needed and iterates until the optimum strengthening forces are determined.

For the bridge considered here, an attempt was made to reduce the overstresses at the critical locations using post-tensioning only. However, it was determined that using this alternative did not reduce the overstresses at the pier locations to inventory level. Therefore, it was decided to add superimposed trusses on the exterior stringers at the pier locations to help reduce these overstresses. The final design strengthening forces are as follows:

- 43 kips in end-spans of each exterior stringers.
- 58 kips in center-span of each exterior stringers.
- 75 kips in end-spans of each interior stringers.
- 81 kips in end-spans of each interior stringers.
- 167 kips in each superimposed truss on the exterior stringers.

The bottom flange stresses in the bridge stringers due to the post-tensioning forces is given in Fig. 3.7. Figure 3.8 shows the stresses due to the superimposed trusses and the final stress envelopes after strengthening are shown in Fig. 3.9. Note that the stress envelopes do not exceed the 18 ksi inventory stress level at any section along the stringer.

The computed forces were applied to the bridge by post-tensioning the positive moment regions of all the stringers (12 locations) and by adding superimposed trusses at the piers of the exterior stringers only (four locations). A layout of the post-tensioning system employed is shown in Fig. 3.10; photographs of the system are shown in Fig. 3.11.

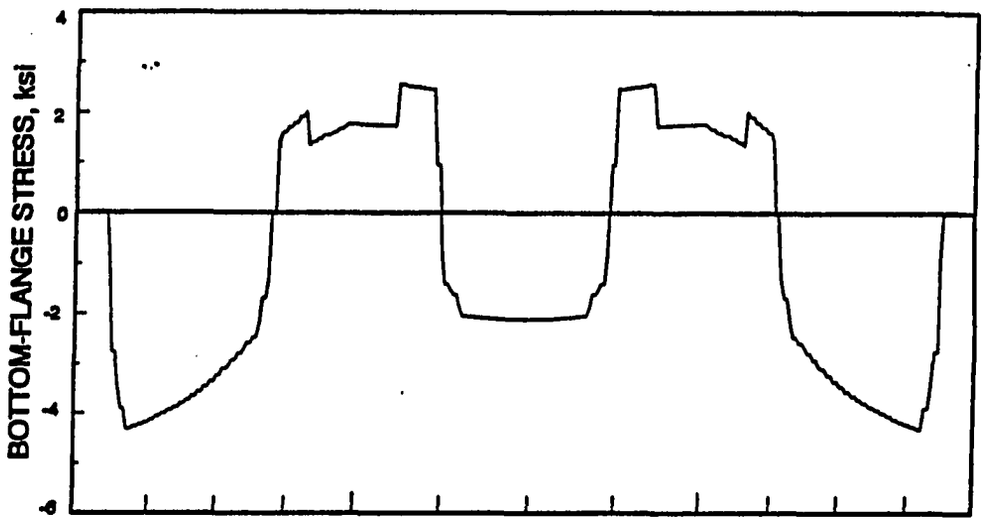

a. EXTERIOR STRINGER

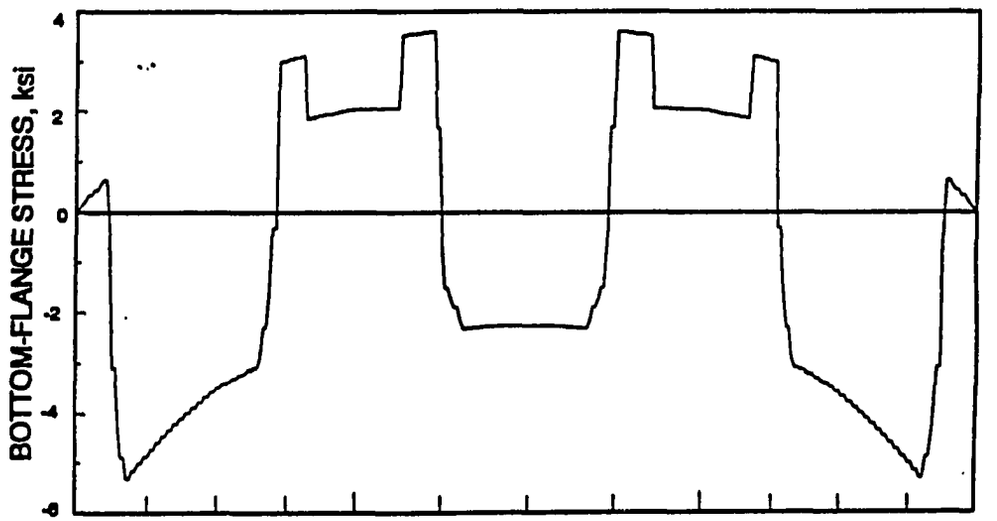

b. INTERIOR STRINGER

Fig. 3.7. Stringer Stresses due to post-tensioning.

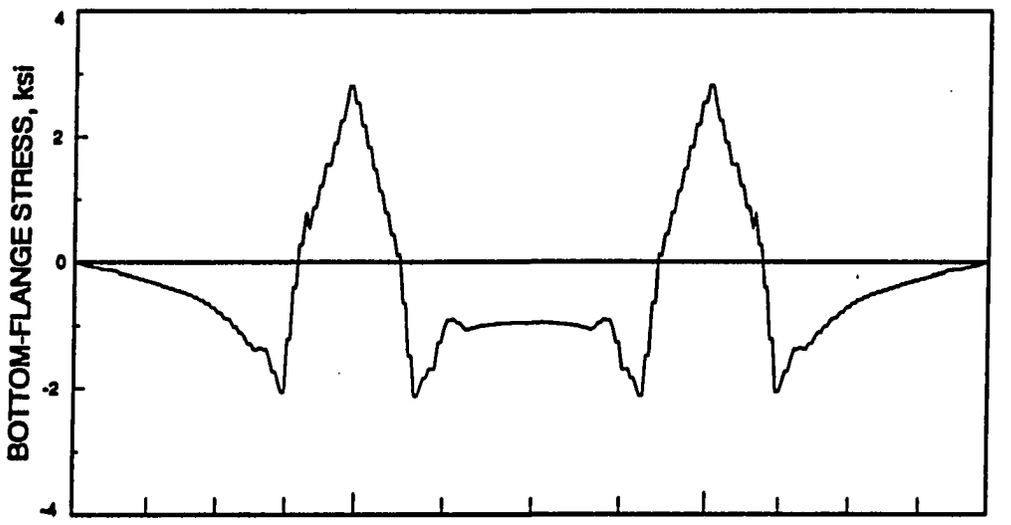

a. EXTERIOR STRINGER

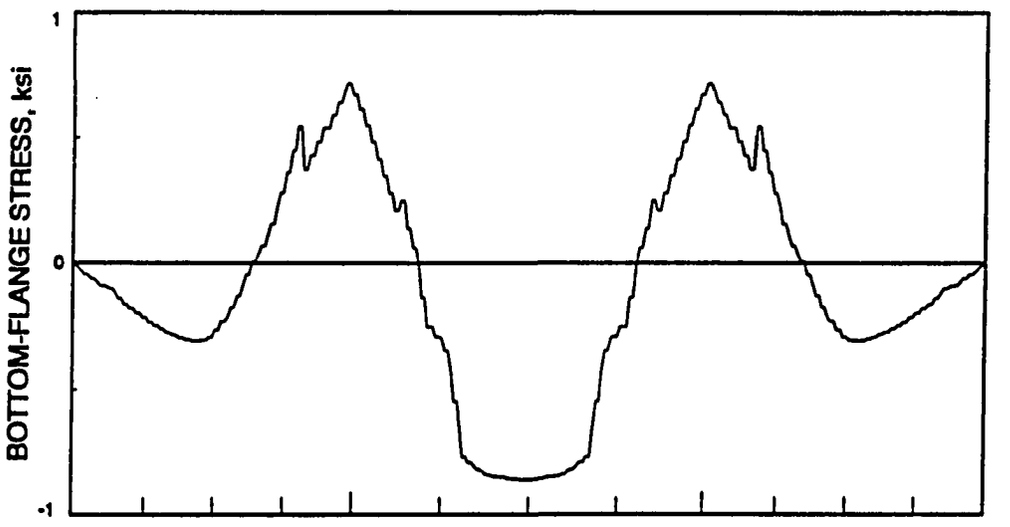

b. INTERIOR STRINGER

Fig. 3.8. Stringer Stresses due to superimposed trusses.

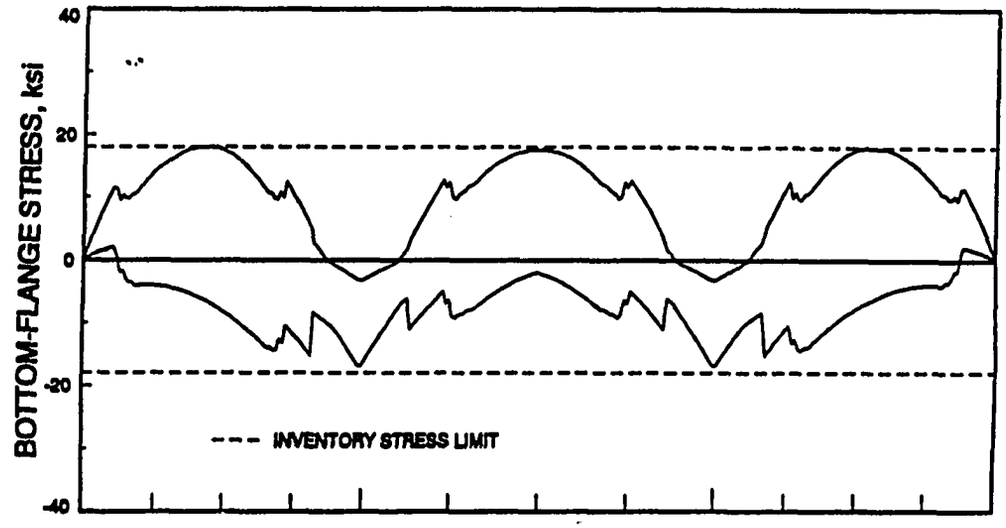

a. EXTERIOR STRINGER

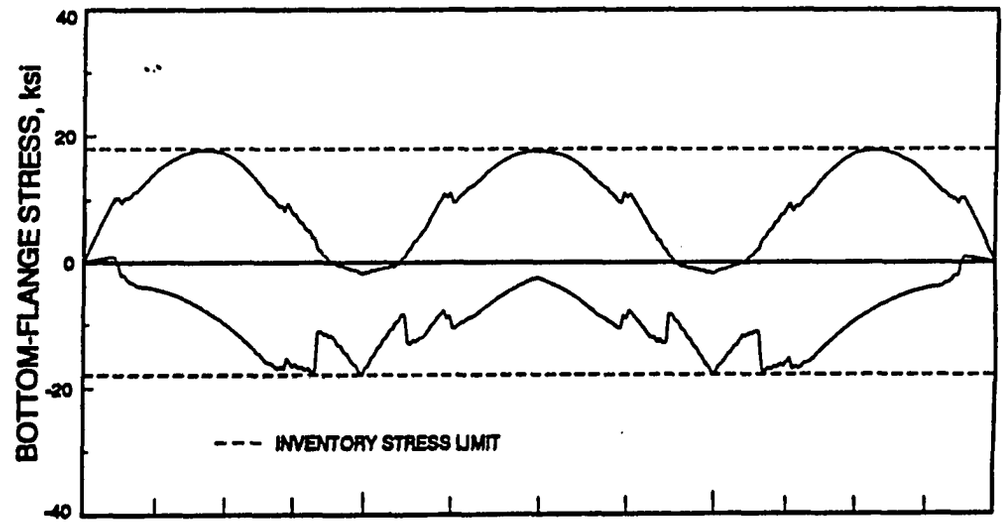

b. INTERIOR STRINGER

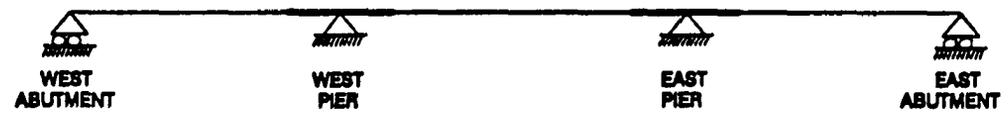

Fig. 3.9. Stringer Stress envelopes due to vertical loads and the strengthening system.

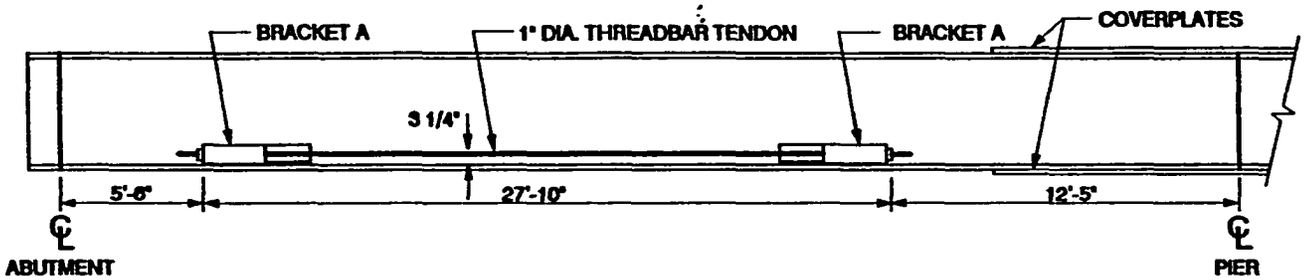

a. END SPAN

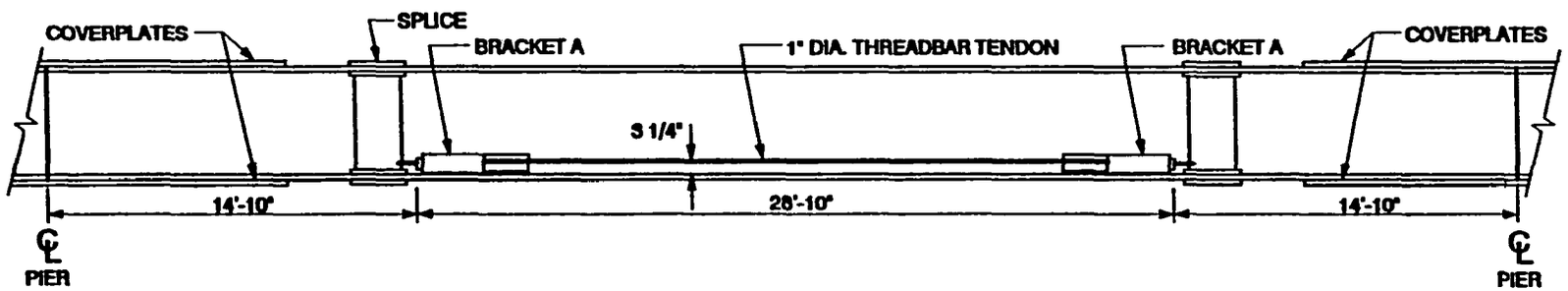

b. MIDDLE SPAN

Fig. 3.10. Post-tensioning layout.

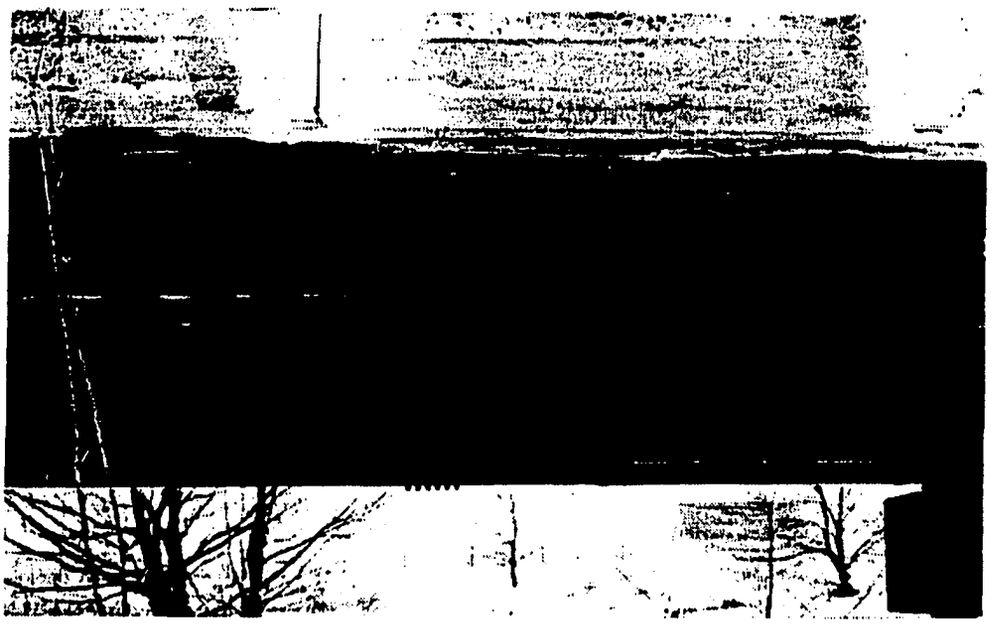

a. POST-TENSIONING BRACKET AND TRUSS BEARING

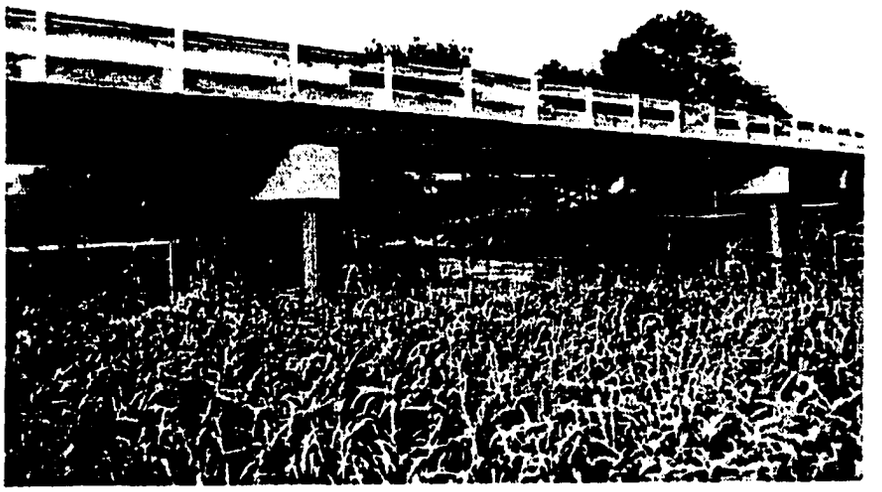

b. TRUSS STRENGTHENING SYSTEM

Fig. 3.11. Photographs of strengthening sytem in place.

Figure 3.12 illustrates the superimposed truss system used at the pier locations (one on each side of the stringer web) on the exterior stringers.

3.3. Field results

The strengthening system was installed on the Mason City bridge and the field-testing was performed during the summers of 1992 and 1993. In this section, some of the field-test results are given and compared to those predicted by the finite element analysis. A detailed description of the bridge instrumentation and testing is given in Ref. 2.

Several stages were necessary to install the strengthening system on the bridge because of the limited strengthening equipment available. The various stages used are presented in Fig. 3.13. In this section, the response of the bridge to the strengthening system is presented.

The forces that were applied in each stage of the strengthening process are shown in Fig. 3.14 and are indicated by the highlighted boxes for each stage.

As previously noted, the theoretical strengthening forces were calculated using a finite element model (Chp. 2). The forces applied in the field were slightly different than the required theoretical forces. The actual forces applied are shown in Fig. 3.15.

Based on the finite element model developed, the strain profile was predicted for the exterior and interior stringers as each symmetric strengthening stage was activated. Because the bridge was modeled using 1/4 symmetry; only symmetric results could be predicted. The predicted theoretical strain profiles and experimental strains in the exterior and interior stringers are presented in Figs. 3.16 through 3.20 for Stages 2, 4, 6, 7, and 8,

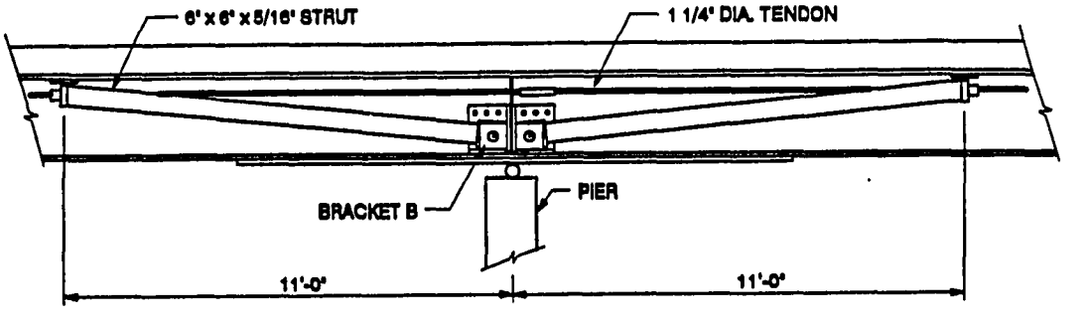

a. SUPERIMPOSED TRUSS

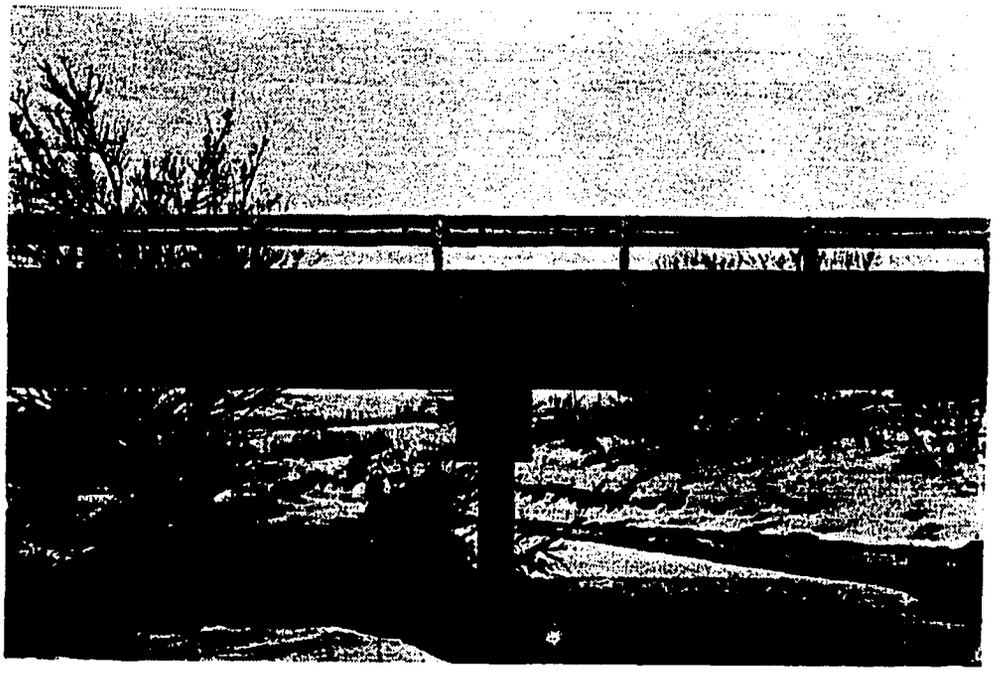

b. SUPERIMPOSED TRUSS PHOTOGRAPH

Fig. 3.12. Superimposed truss system.

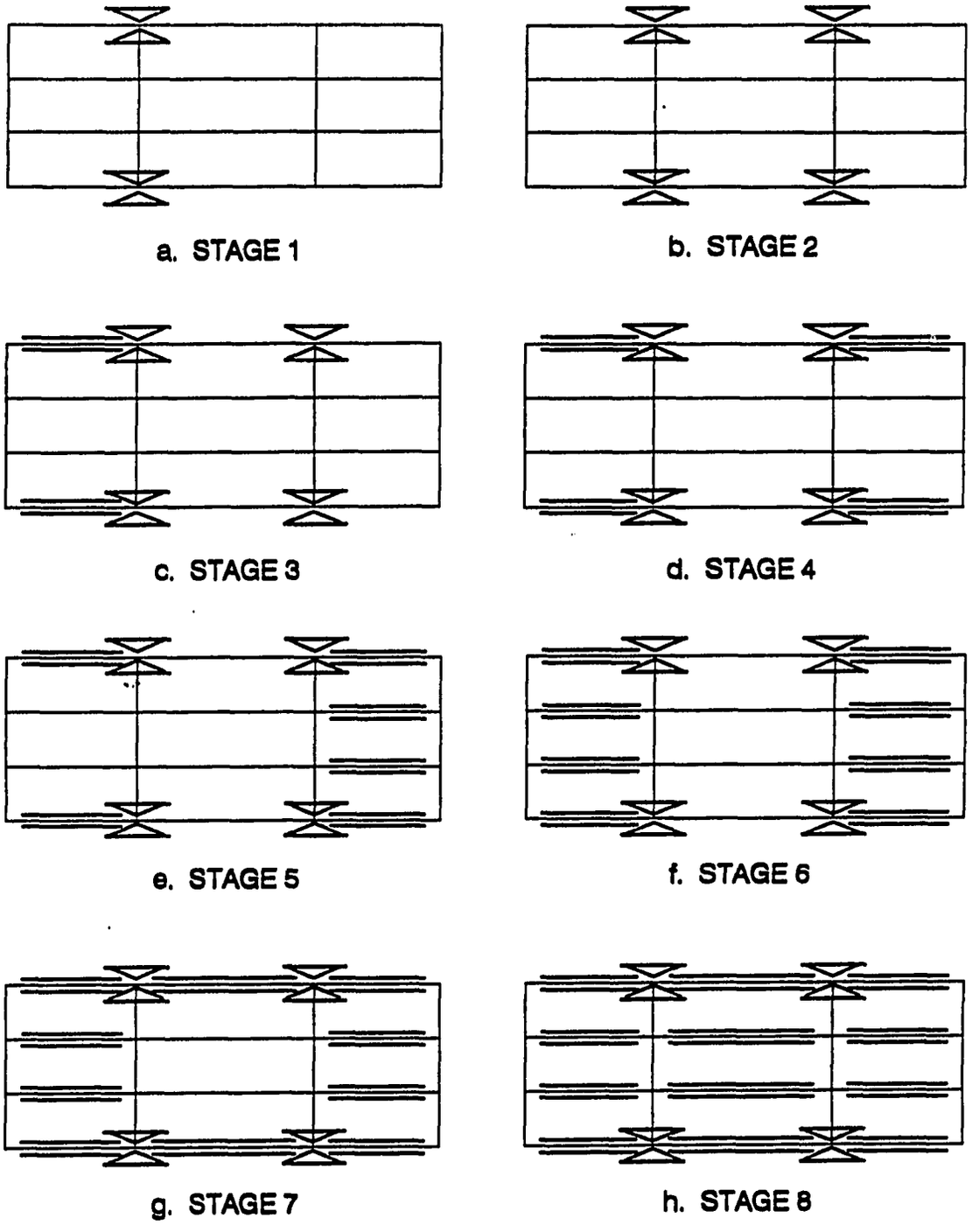

Fig. 3.13. Order strengthening system was applied to bridge.

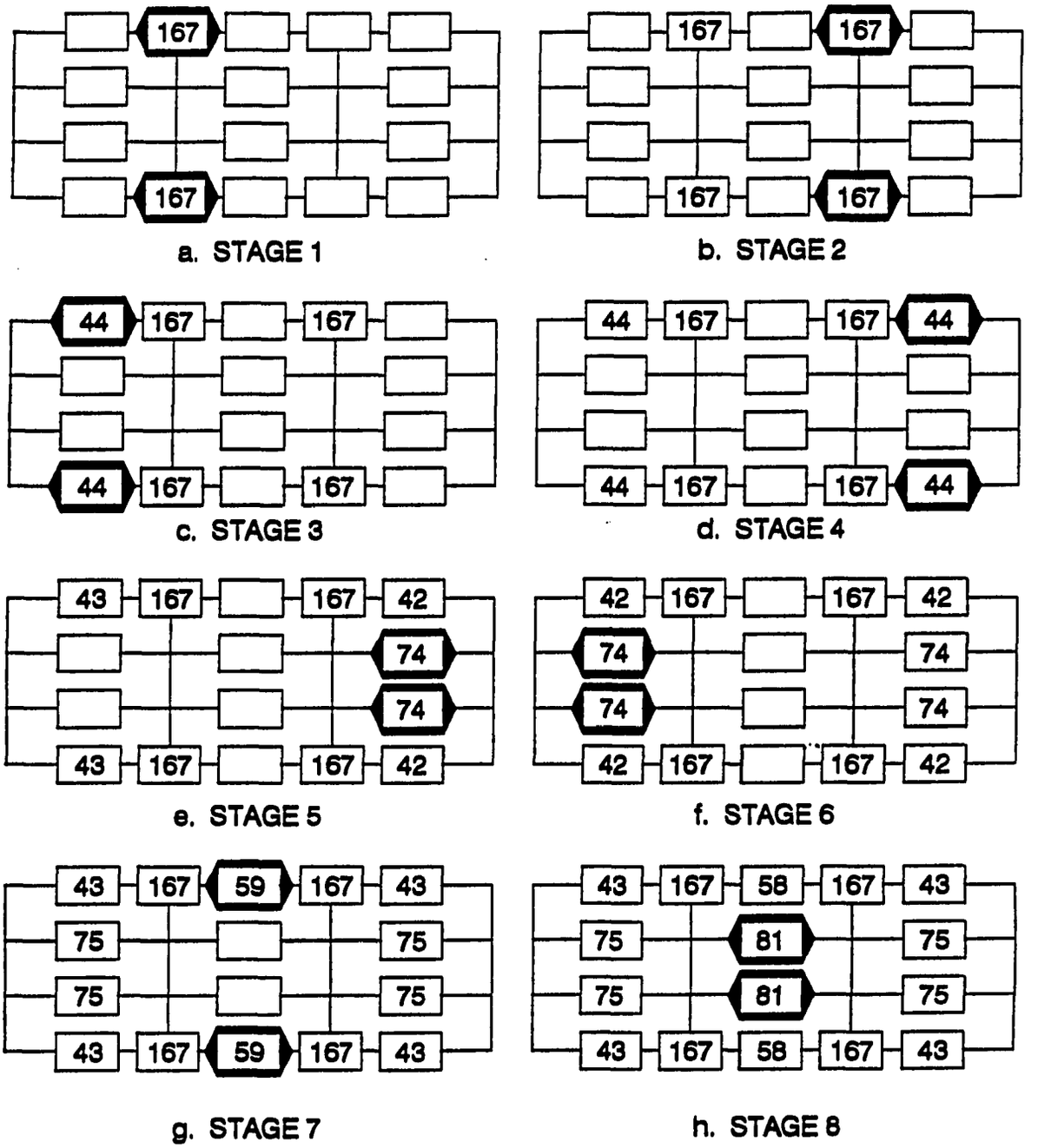

Fig. 3.14. Theoretical strengthening forces (kips) required per stage.

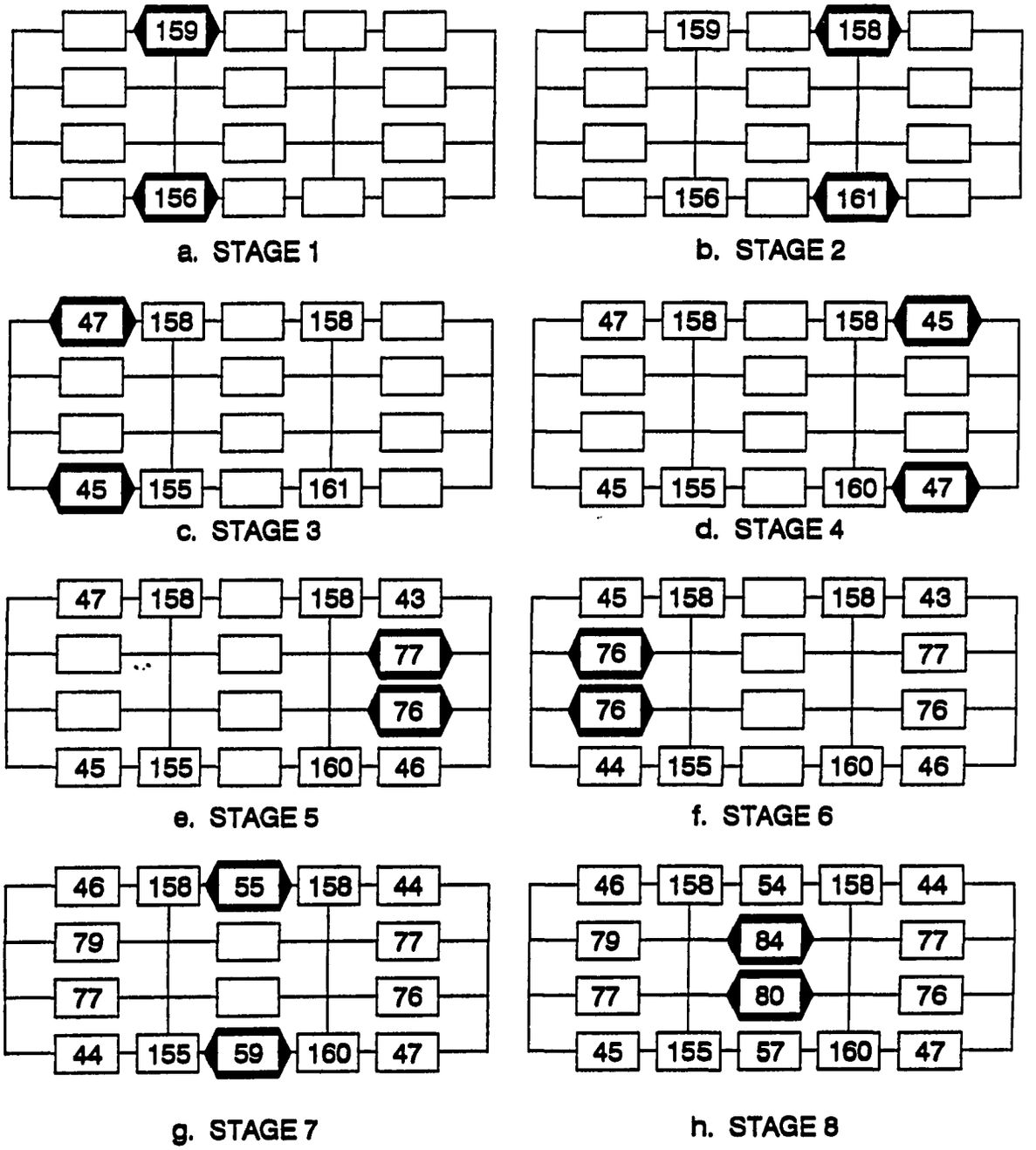

Fig. 3.15. Actual strengthening forces (kips) applied per stage.

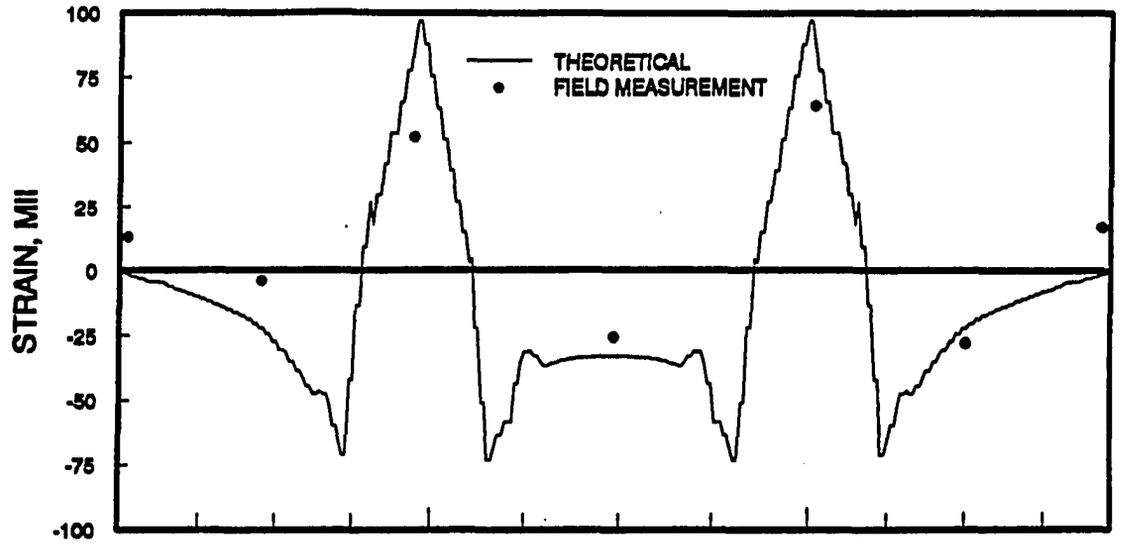

a. EXTERIOR STRINGER

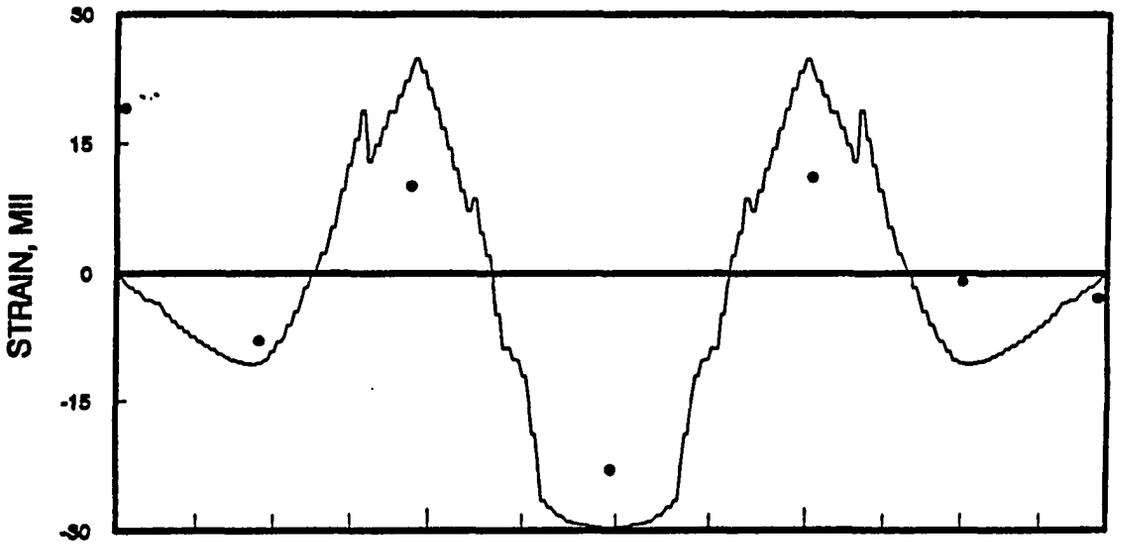

b. INTERIOR STRINGER

Fig. 3.16. Bottom-flange stringer strains: Stage 2 strengthening.

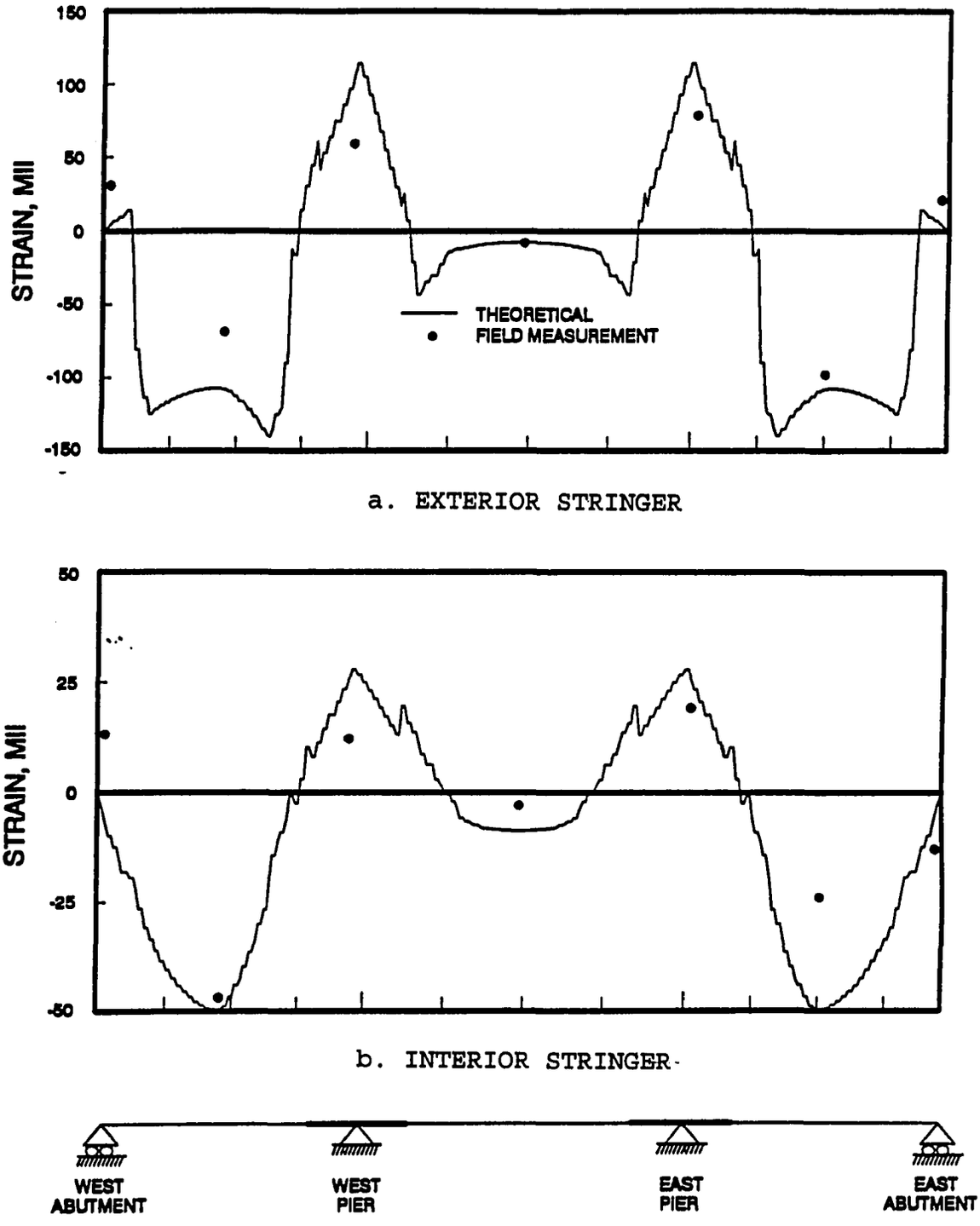

Fig. 3.17. Bottom-flange stringer strains: Stage 4 strengthening.

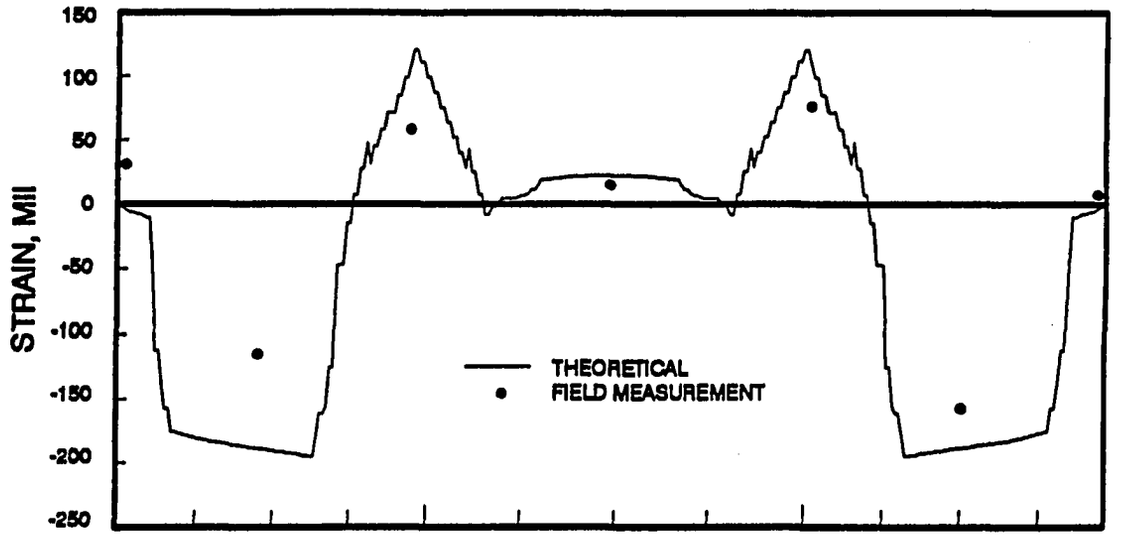

a. EXTERIOR STRINGER

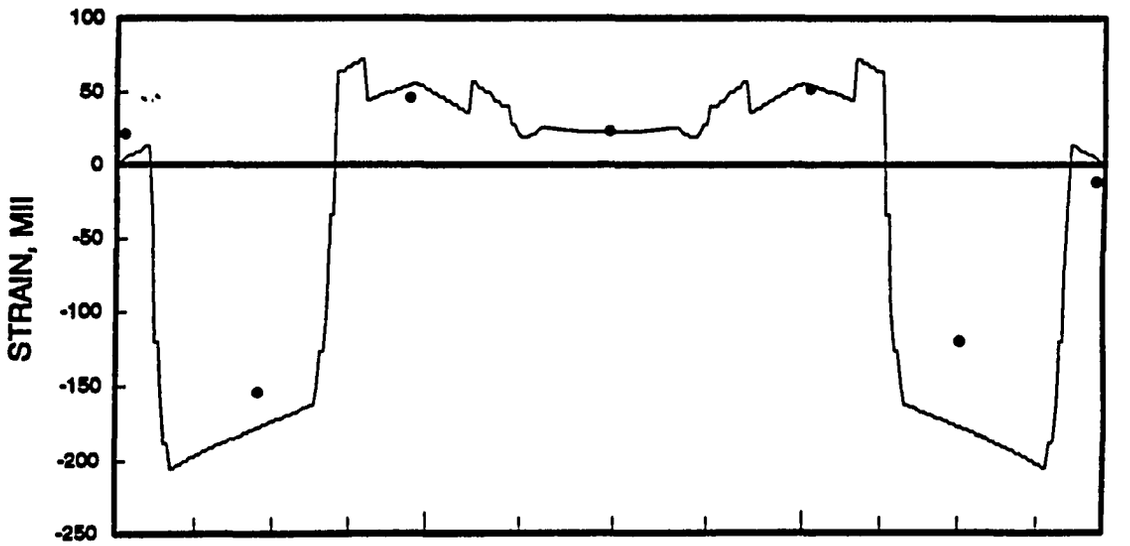

b. INTERIOR STRINGER

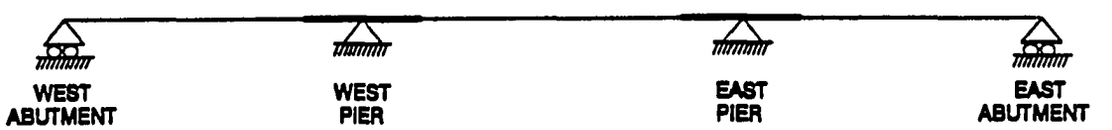

Fig. 3.18. Bottom-flange stringer strains: Stage 6 strengthening.

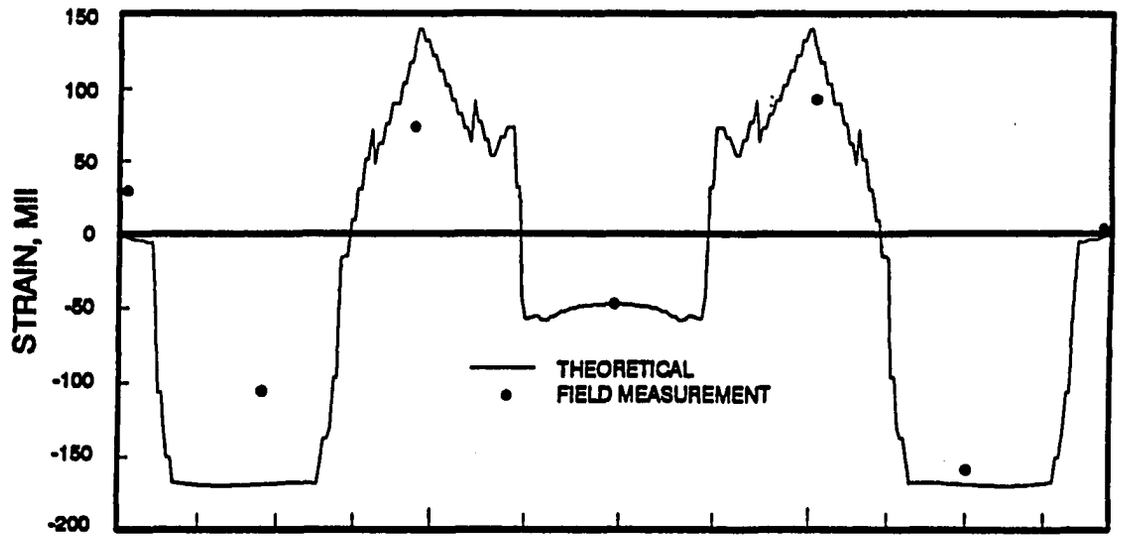

a. EXTERIOR STRINGER

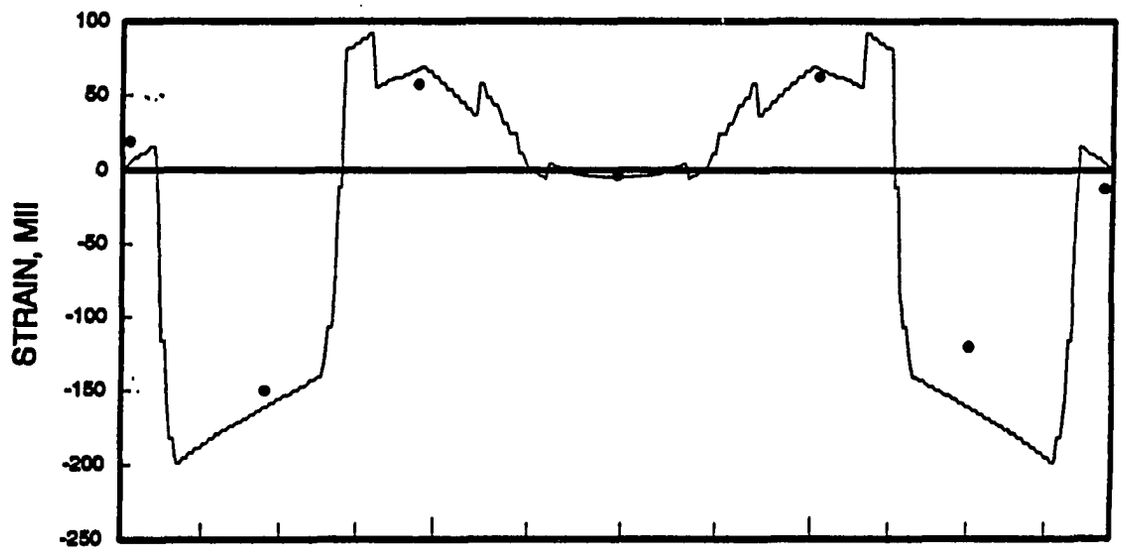

b. INTERIOR STRINGER

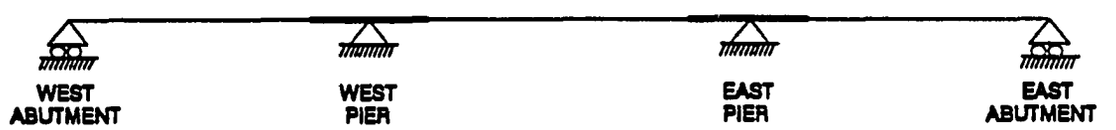

Fig. 3.19. Bottom-flange stringer strains: Stage 7 strengthening.

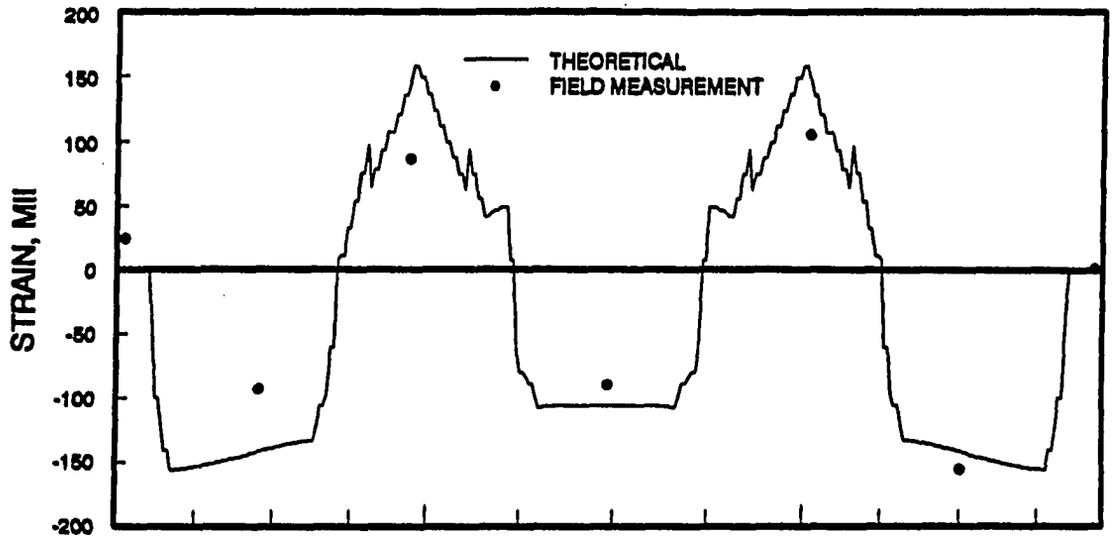

a. EXTERIOR STRINGER

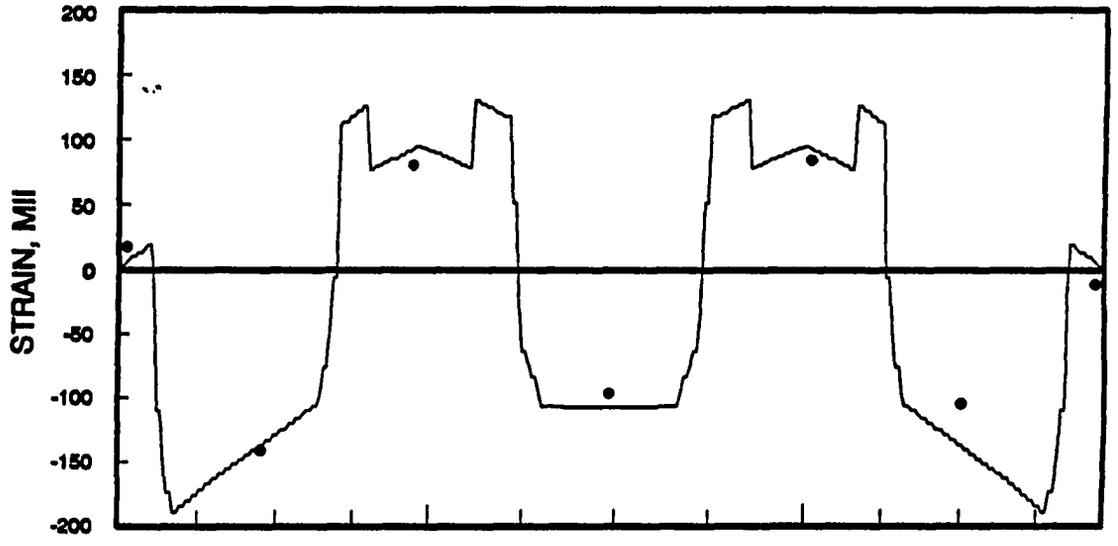

b. INTERIOR STRINGER

Fig. 3.20. Bottom-flange stringer strains: Stage 8 strengthening.

respectively. Note that different vertical scales have been used for each figure.

Each field strain shown in the figures was calculated by averaging four strain gage readings associated with the pairs of interior and exterior stringers, respectively. In other words, the four strains for the two exterior stringers were averaged as well as the four strains for the interior stringers.

The theoretical strains assume roller supports at the abutments as indicated by the zero strains shown at the west and east abutments in all of the theoretical curves. The figures indicate that field strains occurred at the abutments during strengthening. Note that these strains are measured 15 in. from the centerline of the abutments. Also, inherent end restraint existed due to continuity between the deck and the abutment.

Further review of the figures indicates that the west abutment strains were larger than the east abutment strains. This result is consistent for both interior and exterior stringers throughout all strengthening stages. Although the abutment bearings were cleaned and treated with a silicone spray prior to testing, it is possible that some of the bearing pads were not moving freely. Crack monitors were attached at each abutment bearing location and monitored during the strengthening process. Data from the crack monitors indicated that the bearing pads did slide relative to one another. Therefore, most of the strain at the abutments is the result of rotational restraint.

Figure 3.16 shows the strains with the truss system completely activated (Stages 1 and 2). The purpose of the superimposed trusses was to apply upward forces that induce moments to oppose the moments induced by live load. Therefore, negative (compressive) bottom-flange strains due to live load should be opposed by a positive (tensile)

strain from the trusses. The magnitude of the desired positive strain from the trusses was determined using the finite element model discussed earlier; 87 MII (micro-in. per in.) on the exterior stringers and 24 MII on the interior stringers. However, the average strain achieved by the truss system was 58 MII and 11 MII for the exterior and interior stringers, respectively. Therefore, the actual strain applied on the exterior stringer was 67% of the predicted value.

Part of this discrepancy at the piers can be attributed to the way that the finite element model simulated the truss uplift points on the bridge. The model assumed a concentrated force acting at the contact point, when in fact the force was distributed over an area of eight in. x eight in. (i.e., the area of the 1/2 in. bearing plate). This assumption thus overestimates the analytical strains in the vicinity of the pier.

The superimposed truss system also introduced beneficial strains in the positive moment regions due to longitudinal distribution. The experimental results for these midspan regions agree well with the predicted values at all but two locations; the west span in Fig. 3.16a and the east span in Fig. 3.16b. These experimental data are questionable. Review of the figures shows that the strain at these two locations was always significantly below the predicted values.

Figure 3.20 displays the final strain profiles for the completely strengthened bridge. The midspan strains were, on the average, 88.4% of the predicted values. Bottom-flange strains at the piers were 76.8% of the predicted values. Considering interior stringers only, this value is 88.5%.

Several factors contributed to the differences between the actual and theoretically predicted values. Significant

guardrail strains were observed, which shows that the bridge guardrails carry a portion of the applied loads. This can be explained by the fact that the guardrails along with the exterior stringers are acting as vierendeel trusses along the side of the bridge. Another important factor is the existence of end-restraint at the abutments due to the connection between the abutment and slab reinforcement.

The guardrails were not modeled as structural elements in the finite element model because they are usually not considered in the rating procedure for these bridges under vertical loads. Also, the contribution of end restraint was not taken into account in the theoretical model since the amount of end restraint is variable and can not be predicted.

In general, the field results show good agreement with the finite element model. The strains predicted by the finite element model were closer to the field results in case of the post-tensioning system than in case of the superimposed trusses.

4. DEVELOPMENT OF A STRENGTHENING DESIGN METHODOLOGY

The objective of developing a design methodology was to provide the practicing engineer with a simple method for computing the axial forces and moments (and consequently stresses) induced in the bridge stringers when subjected to the strengthening forces without having to perform a finite element analysis. To allow flexibility in design, the strengthening system (i.e., post-tensioning and superimposed trusses) was divided into the five strengthening schemes shown in Fig. 4.1. Each of these strengthening schemes was treated separately. The design methodology as developed has the practicing engineer compute the axial forces and moments along the lengths of the bridge stringers due to each strengthening scheme separately and add them to obtain the final axial forces and moments. This allows the designer the flexibility of using any combination of these five schemes to achieve the required stress reduction in the bridge stringers.

The procedure for determining the axial forces and moments in the bridge stringers due to the strengthening system can be summarized in the following steps:

1. The axial forces and moments on the total bridge section are computed by analyzing the bridge using "continuous beam analysis" as described in Sec. 4.1.
2. The axial forces and moments on the individual stringers are computed using force and moment distribution fractions. The definition of these distribution fractions and the development of formulas for their computation are described in Sec. 4.2.

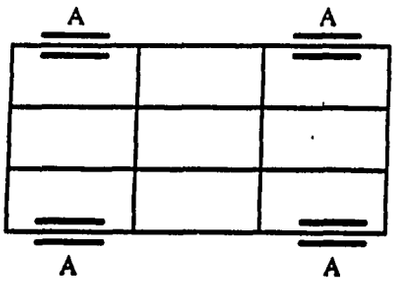

a. STRENGTHENING SCHEME [A]: POST-TENSIONING END SPANS OF THE EXTERIOR STRINGERS

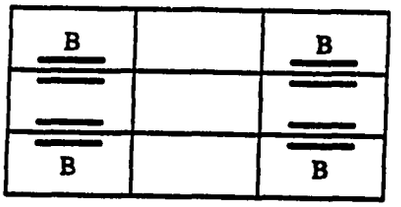

b. STRENGTHENING SCHEME [B]: POST-TENSIONING END SPANS OF THE INTERIOR STRINGERS

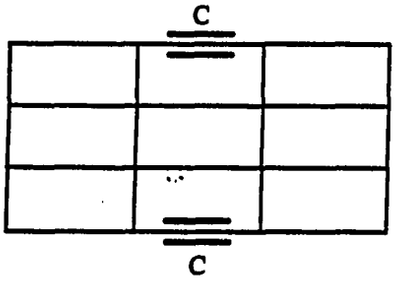

c. STRENGTHENING SCHEME [C]: POST-TENSIONING CENTER SPANS OF THE EXTERIOR STRINGERS

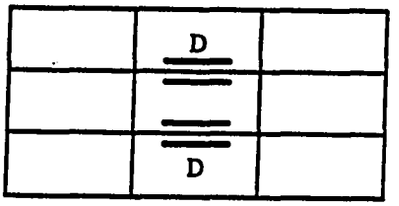

d. STRENGTHENING SCHEME [D]: POST-TENSIONING CENTER SPANS OF THE INTERIOR STRINGERS

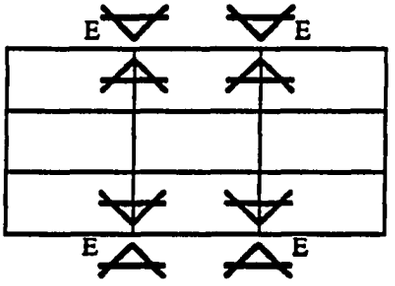

e. STRENGTHENING SCHEME [E]: SUPERIMPOSED TRUSSES AT THE PIERS OF EXTERIOR STRINGERS

Fig. 4.1. Various locations of post-tensioning and superimposed trusses.

4.1. Computation of axial forces and moments on the total bridge section

The axial force acting on the total bridge section is equal to the post-tensioning force in the post-tensioned portions of the bridge spans and equal to zero at other locations. The computation of the total moment on the bridge section at a certain location is more difficult due to the indeterminancy of the bridge model.

In order to develop a simple method for computing the moments on the total bridge section along the bridge length, the author analyzed a number of continuous-span bridges using two methods of analysis. In the first method, the bridges were analyzed using the finite element model developed in Chapter 2. In the second method, each bridge was analyzed as a continuous beam with inertias equal to those of the total bridge composite section at the different locations. A comparison between the results of the two types of analysis for these bridges showed that the difference between the moments computed using the two methods did not exceed 7% at most locations. Fig. 4.2 is a representative sample which shows the results of the two types of analysis for a typical continuous span bridge due to the effect of strengthening scheme [C]. It should be noted that no vertical scale is provided in the figure since the comparison is independent of the magnitude of the strengthening forces. It was therefore determined that the moments on the total bridge section can be determined using a "continuous-beam analysis" with good accuracy.

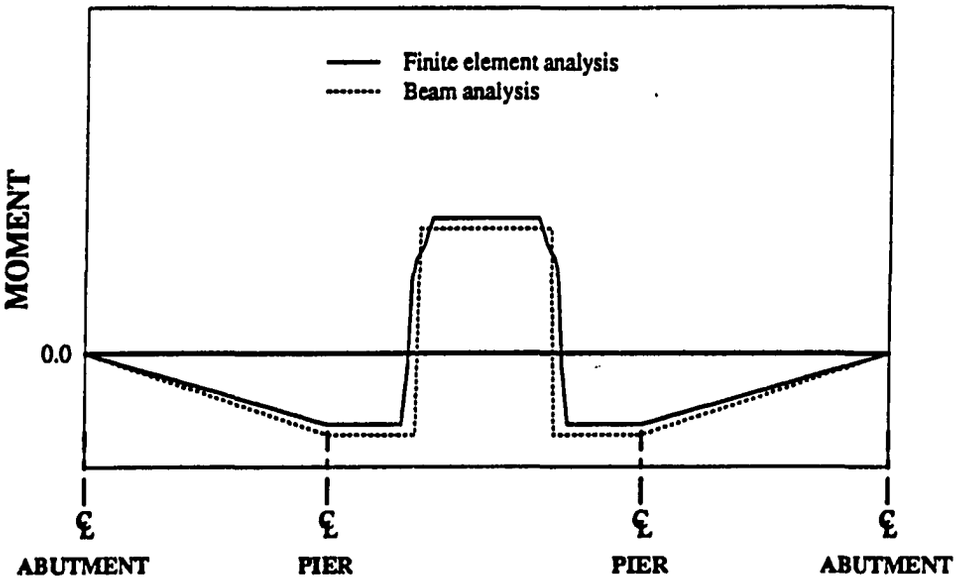

Fig. 4.2. Total moments on the bridge section: Strengthening scheme [C].

4.2. Computation of axial forces and moments on the individual bridge stringers

In order to simplify these computations, the force and moment diagrams on the individual stringers resulting from the finite element analysis of the bridge model were idealized into a number of straight line segments. The segments are defined by a number of critical sections on the axial force and moment diagrams. The positions of the critical sections have been chosen so that the idealized diagrams represent the actual axial forces and moments on the stringers very closely. Fig. 4.3 is a representative sample which shows this idealization for strengthening scheme [A]. It should be noted that no vertical scale is provided in this figure as the force and moment fractions are independent of the magnitude of the strengthening force and the axial forces and moments developed in the stringers.

As mentioned in Chapter 2, the AASHTO Standard Specifications for Highway Bridges [23] provides the designer with wheel-load fractions to compute the distribution of the vertical truck loads to the exterior and interior stringers. In this section, distribution fractions are developed to describe the distribution of the axial forces and moments induced by the post-tensioning system and the superimposed trusses to the various bridge stringers. The definition of the distribution fractions is presented in Sec. 4.2.1. The development of regression formulas for the computation of the distribution fractions is described in Sec. 4.2.2.

4.2.1. Definition of force and moment fractions

The force (or moment) distribution fractions at the critical sections are defined as follows:

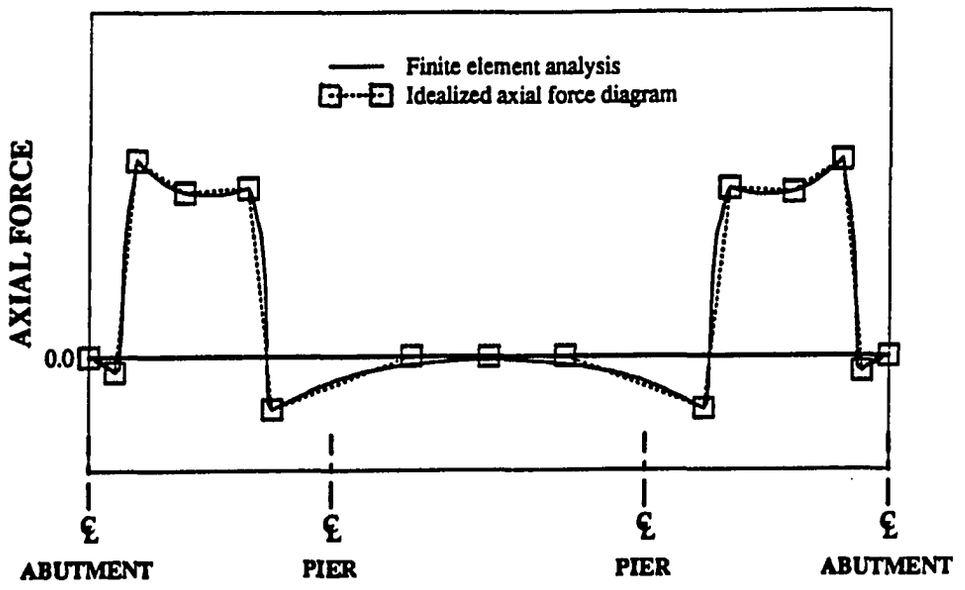

a. AXIAL FORCE ON EXTERIOR STRINGER

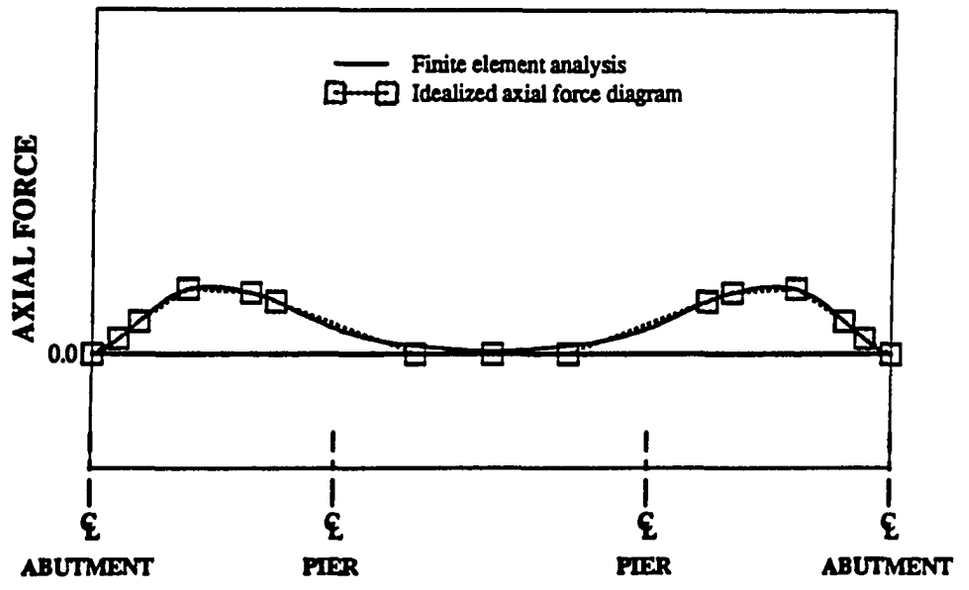

b. AXIAL FORCE ON INTERIOR STRINGER

Fig. 4.3. Idealization of axial force and moment diagrams on the stringers due to the strengthening system: Strengthening scheme A.

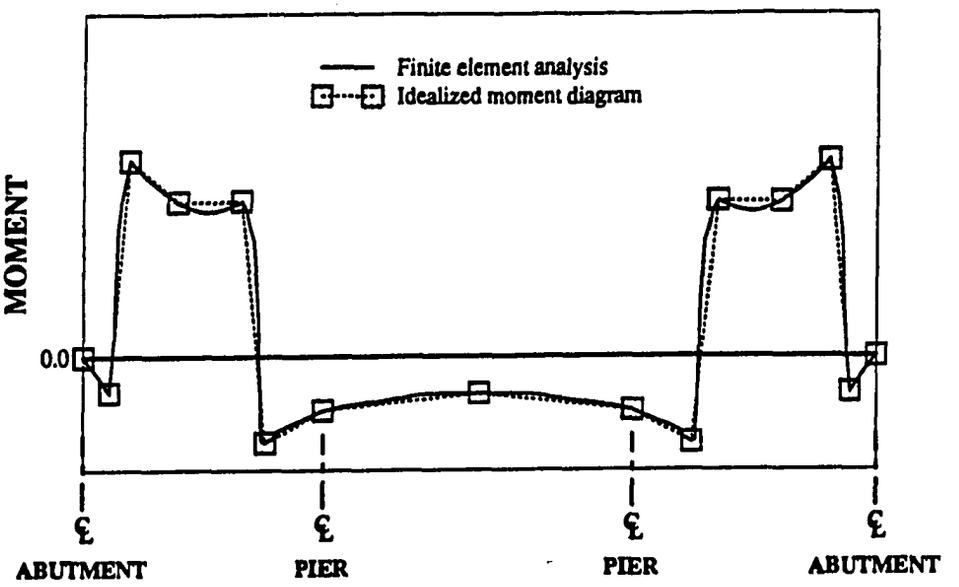

c. MOMENT ON EXTERIOR STRINGER

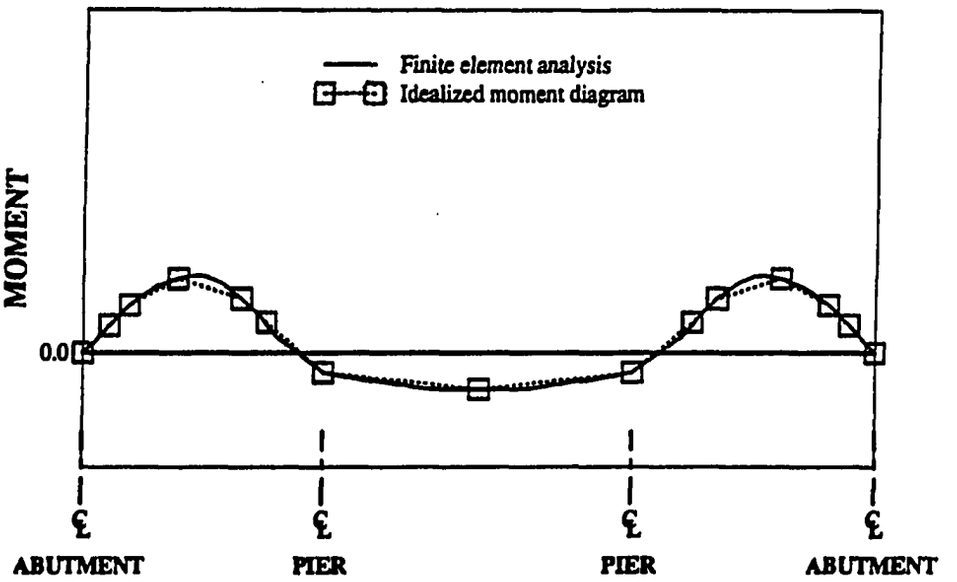

d. MOMENT ON INTERIOR STRINGER

Fig. 4.3. Continued.

1. For strengthening schemes A, C, and E:

   Force fraction at sec (i) =

$$\frac{\text{Axial force in the exterior stringers at sec (i)}}{\text{Total axial force on the bridge at sec (i)}}$$

   Moment fraction at sec (i) =

$$\frac{\text{Moment in the exterior stringers at sec (i)}}{\text{Total moment on the bridge at sec (i)}}$$

2. For strengthening schemes B, and D:

   Force fraction at sec (i) =

$$\frac{\text{Axial force in the interior stringers at sec (i)}}{\text{Total axial force on the bridge at sec (i)}}$$

   Moment fraction at sec (i) =

$$\frac{\text{Moment in the interior stringers at sec (i)}}{\text{Total moment on the bridge at sec (i)}}$$

Figure 4.4 is a representative sample which illustrates the axial force and moment diagrams on the bridge stringers resulting from the finite element analysis due to strengthening scheme [A], i.e., post-tensioning forces in the end-spans of the exterior stringers. Similar to Fig. 4.2, no vertical scale is provided. As shown in the figure, four critical sections were chosen for the computation of axial force fractions and six critical locations were chosen for the computation of moment fractions. The choice of these critical locations was done so that axial forces and moments computed at these sections would be sufficient for the reconstruction of the axial force and moment diagrams along the lengths of the stringers. The locations chosen for the computation of the force and moment fractions for strengthening schemes [A through E] are given in Figs. A.1 to A.5 of Appendix A.

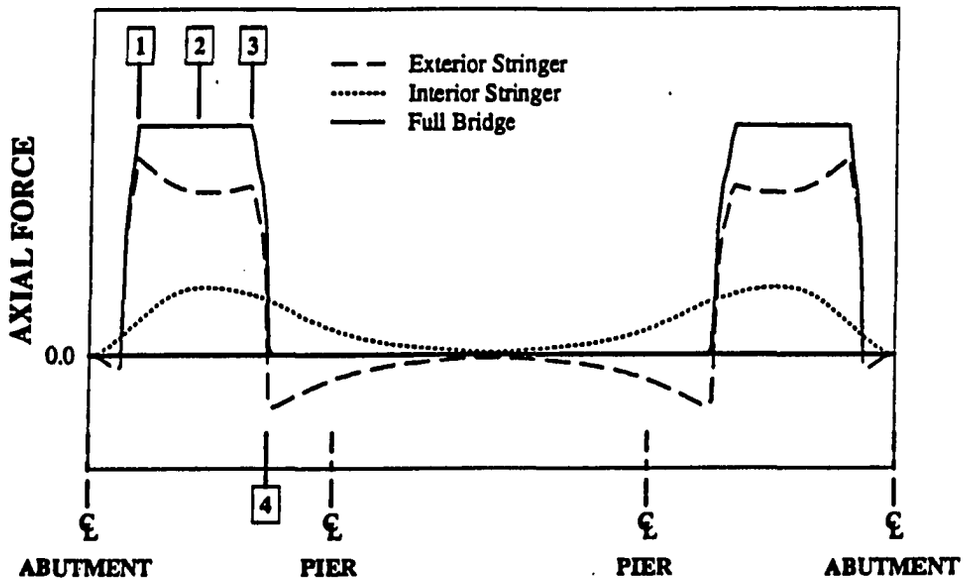

a. AXIAL FORCE

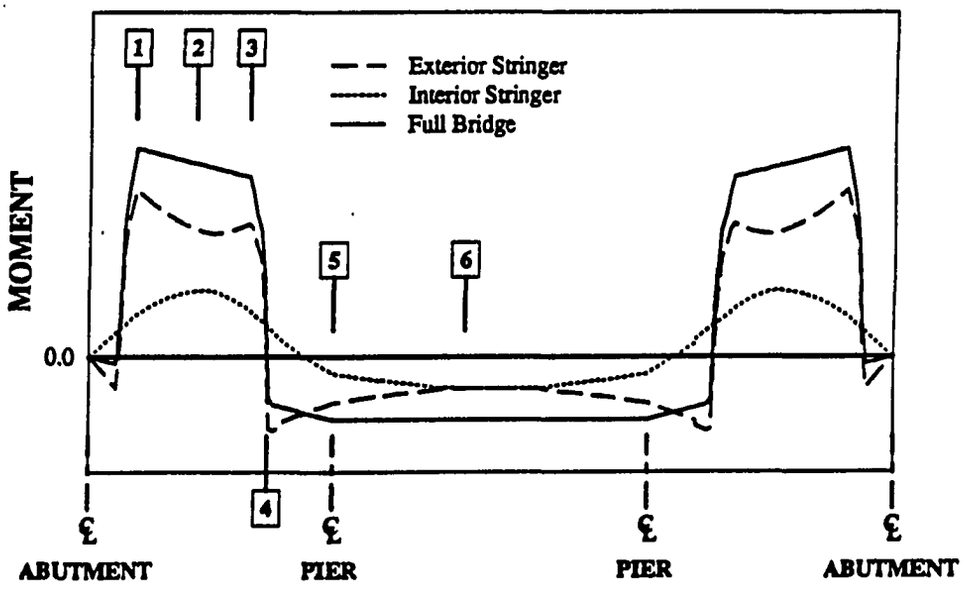

b. MOMENT

Fig. 4.4. Locations of distribution fractions: Strengthening scheme [A].

4.2.2. Development of force and moment fraction formulas

In order to develop regression formulas for the force and moment fractions, several bridges were modeled and analyzed using the finite element model developed in Chapter 2. The bridges analyzed included both standard Iowa DOT bridges and nonstandard bridges.

The standard bridges analyzed were of the V12 and V14 Iowa DOT standard bridge series. Analysis runs were performed for these bridges utilizing variable tendon lengths for each of the five strengthening schemes shown in Fig. 4.1. The analysis runs performed on the standard bridges are listed in Table 4.1.

The non-standard bridge models were developed by changing some of the dimensions of the standard Iowa DOT bridges within practical limits. As in case of the standard bridges, analysis runs were performed for the non-standard bridges utilizing variable tendon lengths for each of the strengthening schemes. The analysis runs performed on the non-standard bridges are listed in Table 4.2.

As shown in Tables 4.1 and 4.2, a total of 2400 analysis runs were performed. 1200 analysis runs were performed for the Iowa DOT standard bridges and 1200 analysis runs were performed for the non-standard bridges.

For each of the above-mentioned analysis runs, the finite element results were used to compute force and moment distribution fractions at the critical locations. The computation of the distribution fractions is illustrated in Tables 4.3 and 4.4. Table 4.3 is an extract from the output file resulting form the finite element analysis of a V12-2 standard Iowa DOT bridge due to post-tensioning forces of 1000 kips applied to the end-spans of the exterior stringers (i.e., strengthening scheme [A]). It should be noted that the (1000 kips) force value is arbitrarily chosen since the

Table 4.1. Iowa DOT standard bridge models included in regression analysis for distribution fractions.

Iowa DOT Series (Date)	V12 (1957)	V14 (1960)
Number of stringers/ Number of lanes	4/2	4/2
Design Live Load	H-15	H-20
Total bridge lengths, ft	125, 150, 175, 200, 250, 300	125, 150, 175, 200, 225, 250
Skew	0°, 15°, 30°, 45°	0°, 15°, 30°, 45°
No. of strengthening schemes *	5	5
No. of runs/scheme on each bridge (variable tendon lengths)	5	5
Total no. of runs	600	600

* See Fig. 4.1.

Table 4.2. Non-standard bridge models. (Developed by changing some of the dimensions of the Iowa DOT standard bridges).

Iowa DOT Series (Date)		V12 (1957)	V14 (1960)
Non-standard dimension	Slab thickness	8 in., 10 in.	8 in., 10 in.
	Stringer spacing	6 ft, 9 ft	8 ft, 11 ft
	Center-span length / End-span length	1.0, 1.1, 1.2, 1.4, 1.5	1.0, 1.1, 1.2, 1.4, 1.5
	I_{ext} * / I_{int}	1.0	1.0
Total bridge lengths, ft		125, 200, 300	125, 175, 250
Skew		0°, 45°	0°, 45°
No. of strengthening schemes **		5	5
No. of runs/scheme on each bridge (variable tendon lengths)		2	2
Total no. of analysis runs		600	600

* I_{ext}: Inertia of the exterior stringer composite section.
I_{int}: Inertia of the interior stringer composite section.

** See Fig. 4.1.

Table 4.3. Finite element analysis results: V12-2 standard Iowa DOT bridge, Strengthening scheme [A], Post-tensioning force = 1000 kips, Tendon length / Span length = 0.61 .

Axial forces at the critical sections				
* Critical section	Distance from support (in.)	Axial force (kips)		
		Exterior Stringer	Interior Stringer	Total Bridge Section
1	108.13	856	144	1000
2	229.38	710	290	1000
3	360.63	733	267	1000
4	416.88	-231	231	---
Moments at the critical sections				
* Critical section	Distance from support (in.)	Moment (in. kips)		
		Exterior Stringer	Interior Stringer	Total Bridge Section
1	108.13	14546	3614	18160
2	229.38	11294	5653	16947
3	360.63	11570	4064	15634
4	416.88	6454	2107	4167
5	549	4032	-1457	5489
6	900	2756	-2734	5490

* See Fig. 4.4.

Table 4.4. Computation of force and moment fractions:
V12-2 standard Iowa DOT bridge,
Strengthening scheme [A],
Post-tensioning force = 1000 kips,
Tendon length / Span length = 0.61 .

Computation of force fractions		
Critical Section *	Distance from support (in.)	Force Fraction
1	108.13	856 / 1000 = 0.856
2	229.38	710 / 1000 = 0.710
3	360.63	733 / 1000 = 0.733
4	416.88	231 / 1000 = 0.231
Computation of moment fractions		
Critical Section *	Distance from support (in.)	Moment Fraction
1	108.13	14546 / 18160 = 0.801
2	229.38	11294 / 16947 = 0.666
3	360.63	11570 / 15634 = 0.740
4	416.88	6454 / 4167 = 1.549
5	549	4032 / 5489 = 0.735
6	900	2756 / 5490 = 0.502

* See Fig. 4.4.

distribution fractions are independent of the magnitude of the strengthening force. Table 4.4 illustrates the use of the output results in Table 4.3 for the computation of force and moment distribution fractions.

All bridges were analyzed with the tendons positioned at an elevation of 3 1/2 in. above the top surface of the bottom flange. The effect of changing the elevation of the tendons above the top surface of the bottom flange in the range of 3 in. to 5 in. was investigated. The results revealed that this change in elevation has a minimal effect on the force and moment fractions. Thus, the force and moment fractions determined in this investigation are valid for elevations above the bottom flange in this range.

The statistical analysis software package, SAS, was used to perform the regression analysis. A program was prepared on SAS utilizing the standard SAS routine "PROC.REG". This standard SAS routine performs several iterations of the regression analysis to eliminate the least significant variables in each regression equation.

The program uses input files containing the various bridge parameters and the force and moment distribution fractions for the analyses performed. The program output contains the coefficients of the different parameters in the regression formulas. It also includes the coefficient of determination (R^2) and the error range for each formula. Table 4.5 is an extract from the input files used by the program. Table 4.6 is an extract from the program output.

As mentioned earlier in this Section, the bridges analyzed using the ANSYS finite element model included both standard Iowa DOT bridges and non-standard bridges. When developing regression formulas for the force and moment fractions, it was found more practical to develop the formulas only for the standard bridges; this limitation resulted in formulas which are both more accurate and

Table 4.5. Input data* for the regression analysis: Strengthening scheme [A], Force Fraction at section 1.

Finite Element Analysis Run No.	Independent variables			Dependent variable
	X_L	X_S	X_{P1}	Strengthening scheme [A] : FF1
1	0.652	0.645	0.923	0.259
2	0.652	0.645	0.811	0.250
3	0.652	0.645	0.700	0.253
4	0.652	0.645	0.589	0.222
5	0.978	0.645	0.923	0.263
6	0.978	0.645	0.811	0.254
7	0.978	0.645	0.700	0.242
8	0.978	0.645	0.589	0.224

* This data is part of the data included in the input files used for the SAS regression analysis performed to develop a formula for the force fraction at critical section (1) in case of strengthening scheme [A].

Table 4.6. Regression analysis output,
Strengthening scheme A, Force Fraction at Sec. 1.

Model: MODEL A
Dependent Variable: FF1

Analysis of Variance

Source	DF	Sum of Squares	Mean Square	F Value	Prob>F
Model	3	0.06788	0.02263	647.188	0.0001
Error	32	0.00112	0.00003		
C Total	35	0.06900			

Root MSE	0.00591	R-square	0.9838
Dep Mean	0.83389	Adj R-sq	0.9823
C.V.	0.70905		

Parameter Estimates

Variable	DF	Parameter Estimate	Standard Error	T for H0: Parameter=0	Prob > |T|
INTERCEP	1	0.165999	0.03500144	4.743	0.0001
1/XS	1	0.417187	0.02130132	19.585	0.0001
1/XL	1	0.049060	0.00203238	24.139	0.0001
XP1	1	-0.103535	0.01488908	-6.954	0.0001

simple. The formulas were therefore developed for the standard Iowa DOT V12 and V14 series [26,27] which are summarized in Table 4.1.

A sensitivity study was conducted to determine the parameters which significantly affect the largest number of force and moment fractions. The parameters investigated included bridge length, angle of skew, end-span to center-span length ratio, deck thickness, stringer spacing, stringer moments of inertia (composite and noncomposite) and the ratio of the post-tensioned portion of the span to the span length for the various strengthening schemes. To simplify the formulas, the bridge variables were put in the form of dimensionless parameters as follows:

$$X_L = 0.0167 \times \frac{\textit{Total bridge length}}{\textit{Stringer spcaing}} + 0.3$$

$$X_S = 9.0 \times \frac{\textit{Deck thickness}}{\textit{Stringer spacing}}$$

$$X_{P1} = 1.5 \times \frac{\textit{Length of post-tensioned portion of end span}}{\textit{Length of end span}}$$

$$X_{P2} = 1.5 \times \frac{\textit{Length of post-tensioned portion of center span}}{\textit{Length of center span}}$$

$$X_{P3} = 1.5 \times \frac{\textit{Length of superimposed truss tendon}}{\textit{Length of end span}}$$

$$X_R = \frac{\textit{Length of center span}}{\textit{Length of end span}}$$

$$X_K = \frac{\textit{Angle of skew (in degrees)}}{90}$$

$$X_I = \frac{\textit{Moment of inertia of full composite section of exterior stringer}}{\textit{Moment of inertia of full composite section of interior stringer}}$$

Statistical tests were performed to determine the effect of each parameter on the various force and moment fractions. The coefficient of determination, R^2 was used as a measure of the prediction accuracy of the formulas. As a result of these tests, some of the variables considered were excluded from the final regression analysis. Table 4.7 shows the elimination process for the variable X_I. As shown in the table, the change in the coefficient of determination when adding X_I to the regression variables was computed for each formula. This change was less than 5% for all formulas, and less than 2% for most formulas. For formulas in which the percentage change in R^2 was more than 2%, the change in error range due to X_I was checked and was found insignificant. It was therefore determined that the variable X_I does not have a significant effect on the prediction accuracy of the developed formulas. X_I was therefore not included in the final regression analysis.

After performing several tests on the various parameters and combinations thereof, the parameters X_R, X_K, and X_I were eliminated. The variables X_L, X_S, X_{P1}, X_{P2}, and X_{P3} were found to have a significant effect on most distribution fractions, and were therefore chosen for the final regression analysis. Fig. 4.5 illustrates the bridge dimensions used for computing these parameters.

It should be noted that some of the variables excluded from the regression analysis were eliminated because their variation within the limits of the standard Iowa bridges is small and therefore their effect on the variation of the distribution fractions was insignificant (e.g. X_R values range from 1.25 to 1.35 for the V12 and V14 standard Iowa

Table 4.7. Effect of variable X_I on the accuracy of the developed regression formulas.

Strengthening scheme *	Distribution fraction **	Coefficient of determination, R^2		Change in R^2 due to X_I
		Formulas developed using X_L, X_S, X_{P1}, X_{P2}, and X_{P3}	Formulas developed using X_L, X_S, X_{P1}, X_{P2}, X_{P3}, and X_I	
A	FF1	98.38 %	98.58 %	0.20 %
	FF2	97.33 %	98.09 %	0.76 %
	FF3	97.31 %	97.48 %	0.17 %
	FF4	96.24 %	97.33 %	1.09 %
	MF1	98.33 %	99.61 %	1.28 %
	MF2	98.62 %	99.20 %	0.58 %
	MF3	98.16 %	98.71 %	0.55 %
	MF4	99.51 %	99.72 %	0.21 %
	MF5	98.24 %	98.45 %	0.21 %
	MF6	95.79 %	99.53 %	3.74 %
B	FF1	96.13 %	97.75 %	1.62 %
	FF2	95.79 %	97.32 %	1.53 %
	FF3	96.32 %	97.52 %	1.20 %
	FF4	96.87 %	97.51 %	0.64 %
	MF1	95.50 %	99.04 %	3.54 %
	MF2	96.06 %	99.59 %	3.53 %
	MF3	93.01 %	95.31 %	2.30 %
	MF4	99.47 %	99.59 %	0.12 %
	MF5	98.34 %	98.90 %	0.56 %
	MF6	95.48 %	98.84 %	0.36 %
C	FF1	83.79 %	84.03 %	0.24 %
	FF2	92.96 %	93.23 %	0.27 %
	FF3	93.20 %	93.87 %	0.67 %
	MF1	99.52 %	99.54 %	0.02 %
	MF2	93.01 %	93.32 %	0.31 %
	MF3	97.53 %	97.86 %	0.33 %
	MF4	98.08 %	98.35 %	0.27 %
D	FF1	87.94 %	88.61 %	0.67 %
	FF2	90.76 %	91.93 %	1.17 %
	FF3	89.55 %	91.73 %	2.18 %
	MF1	96.23 %	97.30 %	1.07 %
	MF2	95.45 %	95.48 %	0.03 %
	MF3	92.84 %	97.81 %	4.97 %
	MF4	94.01 %	96.92 %	2.91 %
E	MF1	99.68 %	99.91 %	0.23 %
	MF2	97.15 %	97.29 %	0.14 %
	MF3	99.71 %	99.89 %	0.18 %
	MF4	99.30 %	99.58 %	0.28 %
	MF5	99.68 %	99.75 %	0.07 %

* See Fig. 4.1. ** See Figs. A.1. through A.5 of Appendix A.

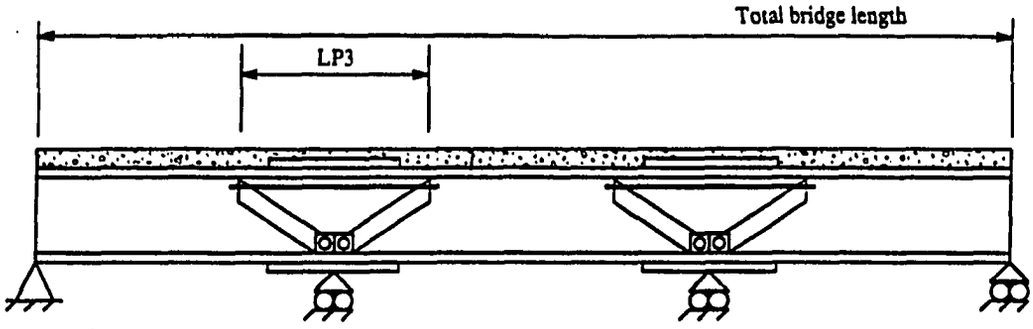

a. SUPERIMPOSED TRUSSES (EXTERIOR STRINGERS)

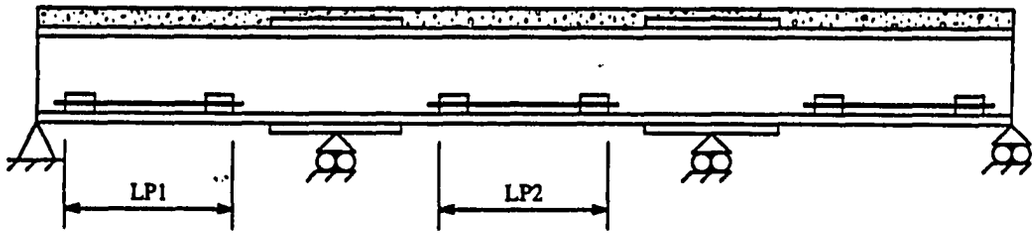

b. POST-TENSIONING (EXTERIOR AND INTERIOR STRINGERS)

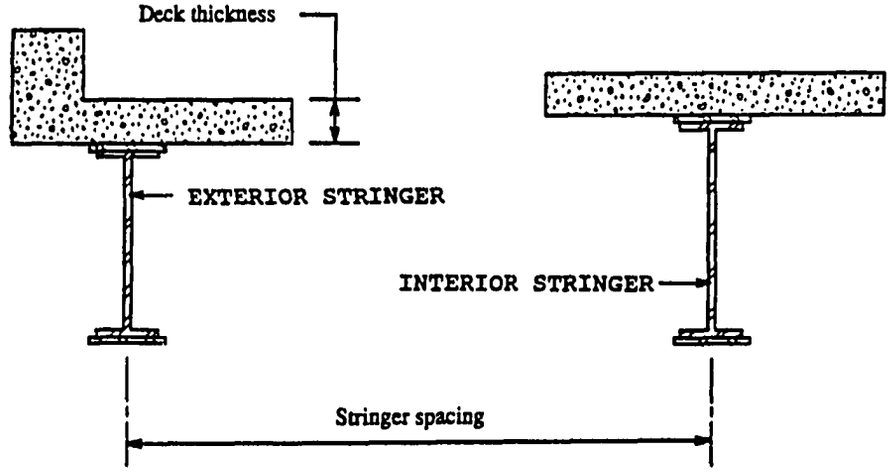

c. PARTIAL CROSS-SECTION

Fig. 4.5. Regression formula variables.

DOT bridges). It is therefore recommended not to use these distribution fraction formulas for bridges whose properties are significantly different from those of the standard Iowa DOT bridges listed in Table 4.1.

The final regression analysis was performed using the chosen parameters X_L, X_S, X_{P1}, X_{P2}, and X_{P3}. The formulas developed for the force and moment fractions for each strengthening scheme are listed in Tables A.1 through A.9 of Appendix A. In developing each formula, the author attempted to minimize the number of terms, while obtaining good accuracy (generally, coefficients of determination, R^2 >> 90%). In a few formulas, this was not possible, especially in case of the fractions with very low average values. Nevertheless, the error range was small enough in these formulas so that the effect on the forces or moments computed at that section is generally very small.

As shown in Appendix A, the error range is generally less in the moment fractions than in the force fractions. This further minimizes the errors in the design methodology as the moment fractions have a greater effect on the final stringer stresses.

Limits have been provided for the variables, and for the force and moment fractions computed using the regression formulas. Variables and the computed force and moment fractions of the Iowa standard V12 and V14 series bridges are well within the established limits. For bridges with lengths, widths, etc, that vary significantly from those of the standard bridges, the formulas do not give accurate force and moment fractions. In these cases, it is strongly recommended that a finite element analysis be performed to determine the axial forces and moments in the bridge stringers.

4.3. Accounting for approximation errors and post-tensioning losses

As previously described, several approximations have been made to provide the designer with a simplified procedure for determining the response of the bridge to the strengthening system, and for designing the required strengthening system. Although the errors resulting from these approximations are small, their collective effect might be significant in some cases. A method of accounting for these errors is suggested in this Section.

Potential sources of error in the design methodology developed are summarized below:

- The assumption that the moments in the bridge are equal to those obtained from the analysis of the bridge as a continuous beam with equivalent moments of inertia.
- Idealizing the axial force and moment diagrams as diagrams composed of straight line segments.
- Errors in the force and moment fractions obtained using the regression formulas.
- Post-tensioning losses such as:
  - Steel relaxation.
  - Concrete creep.
  - Temperature differential between the tendons and the bridge.
  - Anchor seating.

Due to the complexity of the design procedure, and the large number of formulas, it is difficult to account for the errors in the regression formulas using the error limits corresponding to each formula. In order to account for these losses and approximation errors, it is recommended to increase all strengthening forces by a conservative percentage; an 8% increase is recommended. The designer must check that the stringer stresses based on the original

strengthening forces and the increased strengthening forces are both within the allowable limits.

4.4. Recommended design procedure

This section describes the various steps required in the design of a strengthening system for a typical continuous-span, composite bridge. It should be noted that this procedure is not intended to be a detailed explanation of the design process but rather a summary of the basic steps involved. A detailed example is given in Chp. 5 to illustrate the use of this procedure in designing a strengthening system for a typical continuous span composite bridge.

A LOTUS 1-2-3 spreadsheet was developed to assist the engineer with designing the required strengthening system. The spreadsheet calculates the required strengthening forces and provides the designer with the final stress envelopes of the bridge stringers. The use and organization of the spreadsheet are presented in detail in Chp. 5.

A few of the steps outlined must be completed by the user; however the majority of the steps are performed by the spreadsheet. Fig. 4.6 illustrates the steps of the design procedure. To determine the configuration of the strengthening system and the required tendon forces, the following procedure is suggested:

1. Load the spreadsheet "STRCONBR.WK1" into LOTUS 1-2-3, and become familiar with the different sections of the spreadsheet. All spreadsheet sections have a "HELP" area provided for guidance.
2. Determine section properties of the exterior and interior stringers for the following sections:
   - Steel beam

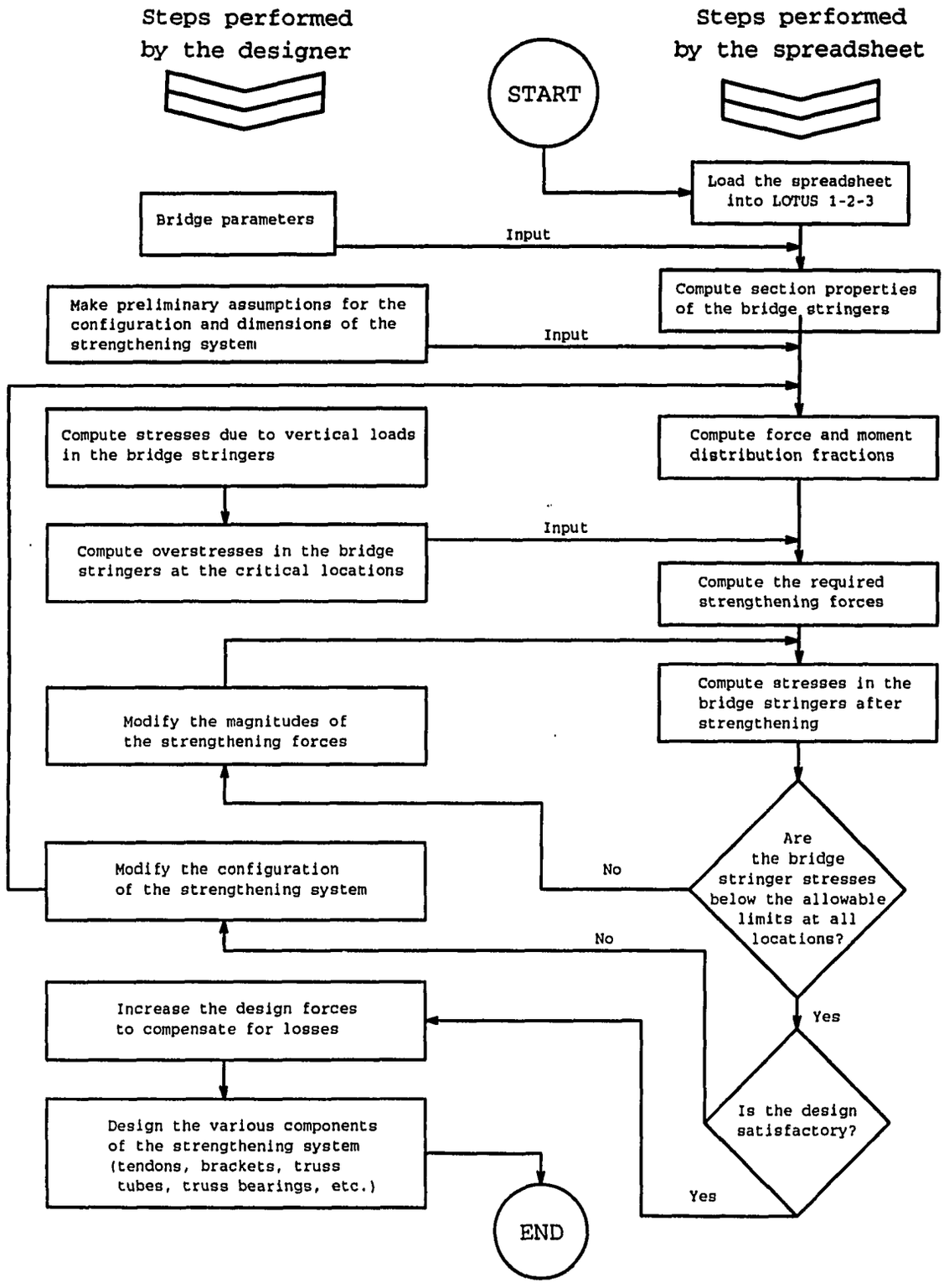

Fig. 4.6. Design procedure for strengthening system.

- Steel beam with coverplates
- Composite stringer (steel beam + deck)
- Composite stringer with coverplates (steel beam + coverplates + deck)

Also determine the location of the "standard" neutral axis,i.e., the neutral axis location of the composite bridge without coverplates.

3. Determine all loads and load fractions for exterior and interior stringers for:
   - Dead load
   - Long-term dead load
   - Live load and impact
4. Compute the moments induced in the exterior and interior stringer due to:
   - Dead load
   - Long-term dead load
   - Live load and impact
5. Compute the stresses in the exterior and interior stringers at numerous sections along the length of the bridge due to:
   - Dead load
   - Long-term dead load
   - Live load and impact
6. Make an initial assumption of the strengthening scheme (see Sec. 3.3.1), the tendon lengths and bracket locations (see Sec. 3.3.2). Use these values to compute the initial force and moment fractions.
7. Compute the overstresses at the critical section locations to be removed by strengthening.
8. Determine the post-tensioning forces and the vertical truss force which produce the desired stress reduction at the critical sections.
9. Check the final stresses in the exterior and interior stringers at various sections along the length of the

bridge; one should especially check the stresses at the coverplate cutoff points, bracket locations, and truss bearing points.

10. Increase the strengthening design forces by 8% to account for post-tensioning time-losses and errors due to approximations in the design methodology.

The design example in Chp. 5 of this thesis illustrates the computation details for each of these steps. Sections 5.1. through 5.10. of Chp. 5 correspond to the ten steps outlined above.

4.5. Recommendations for design

The following are helpful guidelines to obtain an efficient and practical design for the strengthening system. In the following sections, information is provided on selecting the strengthening scheme, bracket locations, and tendon and truss design considerations.

4.5.1. Selection of the strengthening scheme

- Due to the extra cost and installation time required when superimposed trusses are used, it is recommended to use only post-tensioning whenever possible.
- A recommended design procedure is to use the post-tensioning forces to compensate for the overstresses in the positive moment regions. This will also reduce some of the overstress in the pier negative moment regions. If the remaining overstress in the negative moment regions is small, the post-tensioning forces can be increased to compensate for this overstress. If the negative moment overstress is not eliminated using this procedure, superimposed trusses should be used to

obtain the desired stress reduction in the negative moment regions.

- One may increase the post-tensioning forces significantly beyond what is required to compensate for the overstress in the positive moment regions. Although the stresses along the stringers may still be within the allowable stress limits, large post-tensioning forces may cause excessive cracking in the deck and curbs. Such cracking can be avoided by using superimposed trusses (which are very efficient in reducing overstresses at the piers) coupled with the post-tensioning of positive moment regions.

4.5.2. Selection of the bracket locations

- The initial positions of the brackets may be determined by using the following guidelines:
  - Length of post-tensioned portion of end-span = 0.60 x Length of end-span.
  - Length of post-tensioned portion of center-span = 0.50 x Length of center-span.
  - Length of truss tendon = 0.50 x Length of end-span.
  - Distance of first bracket from abutment = 0.12 x Length of end-span.
  - Bracket length = 1.50 ft.

  These values can be used in the preliminary stages of calculating the required strengthening forces and modified later within the allowable limits (given in Appendix A) to obtain a better design.
- Numerous practical considerations should be taken into account when one positions the brackets. For example, adequate clearance should be provided for the post-tensioning hydraulic cylinder as well as the jacking

chair. The tendon extension beyond the end of the bracket, and tendon elongation during the stressing must also be considered. Special consideration must be given to the splice locations to ensure that they do not interfere with the stressing.

- It is often difficult to give adequate clearance between the bracket locations and the stringer splice location in the center span since reducing the length of the center span tendons to avoid this interference may not allow the achievement of the desired stress reduction. In such situations, larger brackets may be used to increase the distance between the tendon and the bottom flange and the web. By increasing the clearances between the tendon and the stringer flange and web, one will be able to use the chair and hydraulic cylinder above the splice plates. Another option would be to use special jacking chairs which clear the splice area. When there is sufficient clearance under the bridge, one could position brackets (and thus the tendons) under the bottom flange. The center span of the bridge in Ref. 4 was strengthened with post-tensioning under the bottom flange in the center span. See additional comments which follow on this under the flange location.
- It is not recommended to place the brackets outside the splice locations in the center span, as this would subject the splice to post-tensioning forces.
- For skewed bridges (45 degrees or less), the bracket locations on the stringers can be determined as in the case of right-angle bridges.
- Placing the tendon and the brackets under the stringer creates a large eccentricity, and therefore smaller tendon forces are required. However, this arrangement reduces clearance under the bridge. Therefore, it is

recommended to position the brackets above the lower flanges of the stringers. This location allows the brackets to be bolted to both the stringer flange and web and thus requires a smaller bracket. This location also "protects" the strengthening system from unexpected overheight vehicles (when the bridge is over a road) and floating debris (when the bridge is over a flooded stream).

4.5.3. Design considerations for the post-tensioning tendons and superimposed trusses

- The designer should allow for decreases in the tendon forces with time. Therefore, stresses should be checked for both initial and final forces. Some of the most common causes for losses are:
  - Steel relaxation.
  - Temperature differential between the tendons and the bridge.
  - Reduction of end-restraint present at the time of post-tensioning.
  - Removal of the deck and curbs for replacement. This causes a significant decrease in the tendon forces. It is therefore recommended to temporarily remove post-tensioning during deck and curb repairs.
- The post-tensioning tendons used in the strengthening system should be protected from corrosion. Epoxy coating is one method of obtaining this protection. If epoxy-coated Dywidag threadbars are used [28], special nuts should be ordered if the tendons are coated over their entire length. The epoxy coating should be omitted at the ends of the tendons if only ordinary nuts are available.

- The designer should make a careful study of the tendon locations since in some bridges diaphragms and/or other construction details may interfere with the tendons.
- In choosing the bearing points of the superimposed trusses, the angle between the truss tube members and the stringer should not be too small. It is recommended that the inclination of the truss tube be not less than 1 in 15.

4.6. Application of the design methodology to actual bridges

In this section, an example is given to demonstrate the application of the design methodology in strengthening a standard Iowa DOT continuous-span bridge. This example is intended to show only the basic procedure of the design process and to show the possibility of using more than one strengthening scheme to achieve the required stress reduction. This example does not show the details of each design step. The example given in Chp. 5 illustrates the detailed computations and use of the spreadsheet for the design of a strengthening system for a typical bridge.

The bridge selected for use in the current example is a two-lane, three-span, four-stringer, standard Iowa DOT V14 bridge with a total length of 250 ft. This bridge is to be strengthened to meet current Iowa legal load standards.

Since the bottom flange steel stresses in the bridge stringers is usually more critical than the top flange steel stresses and the concrete stresses, the approach utilized in this example is to design the strengthening system to reduce the bottom flange stresses to the allowable inventory stress level. The initial bottom flange stress envelopes in the exterior and interior stringers are obtained from the Iowa DOT rating files and are shown in Fig. 4.7.

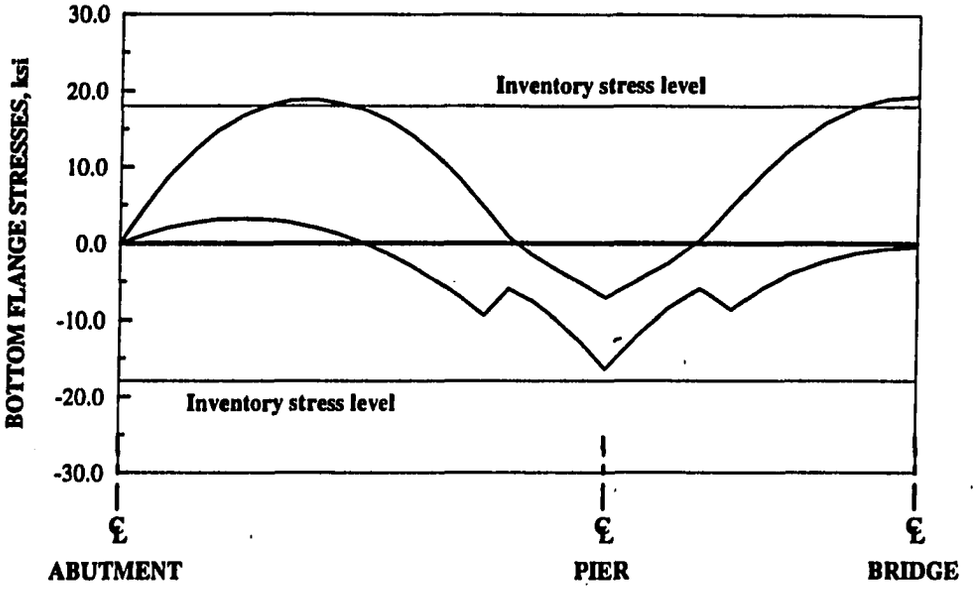

a. EXTERIOR STRINGER

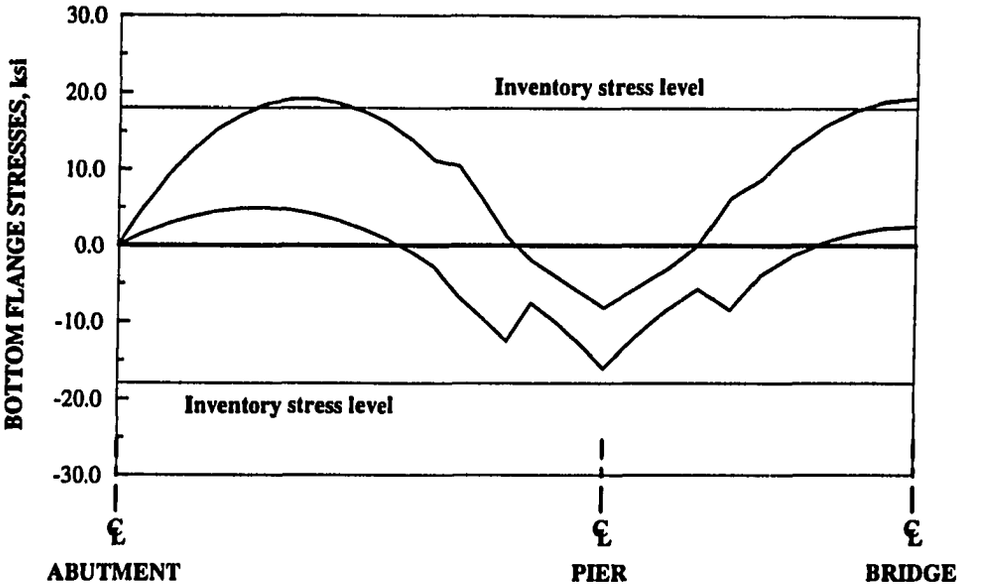

b. INTERIOR STRINGER

Fig. 4.7. Bottom flange stresses for V14 standard Iowa DOT bridge (length = 250 ft.) due to vertical loads.

As shown in Fig. 4.7, the bottom flange stresses exceed the allowable limits in the positive moment regions in both stringers. The maximum overstresses are 0.86 ksi, and 1.33 ksi in the end and center spans of the exterior stringer respectively, and 1.18 ksi and 1.30 ksi in the end and center spans of the interior stringer respectively. The negative moment regions at the piers are not overstressed.

To achieve the required stress reduction, two different combinations of the possible strengthening schemes (shown in Fig. 4.1) are used. The required strengthening forces are computed for each scheme and a comparison is made between the two.

4.6.1. Strengthening system 1

The strengthening system selected in this case is to post-tension all spans of both the exterior and interior stringers (i.e., a combination of schemes [A, B, C and D]). The stress envelopes and the various bridge parameters are input into the design spreadsheet and the required design forces are computed. The post-tensioning forces are:

- 24 kips in end-spans of the exterior stringers.
- 64 kips in center-spans of the exterior stringers.
- 51 kips in end-spans of the interior stringers.
- 60 kips in center-spans of the interior stringers.

The final stress envelopes after strengthening obtained from the spreadsheet are shown in Fig.4.8. The figure shows that the stresses along the lengths of both bridge stringers are below the allowable inventory stress level.

4.6.2. Strengthening system 2

Another combination for strengthening schemes was investigated. In this case, post-tensioning was used on the

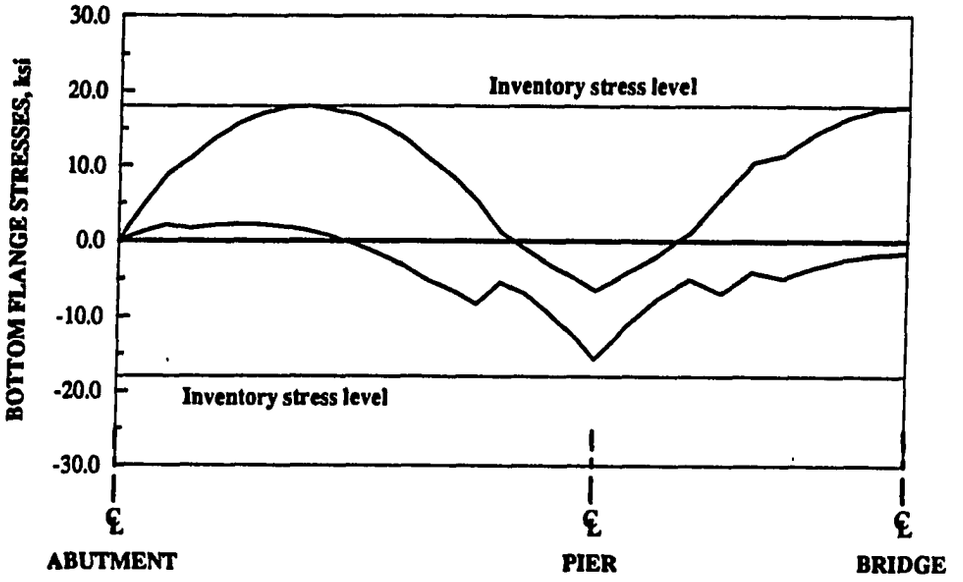

a. EXTERIOR STRINGER

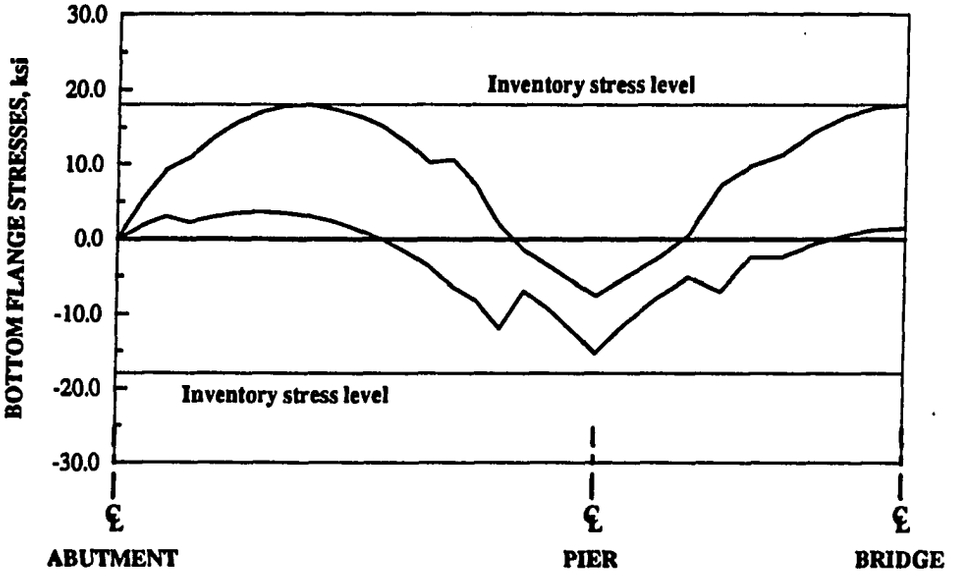

b. INTERIOR STRINGER

Fig. 4.8. Bottom flange stresses for V14 standard Iowa DOT bridge (length = 250 ft.) due to vertical loads and strengthening system (All spans of both stringers post-tensioned).

exterior stringers only (i.e., a combination of schemes [A and C]). Using the spreadsheet, the required design forces are obtained as follows:

- 150 kips in end-spans of the exterior stringers.
- 225 kips in center-spans of the exterior stringers.

The final stress envelopes after strengthening in this case are shown in Fig.4.9. The stresses are within the allowable limits at all points along the bridge stringers, and therefore this strengthening scheme is also suitable for reducing the overstresses on the bridge stringers.

4.6.3. Comparison between the different strengthening systems

As mentioned above, the two strengthening systems are suitable for strengthening this bridge since the required stress reduction has been achieved in both cases. The total post-tensioning force applied to the bridge can be computed as follows:

Total force for scheme (1) =

4 x (24+51) + 2 x (64+60) = 548 kips.

Total force for scheme (2) =

4 x 150+ 2 x 225 = 1050 kips.

The total force applied to the bridge in case of scheme (2), is 90% more than the total force applied in case of scheme (1). The reason for this is that the effect of post-tensioning one stringer on the stresses in the other stringer is small; thus large forces were required on the exterior stringers to achieve the required stress reduction on the interior stringer.

The second system has the advantage of using a smaller number of tendons and brackets and less construction time

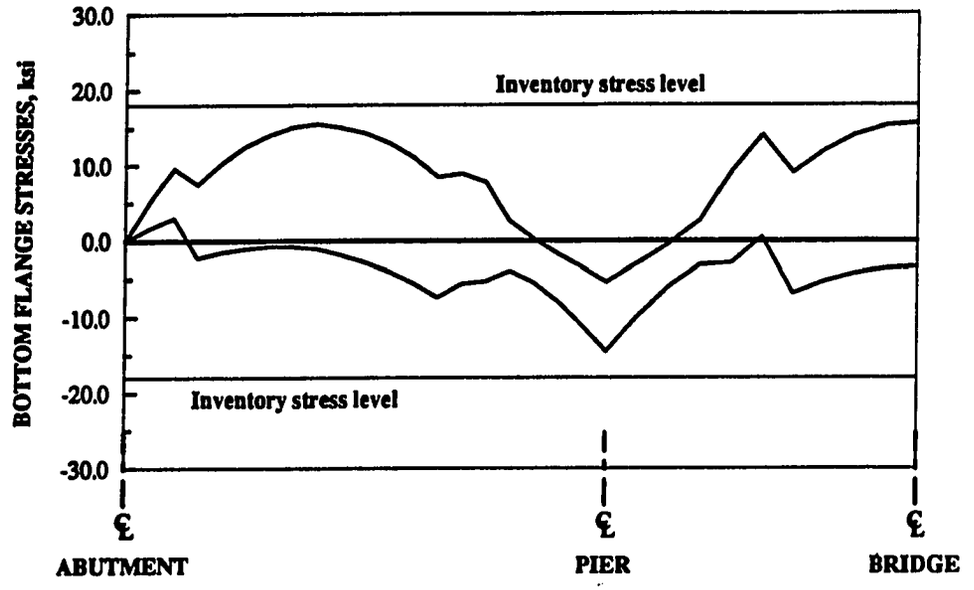

a. EXTERIOR STRINGER

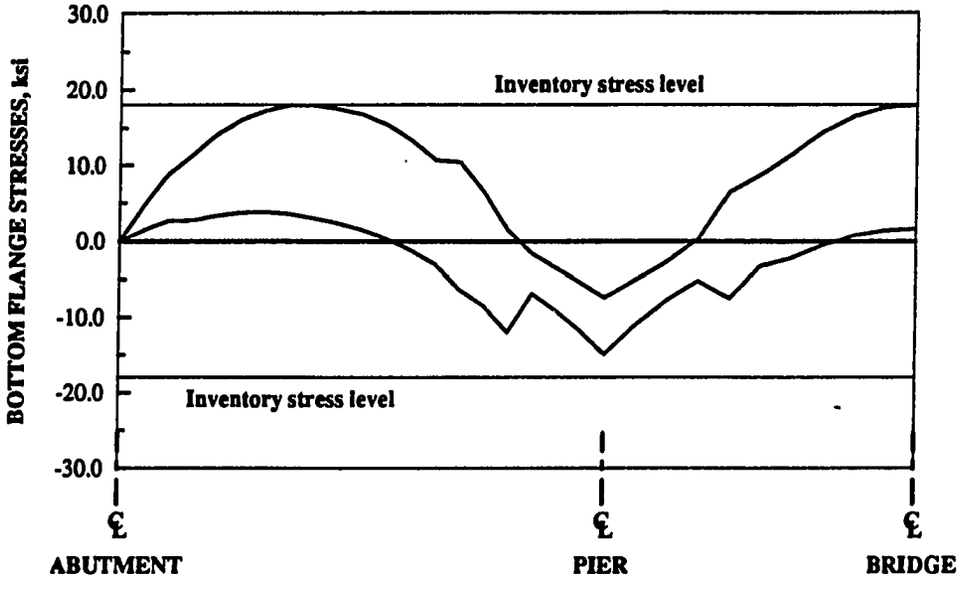

b. INTERIOR STRINGER

Fig. 4.9. Bottom flange stresses for V14 standard Iowa DOT bridge (length = 250 ft.) due to vertical loads and strengthening system (All spans of exterior stringers post-tensioned).

and effort, while the first system has the advantage of using smaller size tendons due to the relatively smaller post-tensioning forces required. The author recommends the use of strengthening system (1) since the relatively small strengthening forces applied in this case give a smaller chance for overstressing of the bracket locations in case of an overload on the bridge causing high stresses in these areas. However, it is left for the designer's judgment to decide which of these two systems to use. The designer can also select other strengthening schemes and repeat the design process until an optimum design is reached.

5. DESIGN EXAMPLE

In this section, the procedure for designing a strengthening system for a typical steel-stringer, composite, concrete-deck, continuous-span bridge is illustrated using the procedure presented in Chapter 3. The example is divided into ten sections - Secs. 5.1 through 5.10 which correspond to the ten steps outlined in Sec. 4.4. The illustrative example utilizes the spreadsheet (STRCONBR.WK1) developed as part of this research project.

The example is prepared assuming the user to be interacting simultaneously with the spreadsheet. The example is organized in steps each of which is denoted with the symbol: ◘; brief descriptions of the various steps are typed in CAPS. These steps include both computations to be performed by the user outside the spreadsheet, and commands to be executed on the spreadsheet. Each step is followed by an explanation and the required computations.

The design process described in this example is composed of two parts. The first part is the computation of the stresses along the lengths of the bridge stringers due to vertical loading and is described in Secs. 5.2 through 5.5, while the second part comprises the design of the strengthening system which is described in Secs. 5.6 through 5.10. If the stringer stresses due to vertical loading are available from the Iowa DOT rating files for the bridge, the user has the option to skip Secs. 5.2 through 5.5 and continue with the balance of the design procedure. The example as well as the spreadsheet are prepared to allow the user to skip these sections.

The bridge used in this example is a two-lane, three-spans,four-stringer, standard Iowa DOT V12 bridge with a total length of 150 ft. This bridge is strengthened to meet current Iowa legal load standards.

The bridge consists of four steel stringers acting compositely with the concrete deck. Coverplates are added to the steel stringers at the piers. In the transverse direction, steel diaphragms are provided at the abutments, piers, and several intermediate locations. A general layout of the bridge is shown in Fig. 3.1.

In order to simplify computations, the transverse section of the bridge has been idealized as shown in Fig. 5.1. The curb cross-section is idealized as a rectangle, the deck is assumed to be horizontal at each of the steel stringers, and the 1/2 in. wearing surface has been removed. Since the actual thickness of the deck varies slightly across the bridge width, an average value of 6.6 in. has been used.

5.1. Using the spreadsheet

The spreadsheet is composed of four parts containing a number of tables and macros (i.e., a subroutine within the spreadsheet). Part I of the spreadsheet computes the section properties of the bridge stringers and the total bridge section. In Part II, the different bridge parameters are input and used to compute the force and moment fractions. In Part III of the spreadsheet, the strengthening system design forces are computed, and in Part IV, the check of final stresses on the bridge stringers is completed.

A HELP section is provided in the spreadsheet, providing directions and explanations on the use of the various tables and macros. It is recommended that initially the user read and study the notes given in the HELP section

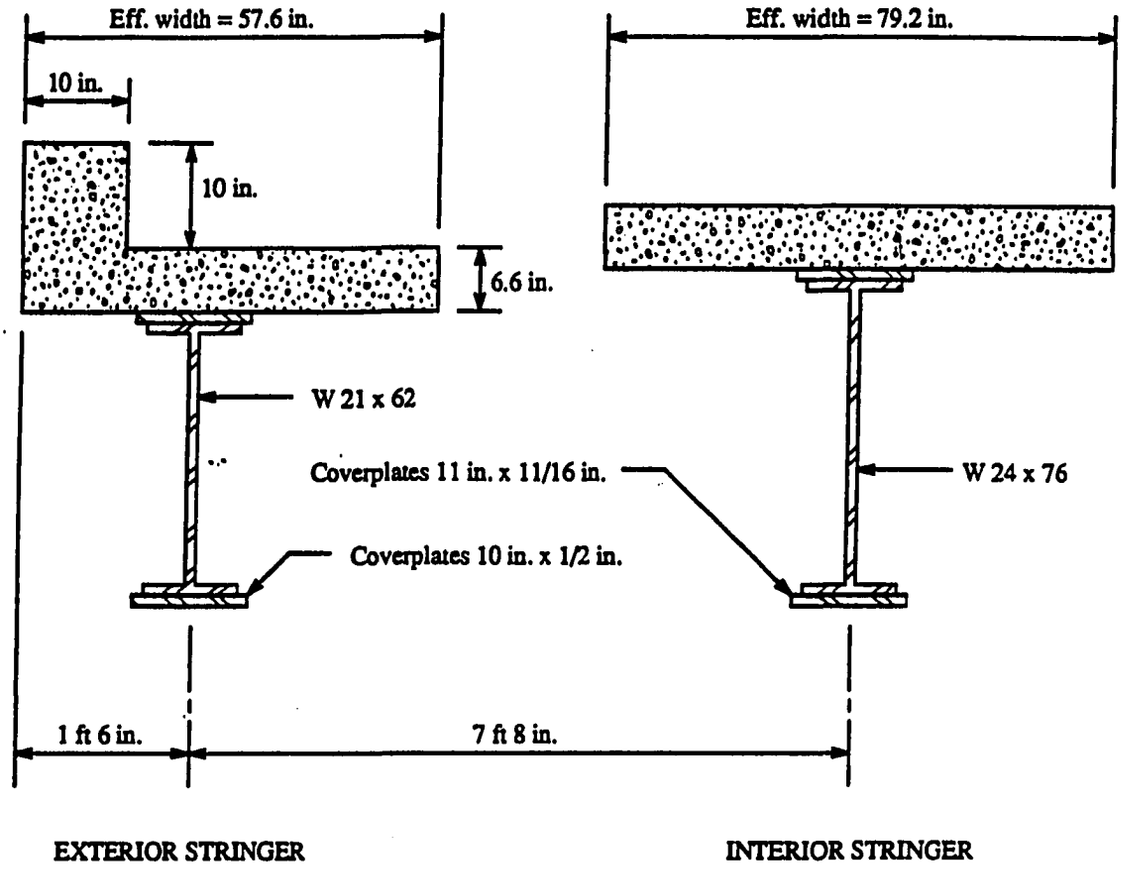

Fig. 5.1. Idealized transverse section of composite bridge.

of the spreadsheet before starting to work on each table or macro.

5.1.1. Retrieving the spreadsheet into LOTUS 1-2-3

Two spreadsheet files (on a 3.5 in. floppy disk) are provided with this manual. The user should start with the spreadsheet file "START.WK1", which is used to initialize the spreadsheet settings so that the design spreadsheet "STRCONBR.WK1" can be retrieved. The following steps describe the use of the spreadsheet:

- **Turn on the computer and start LOTUS 1-2-3**

- **Retrieve "START.WK1" into LOTUS 1-2-3**

To do this, use "/ FILE RETRIEVE A:\START.WK1 " . Some versions of LOTUS have an UNDO option. This option takes a considerable amount of memory. Due to the large size of the spreadsheet, there may be insufficient memory to retrieve the spreadsheet "STRCONBR.WK1", if the UNDO option is ON. The "START.WK1" spreadsheet provides a macro ALT-A to turn the UNDO option OFF.

- **If the signal UNDO shows at the bottom of the screen, Press ALT-A**

- **Retrieve "STRCONBR.WK1" into LOTUS**

To do this, use " / FILE RETRIEVE A:\STRCONBR.WK1 ".

5.1.2. Getting acquainted with the spreadsheet

- **Use the PAGE UP and PAGE DOWN keys to move up and down the spreadsheet**

Most of the time throughout the design, the user will only need to view columns [A through H] of the spreadsheet. However, some tables occupy more than these columns. In these cases, a "Table cont." sign is given to direct the user to the balance of the table.

- **Press ALT-H**

This moves the cursor from the user interactive area [Columns A through H] into the HELP area [Columns I through P] which is normally hidden from view.

- **Press ALT-B**

This returns the cursor to the user interactive area.

Throughout the spreadsheet, the values to be input by the user are designated as input cells, which appear with a different color on the screen. The user is allowed to input values only into these "input cells". When inputting data, the user can activate the INPUT mode in LOTUS using a macro ALT-P.

- **Press ALT-P**

This allows the cursor to move only to cells designated as "input cells". When inputting data, the user can activate this macro to avoid overwriting cells not designated as "input cells". However, in the INPUT mode,

the user can not move freely through the spreadsheet to view the various instructions and the HELP area. To do this, the user needs to leave the INPUT mode.

- **PRESS ESC**

The INPUT mode is off, and the user is able once again to go through the rest of the spreadsheet and the HELP area.

In this example, printouts from the spreadsheet are shown in each step to allow the user to check the results from the computer screen. All spreadsheet tables in this example are shaded to be easily distinguished from other tables used in the example, and the "input cells" within these tables are underlined.

5.2. Computation of section properties:

5.2.1. Section properties of the exterior stringers

The following steps should be performed to compute the section properties of the exterior stringers of the bridge:

- **COMPUTE THE EFFECTIVE FLANGE WIDTH FOR THE EXTERIOR STRINGERS**

The composite action between the concrete deck and the steel stringer requires the determination of an effective flange width of the deck. Since the deck extends a distance of 18 in. beyond the centerline of the exterior steel stringer, the exterior stringer is assumed to have a flange on both sides. Based on Sec. 10.38 of Ref. 23, the flange width should be taken as the smallest of the following:

a. Cantilever deck length + span length / 8
(not to exceed span length / 4)
= 18 + 45.75 x 12 / 8 = 86.625 in. < 137.25 in.
(Note: The end-span length has been used since it is more conservative to use the smaller length).

b. Cantilever deck length + stringer spacing / 2
(not to exceed stringer spacing)
= 18 + 92 / 2 = 64 in. < 92 in.

c. Cantilever deck length + 6 x deck thickness
(not to exceed 12 x deck thickness)
= 18 + 6 x 6.6 = 57.6 in. < 79.2 in.

Therefore, the effective flange width of the exterior stringers is 57.6 in.

□ COMPUTE THE MODULAR RATIO (n)

The modular ratio, n, is the ratio of the modulus of elasticity of the steel to that of the concrete. According to Sec. 10.38 of Ref. 23, the modular ratio, n, corresponding to f_c' = 3000 psi is 9.

□ INPUT THE BASIC DIMENSIONS OF THE EXTERIOR STRINGERS INTO TABLE I.1 OF THE SPREADSHEET

The following is a list of these input values:

W-shape properties: (W21x62)	Height = 21 in.
	Area = 18.30 in^2
	Moment of inertia = 1330.0 in^4
Coverplate dimensions:	Width = 10 in.
	Thickness = 0.5 in.
Deck dimensions:	Effective flange width = 57.6 in.
	Thickness = 6.6 in.
Curb dimensions:	Width = 10 in.
	Height = 10 in.

Modular ratio: n = 9

The remaining values in Table I.1 are computed automatically after the input of these values.

TABLE I.1

Section Properties for Exterior Stringer:

	Width (in.)	Height (in.)	Area (in.^2)	Inertia (in.^4)	Neutral axis elev. (in.)	Y from bot.fiber to Neut. axis(in.)	I at NA of beam X-sec. (in.^4)
W-shape	---	21.00	18.30	1330.00	10.50	10.50	1330.00
Cover PL	10.00	0.50	10.00	1155.83	21.25		
Deck	57.60	6.60	42.24	153.33	24.30		
Curb	10.00	10.00	11.11	92.59	32.60		
W-shape+CPs			28.30		10.50	11.00	2485.83
W-shape+deck			71.65		22.06	22.06	5467.71
Full comp. sec.			81.65		20.65	21.15	7796.73

n = Young's modulus of steel / Young's modulus of concrete = 9.00

Definition of terms in Table I.1:

Cover PL: Cover plates; the steel W-shape has two flange coverplates - one on the top and one on the bottom - in the negative moment regions at the piers. The coverplate width and height input is for one coverplate; the area and inertia are computed for both coverplates.

W-shape + CPs: Steel section composed of W-shape and coverplates.

W-shape + deck: Composite section in noncoverplated regions.

Full comp. sec.: Composite section including W-shape, coverplates and concrete deck.

N-A elevation: Measured from the extreme bottom fiber of the exterior stringer W-shape (or coverplates).

Y from bottom fiber to N-A:	The distance from the extreme bottom fiber of the W-shape (or coverplates) to the section neutral axis (to be used later in computing bottom fiber stresses).
I @ N-A of stringer X-sec:	Moment of inertia of the section about its neutral axis.

5.2.2. Section properties of the interior stringers

The following steps should be performed to compute the section properties of the interior stringer of the bridge:

□ COMPUTE THE EFFECTIVE FLANGE WIDTH FOR THE INTERIOR STRINGERS

Based on Sec. 10.38 of Ref. 23, the flange width should be taken as the smallest of the following:

a. Span length / 4 = 45.75 x 12 / 4 = 137.25 in.
b. Stringer spacing = 92.00 in.
c. 12 x deck thickness = 12 x 6.6 = 79.20 in.

Therefore, the effective flange width of the interior stringers is 79.2 in.

□ INPUT THE BASIC DIMENSIONS OF THE INTERIOR STRINGER INTO TABLE. I.2 OF THE SPREADSHEET.

The following is a list of these input values:

Elevation difference between the top of the interior and exterior W-shapes = 2.75 in.

(Since the exterior and interior stringers are of different sizes, have coverplates with different thicknesses, and bear at the same elevation - this results in an elevation difference between the stringer tops. This elevation difference provides a crown in the bridge deck). The section properties of the interior stringer is as follows:

W-shape properties: Height = 24 in.
(W24x76) Area = 22.40 in^2
Moment of inertia = 2100.00 in^4
Coverplate dimensions: Width = 11 in.
Thickness = 11/16 in.
Deck dimensions: Effective flange width = 79.2 in.
Thickness = 6.6 in.

The remaining values in Table I.2 are computed automatically after the input of these values. The table has the following form:

TABLE I.2.

Section Properties for Interior Stringer:

Elevation of int. W-shape top - Elevation of ext. W-shape top = 2.75 in.

	Width (in.)	Height (in.)	Area (in.^2)	Inertia (in.^4)	Neutral axis elev. (in.) fm Bw	Y from bot.fiber to Neut. axis(in.)	I at NA of beam X-sec. (in.^4)
W-shape	---	24.00	22.40	2100.00	11.75	12.00	2100.00
Cover PL	11.00	0.69	15.13	2305.16	24.09		
Deck	79.20	6.60	58.08	210.83	27.05		
W-shape+CPs			37.53		11.75	12.69	4405.16
W-shape+deck			80.48		22.79	23.04	6094.99
Full comp. sec.			95.61		21.04	21.29	9952.41

5.2.3. Section properties of the entire bridge cross-section

□ PROCEED TO TABLE I.3.

No additional input by the user is needed for Table I.3. Due to symmetry, only half of the bridge cross-section needs to be considered. For simplicity, the section properties for half the bridge section are computed by combining those of the two stringers (Note that portions of the deck not included in the effective flange widths of the

stringers are excluded). The neutral axis elevation for the half-bridge section is computed and all moments of inertia given in the table are computed with respect to this location. Table I.3 is as shown below:

TABLE I.3.

Half-bridge section Properties:	Area [A] (in.^2)	Elev. of C.G. [z] (in.)	A*z (in.^3)	Inertias about bridge NA (in.^4) Exterior Stringer	Interior Stringer	Total Bridge
W-shapes+deck	152.13	22.45	3415.07	5478.37	6104.48	11582.85
Full comp. sec.	177.26	20.86	3697.79	7800.50	9955.63	17756.13

Definition of terms in Table I.3:

Half-bridge section: A section composed of the exterior and interior stringers including only the portions of the deck included in the effective flange areas of both sections.

W-shapes + deck: Section composed of both W-shapes together with their effective deck areas and the curb.

Full comp. sec.: Section composed of both W-shapes together with their coverplates, effective deck areas and the curb.

A*z: The sum of the products of the area of each stringer section and its neutral axis elevation (measured from the extreme bottom fiber of the exterior stringer W-shape). These values are used to compute the overall neutral axis of the bridge.

Elev. of C.G.: The neutral axis elevation of the entire bridge cross-section measured from the extreme bottom fiber of the

Inertias about N-A: The moments of inertia of the individual stringers and of the half-bridge cross-section about the neutral axis of the bridge.

□ PRESS ALT-A

This macro copies the section properties from all three tables in the spreadsheet Part I to Parts II, III and IV.

5.3. Computation of vertical loads on the bridge stringers

The computation of vertical loads on the bridge stringers is performed in accordance with the AASHTO specifications [23].

5.3.1. Dead loads

□ COMPUTE DEAD LOADS ON EXTERIOR STRINGERS

Steel W-shape: W21x62	= 62 plf
Coverplates: 2 x 10 x 0.5 x (2x18/150) x (490 pcf / 144 in^2	= 8 plf
(2 coverplates, each 18 ft long, averaged over the total bridge length)	
R.C. deck: (18 + 92/2) x 6.6 x (150 pcf / 144 in^2)	= 440 plf
R.C. curb: 10 x 10 x (150 pcf / 144 in^2)	= 104 plf
Steel diaphragms: (assumed average)	= 10 plf
Steel rail: (assumed average)	= 48 plf
Total dead load on exterior stringer	= 672 plf

□ COMPUTE DEAD LOADS ON INTERIOR STRINGERS

Steel W-shape: W24x76	= 76 plf
Coverplates: 2 x 11 x 11/16 x (2x19/150) x (490 pcf / 144 in^2)	= 13 plf
(2 coverplates, each 19 ft long, averaged over the total bridge length)	
R.C. deck: 92 x 6.6 x (150 pcf / 144 in^2)	= 633 plf
Steel diaphragms: (assumed average)	= 20 plf
Total Dead load on interior stringer	= 742 plf

5.3.2. Long-term dead loads

□ COMPUTE THE LONG-TERM DEAD LOADS FOR EACH STRINGER

The long-term dead loads are assumed to be distributed equally to each stringer, as permitted in Sec. 3.23 of Ref. 23. Therefore, the long-term dead load per stringer can be computed as follows:

Strengthening steel tendons and brackets (estimated average)	= 8 plf
Future wearing surface: 19 psf x (2x18+3x92)/12 /4 (average wt. is assumed to be 19 psf)	= 124 psf
Long-term dead load per stringer	= 132 psf

5.3.3. Live loads

□ DETERMINE THE LIVE LOADS, IMPACT FRACTION, AND THE WHEEL LOAD FRACTIONS ON THE EXTERIOR AND INTERIOR STRINGERS

The six Iowa legal trucks shown in Appendix C were used for the calculation of the maximum positive and negative

moments induced in each stringer. The impact factor used was computed using the impact formula given in Sec. 3.8 of Ref. 23.

$$I = \frac{50}{L + 125} \leq 0.30$$

where L is the length of the span that is loaded to produce the maximum stress in the bridge, in ft.

The wheel load fractions on the stringers were computed according to Sec. 3.8. of Ref. 23. In this example, the wheel load fraction on the exterior stringer is the greater of:

a. Reaction from the truck wheels, assuming the truck to be 2 ft from the curb
   = (1 x 6.33 + 1 x 0.33) / 7.667 = 0.87
b. S / (4 + 0.25 S), where S is the stringer spacing
   = 7.667 / (4.0 + 0.25 x 7.667) = 1.30

Therefore, the wheel load fraction is 1.30 for the exterior stringers.

The wheel load fraction on the interior stringer is the greater of:

a. Reaction from the truck wheels, assuming one of the truck wheels to be above the interior stringer
   = 1 + 1.667 / 7.667 = 1.22
b. S / 5.5 = 7.667 / 5.5 = 1.39

Therefore, the wheel load fraction is 1.39 for the exterior stringers

5.4. Computation of maximum moments due to vertical loads

□ COMPUTE THE MAXIMUM POSITIVE AND NEGATIVE MOMENTS ON THE BRIDGE STRINGERS DUE TO VERTICAL LOADS

The user would normally need a computer program to determine the maximum positive and negative moment envelopes on the stringers. The authors have developed a computer program for analyzing the bridge stringers due to vertical loads. The program analyzes each stringer separately as a continuous beam with variable moments of inertia using the three-moments equation. This program is used to perform all moment and stress computations in this section and the next section (i.e., Secs. 5.4 and 5.5). To shorten this example, details of this program are not included. The user has the option to develop their own program for computing moment envelopes on the bridge or to use the moment envelopes in the Iowa DOT rating files if available.

The limits of the regions where changes in section properties occur are determined by the locations of the coverplate cutoff points. To ensure that the coverplates have sufficient length to allow for the transfer of force from the W-shape to the coverplates, a theoretical cutoff point is assumed for each coverplate; this is obtained by subtracting a distance of $1^1/_2$ times the plate width from the actual coverplate length at each end (Ref. 23, Sec. 10.13.4). The actual coverplate lengths are given in Fig. 1.1.

Theoretical length of exterior stringer coverplates

= 18 - 2 x 1.5 x 10/12 = 15.50 ft

Theoretical length of interior stringer coverplates

= 19 - 2 x 1.5 x 11/12 = 16.25 ft

The boundaries for the change in section properties - measured from the abutment centerline - are computed as follows:

For the exterior stringer, the coverplates start at:

45.75 - 15.50/2 = 38.00 ft

and end at:

45.75 + 15.50/2 = 53.50 ft

For the interior stringer, the coverplates start at:

45.75 - 16.25/2 = 37.62 ft

and end at:

45.75 + 16.25/2 = 53.88 ft

The section properties used for the analysis of the stringers for vertical loads were obtained from Tables I.1 and I.2 of the spreadsheet. The locations of the various section properties used are shown in Fig. 5.2 and the values of the section properties are given in Table 5.1; this structural modeling was obtained as follows:

- For analysis of the stringers due to dead loads, and due to the maximum negative live load, the steel section properties were used throughout the stringer lengths.
- For analysis of the stringers due to the maximum positive live load, the composite section properties were used throughout the stringer lengths.
- For the superimposed dead loads, the factor, n, was taken to be equal to 3 x 9 = 27. To obtain the section properties for this case, the user can change the value of the factor, n, from 9 to 27 in Table I.1. The value of (n=9) should be input again into Table I.1 after obtaining the required section properties since this value is used later in the spreadsheet to compute section properties for computing stresses induced by the strengthening system.

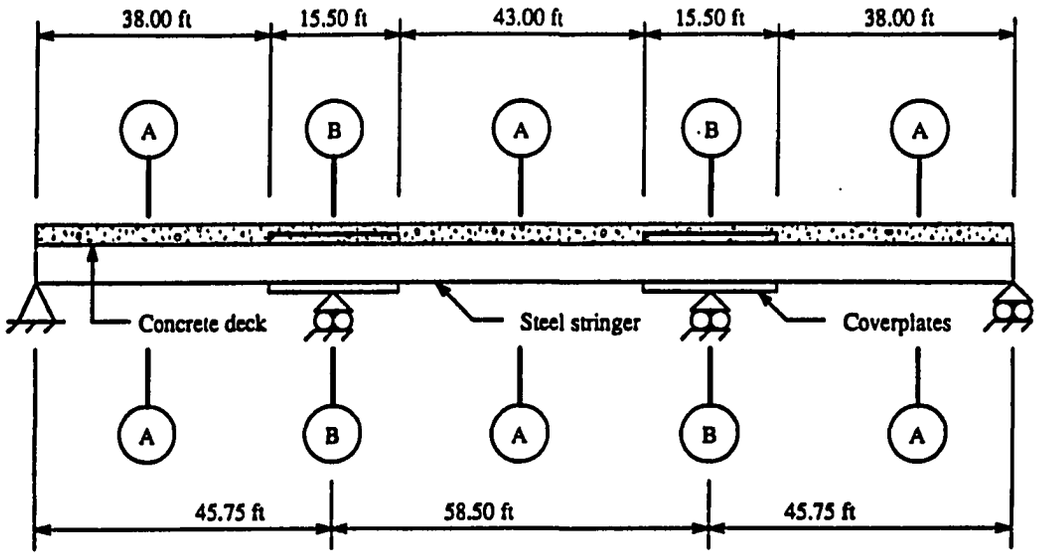

a. EXTERIOR STRINGER

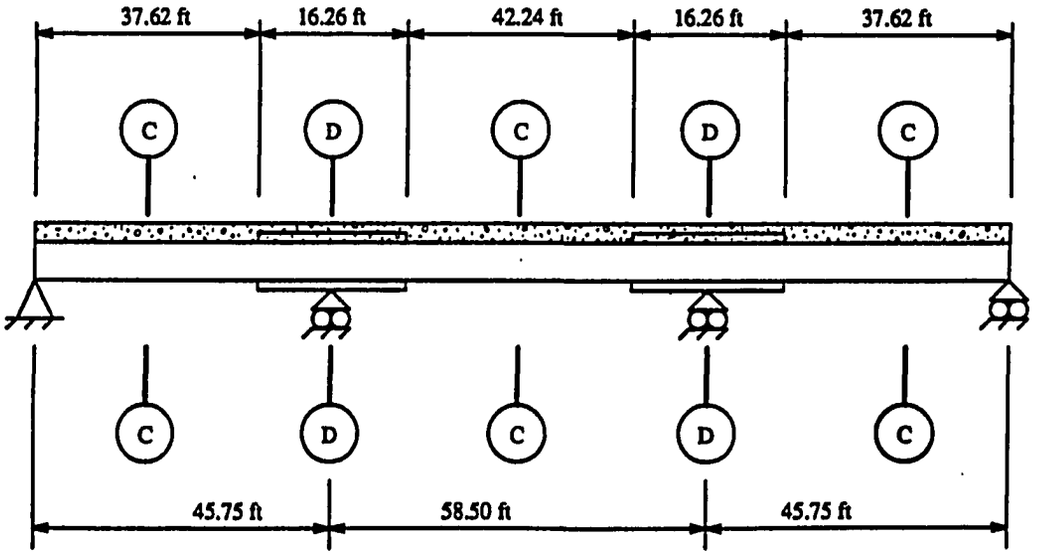

b. INTERIOR STRINGER

b. INTERIOR STRINGER

Fig. 5.2. Locations of various moments of inertia along stringers.

Table 5.1. Section properties used for analysis and stress computations in stringers due to vertical loads.

Loading	Stringer	Section*	Area ($in.^2$)	Inertia ($in.^4$)	Y_{bot} (in.)
Analysis for dead load and for maximum negative moments due to long-term dead load, and live load + impact	Exterior	A-A	18.30	1330.00	10.50
		B-B	28.30	2485.83	11.00
	Interior	C-C	22.40	2100.00	12.00
		D-D	37.53	4405.16	12.69
Analysis for maximum positive moments due to long-term dead load	Exterior	A-A	36.08	3788.82	18.15
		B-B	46.08	5403.27	16.99
	Interior	C-C	41.76	4601.23	19.01
		D-D	56.89	7564.03	17.21
Analysis for maximum positive moments due to live load + impact	Exterior	A-A	71.65	5467.71	22.06
		B-B	81.65	7796.73	21.15
	Interior	C-C	80.48	6094.99	23.04
		D-D	95.61	9952.41	21.29

* See Fig. 5.2.

The moments due to dead loads, and superimposed dead loads, were computed along the lengths of both stringers at sections spaced one ft apart.

To compute the maximum and minimum live load moment envelopes along the stringers, the load fractions and the impact factor were applied to the Iowa legal truck loads. Each truck was positioned at numerous locations along the stringer length, and the maximum and minimum live load moments were computed at sections spaced one ft apart.

5.5. Computation of stresses on the bridge stringers due to vertical loads

- **COMPUTE BOTTOM FLANGE STRESSES ALONG THE LENGTH OF THE STRINGERS DUE TO VERTICAL LOADS**

The moment envelopes computed in Sec. 5.4 have been used to compute the stresses induced by the vertical loads in the bridge stringers at sections spaced one ft apart. The section properties used for computing stresses are the same as those used for the analysis of the stringers due to vertical loads, and are given in Table 5.1. The stresses were computed separately for dead loads, superimposed dead loads, and live loads, and are added to give the final stress envelopes shown in Fig. 5.3.

- **CREATE A FILE "STRESS.VRT" CONTAINING THE STRESS ENVELOPE VALUES DUE TO VERTICAL LOADS AT A NUMBER OF SECTIONS ALONG THE LENGTH OF THE STRINGERS.**

The user needs to prepare this file for later use (see Sec. 5.9.1). This file will be imported into the spreadsheet Table IV.3 to be added to the stresses due to

the strengthening system for determining the stress envelopes after strengthening. The file should be composed of four columns containing the following data:

- Stress envelope for the maximum tensile stresses in the extreme bottom fibers of the exterior stringers.
- Stress envelope for the maximum compressive stresses in the extreme bottom fibers of the exterior stringers.
- Stress envelope for the maximum tensile stresses in the extreme bottom fibers of the interior stringers.
- Stress envelope for the maximum compressive stresses in the extreme bottom fibers of the interior stringers.

It should be noted that the top flange steel stresses and the concrete stresses are not input into the spreadsheet since the bottom flange stresses are usually more critical. The check of stringer top flange stresses and the concrete deck stresses is given in Secs. 5.9.2 and 5.9.3.

The length of the file created should not exceed 80 rows in order to fit into Table IV.3. In this example, the length of the file was 75 rows. A printout of the file is given in Appendix B.

5.6. Input of bridge parameters and computation of force and moment fractions

In this section, the user inputs values into all the designated "input cells" of Table II.1 of the spreadsheet. Preliminary estimates need to be made for some of these values as they will be unknown at this time; these values may be revised at a later stage in the calculations to obtain a better design.

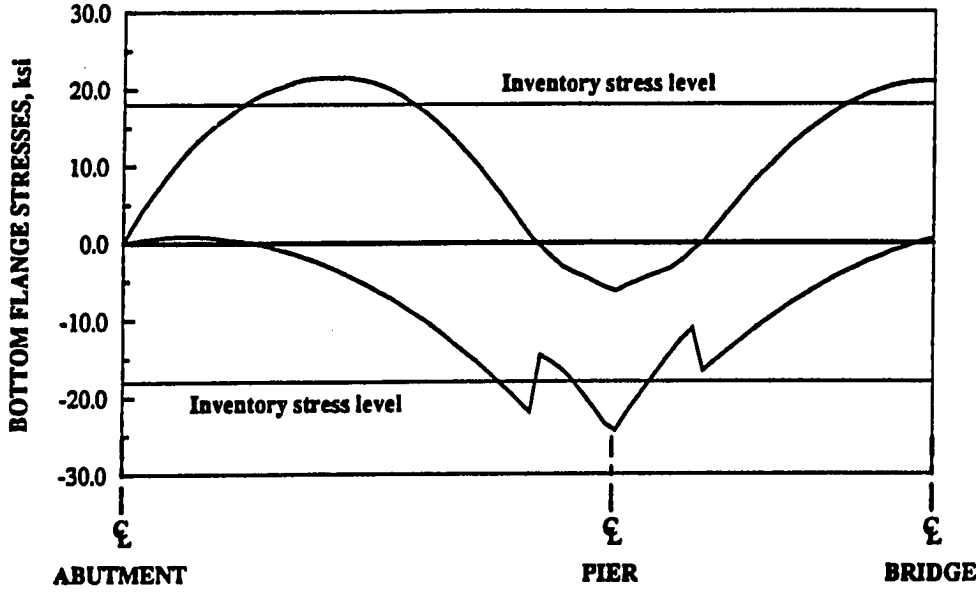

a. EXTERIOR STRINGER

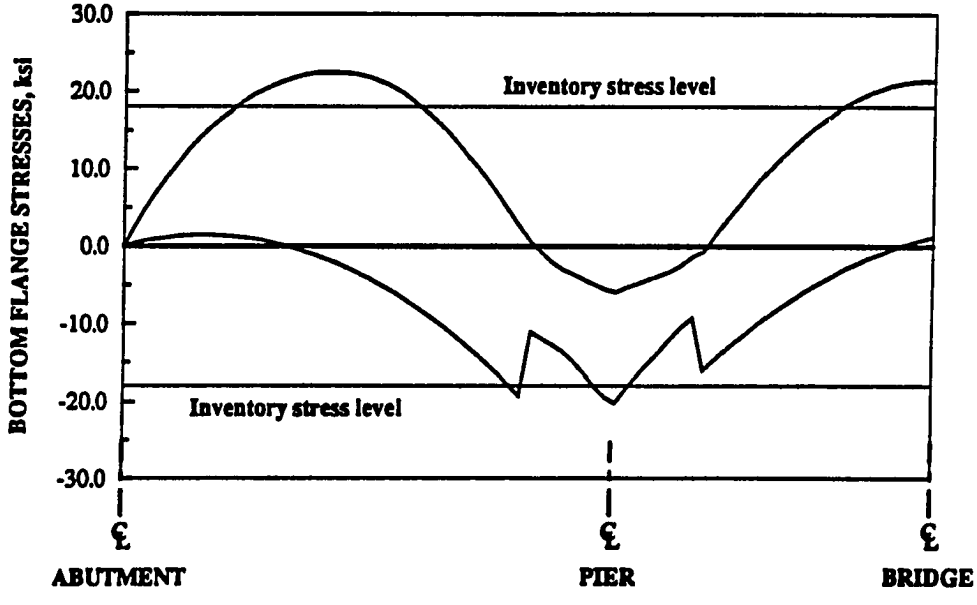

b. INTERIOR STRINGER

Fig. 5.3. Stress envelopes due to vertical loads.

- **MAKE A PRELIMINARY ESTIMATE OF THE TENDON LENGTHS AND POSITIONS, AND THE BRACKET LOCATIONS**

In Sec. 4.3.2, recommended values are provided to assist the engineer in making reasonable assumptions for the lengths and the positions of the post-tensioning tendons, and the superimposed trusses.

Length of end-span tendon	= 0.60 x 45.75 = 28.00 ft
Length of center-span tendon	= 0.50 x 58.50 = 30.00 ft
Length of truss tendon	= 2 x 0.24 x 45.75 = 22.00 ft
Distance of first bracket from centerline of end abutment	= 0.12 x 45.75 = 5.50 ft
Bracket length	= 1.50 ft

- **INPUT THE ESTIMATED VALUES TOGETHER WITH THE BASIC BRIDGE PARAMETERS INTO TABLE II.1 OF THE SPREADSHEET.**

The following is a list of these input values:

Stringer spacing = 92 in.
Deck thickness = 6.6 in.
End-span length = 45.75 ft
Center-span length = 58.50 ft
Inertia of half-bridge section:

- Considering only steel W-shape and reinforced concrete deck
- Considering full composite section including W-shape, coverplates and reinforced concrete deck

Note, these two values have been automatically copied from Table I.3. However, the user has the option of overriding these values and inputting other computed values. This option is needed if the user did not use Tables I.1, I.2, and I.3 to compute the section properties, and is using section properties computed by other means.

Tendon lengths:	for end-span	= 28.00 ft
	for center-span	= 30.00 ft
	for truss	= 22.00 ft

Note, tendon lengths are measured from the outside edges of the brackets. i.e., the bracket lengths are included.

Coverplate lengths:	for exterior stringer	= 18.00 ft
	for interior stringer	= 19.00 ft

First bracket location: = 5.50 ft from abutment C.L.

Bracket length: = 1.50 ft for all stringer spans

(Note: The first and second brackets are in the end span while the third bracket is in the center span; locations of the second and third brackets are automatically computed based on the specified tendon lengths and first bracket location. The bracket locations are the same for all exterior and interior stringers).

Values in Table II.1 are used by the spreadsheet to compute the force and moment fractions described in Sec. 4.1. Although the user does not need to review these computations, they can be seen in the spreadsheet area [R1..Z75].

5.7. Computation of overstresses to be removed by strengthening

The maximum tensile and compressive stresses in the extreme bottom fiber of the W-shape (or coverplate) of the exterior and interior stringers due to dead, live and impact loads were computed in Sec. 5.4. Since the bottom flange of the steel section experiences the largest stringer stresses, actual and allowable stresses are computed for the bottom fibers of the steel sections of both stringers. The strengthening system is initially designed to reduce the

actual stresses to the allowable limits in the bottom fibers at the most critical sections along the stringers. The stresses in the top of the steel section and in the concrete deck are checked after determining the final design forces since they are usually less critical. Modification may be made in the strengthening system if the top flange steel stresses or concrete deck stresses exceed the allowable limits. It should be noted however that the top flange stresses and concrete deck stresses are seldom critical. Table II.1 of the spreadsheet has the following form:

TABLE II.1.

Input of bridge parameters :			
Stringer spacing =	92.00	in.	
Deck thickness =	6.60	in.	
Length of end span =	45.75	ft	
Length of center span =	58.50	ft	
Total bridge length =	150.00	ft	
Inertia of bridge section:			
Steel beam + R.C. deck =	11582.85		in.^4
Full composite section =	17756.13		in.^4
Length of end-span cable =	28.00		ft
Length of center-span cable =	30.00		ft
length of truss cable =	22.00		ft
coverplate length: ext. stringer =	18.00		ft
int. stringer =	19.00		ft
First bracket location =	5.50		ft
Second bracket location =	33.50		ft
Third bracket location =	60.00		ft
Bracket length =	1.50		ft

5.7.1. Allowable stresses

COMPUTE THE ALLOWABLE STEEL TENSION STRESSES

The allowable stresses in the bottom flange of the steel section are given in Sec. 10.32 of Ref. 23. In positive moment locations, the bottom flange is in tension, and the allowable stress (assuming F_y = 33 ksi) is given by:

$F_t = 0.55\ F_y = 0.55 \times 33 = 18$ ksi (to the nearest ksi)

□ COMPUTE THE ALLOWABLE COMPRESSIVE STRESS IN THE BOTTOM FLANGE OF THE EXTERIOR STRINGERS

In the negative moment regions on both sides of the piers, the bottom flange is in compression. According to Sec. 10.32 of Ref. 23, the allowable compressive stress in the bottom flange of the exterior stringers is computed as follows:

The unsupported length of the flange is the minimum of :

a. Distance between diaphragms
   (in end span) = 45.75/2 = 22.88 ft
   (in center-span) = 58.50/3 = 19.50 ft

b. Distance from support to dead load inflection point
   = 13.50 ft

   Therefore, the unsupported length of the flange is 13.50 ft. The radius of gyration, r', of the bottom flange is computed as follows:

$$(r')^2 = \frac{I_{bottom\ flange}}{A_{bottom\ flange}} = \frac{0.5x10^3+0.615x8.24^3}{0.5x10+0.615x8.24} = 6.99\ in^2$$

The allowable compression stress is given by:

$$F_b = 0.55\ F_y \left[1 - \frac{(\frac{l}{r'})^2 F_y}{4\ \pi^2\ E} \right]$$

$$F_b = 0.55\ x\ 33\ x \left[1 - \frac{\frac{(13.5\ x\ 12)^2}{6.99}\ x\ 33}{4\ \pi^2\ x\ 29000} \right] = 16.17\ ksi$$

According to Note (a) of Table 10.32.1.A of Ref. 23, the allowable compression stress at the pier may be increased by 20%, but should not exceed 0.55 F_y. In this case,

F_b = 1.20 x 16.17 = 19.40 ksi > 18 ksi

Hence, the allowable compressive stress is F_b = 18 ksi. (to the nearest ksi)

- **COMPUTE THE ALLOWABLE COMPRESSIVE STRESS IN THE BOTTOM FLANGE OF THE INTERIOR STRINGER**

Since the bottom flange of the interior stringer is larger than that of the exterior stringer, its radius of gyration is larger and consequently its allowable compressive stress is also 18 ksi.

5.7.2. Stresses due to vertical loads at the critical sections

- **DETERMINE BOTTOM FLANGE STRESSES AT THE CRITICAL SECTIONS OF THE EXTERIOR AND INTERIOR STRINGERS RESULTING FROM VERTICAL LOADS**

Three critical stress locations in each stringer are shown in Fig. 5.4. The first section is in the end span at the maximum tensile stress location. This maximum stress location obviously varies depending on the bridge parameters and loads. To simplify the design procedure, the critical section has been assumed to be at a distance of 40% of the span length from the end support. The second section is at the middle of the center span, and the third is at the maximum negative moment location, i.e., at the pier.

Table II.2 of the spreadsheet lists a numbering scheme for the critical sections [1] through [6], as shown in Fig. 5.4. Reference will be made to these sections throughout the example using this numbering scheme. The stresses in the bottom flange - or coverplates - at these sections due to vertical loads are obtained from Fig. 5.3, and are as follows:

Vertical load stress at Sec. [1] = + 21.56 ksi
at Sec. [2] = + 21.02 ksi
at Sec. [3] = - 24.36 ksi
at Sec. [4] = + 22.48 ksi
at Sec. [5] = + 21.42 ksi
at Sec. [6] = - 20.23 ksi

Note, the negative sign indicates a compression stress in the bottom flange.

5.7.3. Computation of overstresses at the critical sections

- **COMPUTE OVERSTRESSES IN THE BOTTOM FLANGES OF THE EXTERIOR AND INTERIOR STRINGERS AT THE CRITICAL SECTIONS**

The overstresses at the critical sections need to be computed by the user. The overstresses are computed as the difference between the stresses due to vertical loads and the allowable stresses at the sections .

Overstress at Sec. [1] = + 21.56 - 18 = + 3.56 ksi
at Sec. [2] = + 21.02 - 18 = + 3.02 ksi
at Sec. [3] = - 24.36 + 18 = - 6.36 ksi
at Sec. [4] = + 22.48 - 18 = + 4.48 ksi
at Sec. [5] = + 21.42 - 18 = + 3.42 ksi
at Sec. [6] = - 20.23 + 18 = - 2.23 ksi

As previously noted, the negative sign indicates a compression stress in the bottom flange.

- **COMPUTE THE DISTANCE FROM THE EXTREME BOTTOM FLANGE FIBER OF THE W-SHAPE TO THE CENTER OF THE TENDONS AT THE CRITICAL SECTIONS**

The engineer needs to make an estimate of the tendon elevations above the bottom flanges of the exterior and interior stringers based on the size of available hydraulic cylinders and jacking chairs. These values will be input

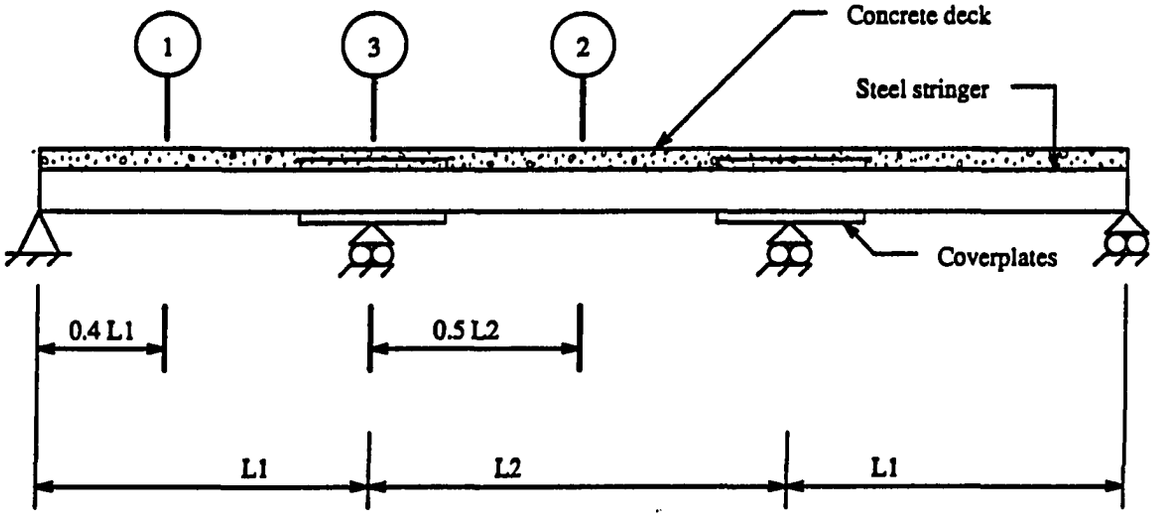

a. EXTERIOR STRINGER

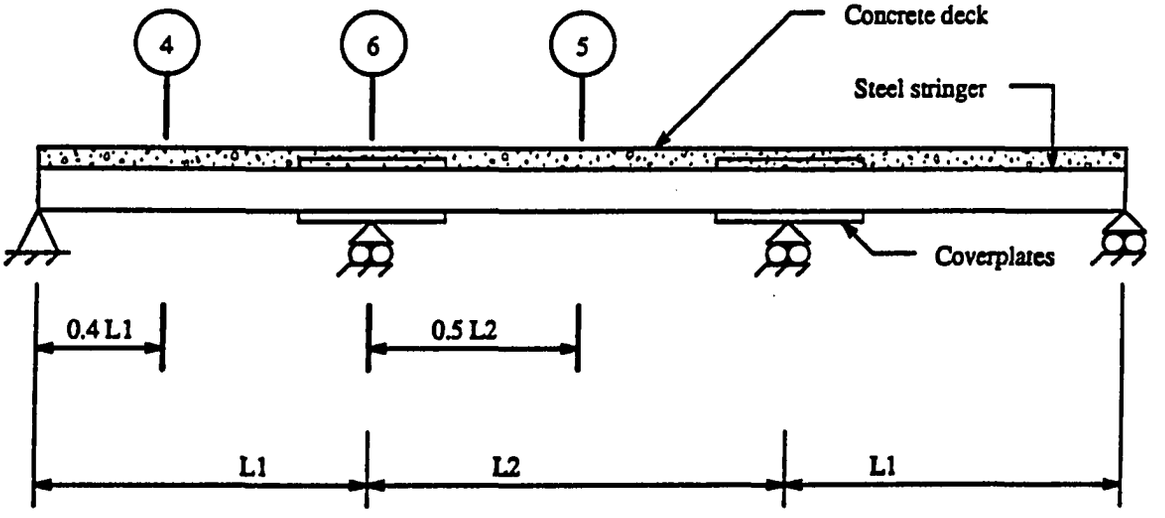

b. INTERIOR STRINGER

Fig. 5.4. Critical stress locations.

into Table II.2 of the spreadsheet together with the overstresses at the critical sections.

As previously noted in Sec. 4.5.2, it is recommended to position the tendons above the bottom flanges of the stringers. In this example, the tendon elevation was estimated based on the diameter of the available hollow-core hydraulic cylinders. In most instances, it is necessary to use a 120 kip capacity hollow-core hydraulic cylinder. Hollow-core cylinders of this capacity frequently have a diameter of $6^1/_4$ in. [29]. Assuming an $^1/_8$ in. clearance, the tendons can be placed so that the centerline of the tendons are $3^1/_4$ in. above the bottom flanges, and $3^1/_4$ in. away from the stringer web. It is desirable to minimize the tendon elevation above the bottom flange to increase the moment arm of the post-tensioning forces about the bridge neutral axis. Therefore, if less post-tensioning force is required, smaller hydraulic cylinders (capacity and diameter) can be used and the $3^1/_4$ in. elevation can be reduced.

The elevation of the tendons above the extreme bottom fiber of the W-shape is equal to the tendon elevation above the top of the bottom flange plus the flange thickness =

3.25 + 0.615 = 3.87 in. for exterior stringers
3.25 + 0.685 = 3.94 in. for interior stringers

□ INPUT DATA INTO THE DESIGNATED "INPUT CELLS" OF TABLE II.2.

The following is a list of values that need to be input by the user:

- The data input in the first three columns of the table are the cross-sectional area, the moment of inertia, and the distance from the extreme bottom fiber of the W-shape (or coverplate) to the neutral axis of the section, respectively. These values were automatically

entered into the table when the user pressed ALT-A, while working on Part I of the spreadsheet. The user needs to make sure that the values in these three columns are the section properties used in computing the vertical load stresses at these sections. If the user did not use Tables I.1 and I.2 of the spreadsheet to compute the section properties of the stringers, the section property values in Table II.2 should be overridden with the values used.

- In the fourth column of the table entitled "Bottom flange overstress", the values +3.56, +3.02, -6.36, +4.48, +3.42, -2.23 ksi are input for the overstresses in Secs. [1] through [6], respectively.
- In the last column of the table, the tendon elevation values are input. A value of 3.87 in. is input into the cells corresponding to Secs. [1] and [2], and 3.94 in. is input for Secs. [4] and [5].

Table II.2 of the spreadsheet now takes the following form:

TABLE II.2.

Overstresses:

Exterior Stringer:	Sec.	X-sec. Area (in.^2)	X-sec. Inertia (in.^4)	Y of bot. flange from NA (in.)	Bottom flange overstress (ksi)	Tendon Elev. (in.)
@ 40 % of end span	[1]	71.65	5467.71	22.06	3.56	3.87
@ middle of center span	[2]	71.65	5467.71	22.06	3.02	3.87
@ pier	[3]	28.30	2485.83	11.00	-6.36	---
Interior Stringer:						
@ 40 % of end span	[4]	80.48	6094.99	23.04	4.48	3.94
@ middle of center span	[5]	80.48	6094.99	23.04	3.42	3.94
@ pier	[6]	37.53	4405.16	12.69	-2.23	---

Comments on Table II.2:

- The section numbering used here [1] through [6] is the same as that in Fig. 5.4.
- In the column titled "Bottom flange overstress", a tension overstress in the bottom flange should be input as positive, and a compression overstress as negative.
- The tendon elevation is measured from the extreme bottom fiber of the W-shape (or coverplate, depending on the section) to the centerline of the tendon.

□ PRESS ALT-Q

Running this macro, the data input into Tables II.1 and II.2 of the spreadsheet are transferred to the rest of the spreadsheet.

5.8. Design of the required strengthening system

5.8.1. Choice of strengthening scheme

□ ASSUME THE STRENGTHENING SCHEME REQUIRED

The different locations for post-tensioning and superimposed trusses are shown in Fig. 5.5. The user can select a configuration composed of any combination of the cases [A, B, C, D, and E] for strengthening a given bridge. Considering the locations of the overstresses in this example, a system composed of post-tensioning tendons on all spans of the exterior and interior stringers together with superimposed trusses at the piers of the exterior stringers, as shown in Fig. 5.6 was assumed. This is specified in the spreadsheet as follows:

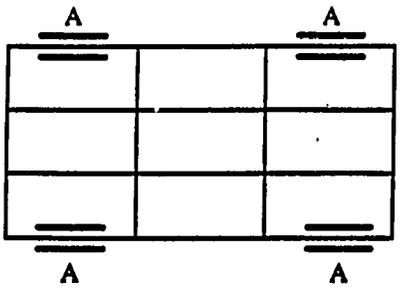

a. STRENGTHENING SCHEME [A]: POST-TENSIONING END SPANS OF THE EXTERIOR STRINGERS

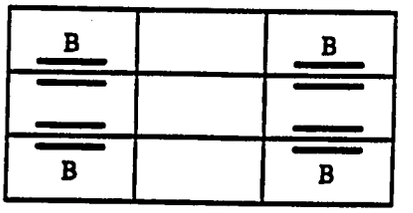

b. STRENGTHENING SCHEME [B]: POST-TENSIONING END SPANS OF THE INTERIOR STRINGERS

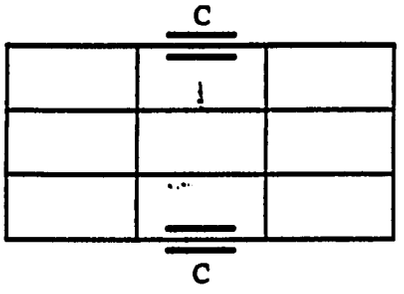

c. STRENGTHENING SCHEME [C]: POST-TENSIONING CENTER SPANS OF THE EXTERIOR STRINGERS

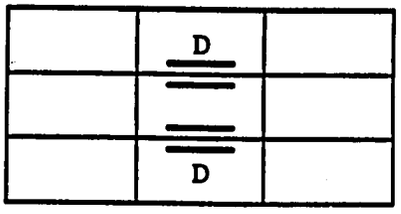

d. STRENGTHENING SCHEME [D]: POST-TENSIONING CENTER SPANS OF THE INTERIOR STRINGERS

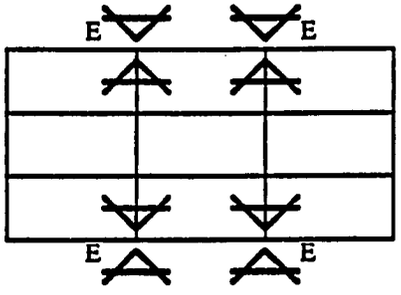

e. STRENGTHENING SCHEME [E]: SUPERIMPOSED TRUSSES AT THE PIERS OF EXTERIOR STRINGERS

Fig. 5.5. Various locations of post-tensioning and superimposed trusses.

Fig. 5.5. Various locations of post-tensioning and superimposed trusses.

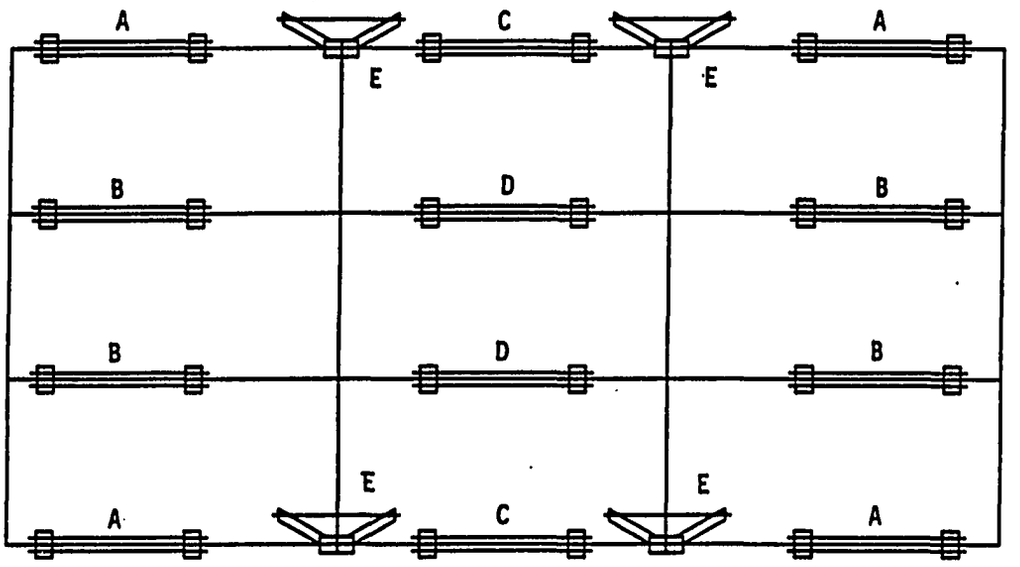

Fig. 5.6. Strengthening system selected for use in example problem.

- **INPUT THE VALUE OF 1 INTO ALL FIVE INPUT CELLS OF TABLE III.1.**

TABLE III.1.

Design of strengthening system: See Help ------>

	System [1/0]
Post-tensioning end spans of exterior stringers	1
Post-tensioning center spans of exterior stringers	1
Superimposed Trusses at piers of exterior stringer	1
Post-tensioning end spans of interior stringers	1
Post-tensioning center spans of interior stringers	1

Comments on Table III.1:

In the system column, 1 = post-tensioning or trusses used in this span

0 = post-tensioning or trusses not used in this span

- **CHECK PRACTICALITY OF THE ASSUMED SYSTEM AND ITS DIMENSIONS**

Practical guidelines for design are given in Sec. 4.5. In this example, it was found that the stringer splices are very close to the bracket locations. Thus, the distance between them is not sufficient for placing the jacking chair and the hydraulic cylinder. To solve this problem, the designer has several options. Reducing the length of the center-span tendon increases the clearance between the splices and the brackets, however, this reduces the effectiveness of the post-tensioning. Another option is to use larger brackets thus increasing the distance between the tendons and the stringer web and flange; this permits the use of the jacking chair and hydraulic cylinder despite the presence of the splice plates. This has the disadvantage of reducing the moment arm of the post-tensioning forces and therefore making them less effective in reducing stresses. A third option is to use special jacking chairs to bypass

the splice locations. In this example, it is assumed that special jacking chairs are available and thus the current design will be continued without modification.

5.8.2. Computation of strengthening forces

Tables III.2 and III.3 are for the computation of the strengthening system forces. These include the post-tensioning forces in the different spans of the exterior and interior stringers as well as the vertical truss forces.

Table III.2 is used to initiate the design and to perform the iterations needed to obtain the required forces. Final force values, after noting practical considerations, are input into Table III.3. These force values are automatically transferred to subsequent sections of the spreadsheet.

□ To start the design, Press ALT-S

This activates a macro which initializes all force values to zero. However, the cells in the column entitled "Force" are designated as "input cells" which provides the engineer the option of inputting assumed values of the forces rather than zeros. Table III.2 has the form:

TABLE III.2.

		Force (kips)	Sec. No.	Stress Reduction Required [Sr] (ksi)	Stress Reduction Achieved [Sa] (ksi)	Diff. [Sa-Sr] (ksi)	Is stress reduction achieved ?
PT EX END	F1 =	0.00	[1]	-3.56	0.00	3.56	NO
PT EX CEN	F2 =	0.00	[2]	-3.02	0.00	3.02	NO
TRUSS EX	F3 =	0.00	[3]	6.36	0.00	-6.36	NO
PT IN END	F4 =	0.00	[4]	-4.48	0.00	4.48	NO
PT IN CEN	F5 =	0.00	[5]	-3.42	0.00	3.42	NO
			[6]	2.23	0.00	-2.23	NO

PT: Post-tensioning EX: Exterior Stringer END: End-spans
TRUSS: Superimposed trusses IN: Interior stringers CEN: Center-spans

Comments on Table III.2:

- Forces in the first column: F1, F2, F4, and F5 are the post-tensioning forces in the tendons. F3 is the vertical force at the truss bearing points.
- The column [Sr] contains the required stress reduction at the six critical sections. These values are automatically copied from Table II.2 of the spreadsheet.
- The column [Sa] contains the actual stress reduction achieved by the forces in the [Force] column. The stress reduction values are computed using the force and moment fractions computed in Sec. 5.5.
- The column [Sa-Sr] gives the difference between the achieved stress reduction and the desired reduction.
- A "NO" in the column [Is stress reduction achieved ?] indicates that the stress reduction is less than that desired at the critical sections. When the desired stress reduction is achieved, it is so designated by the word, "YES".

□ To iterate until the desired stress reduction is attained, Press Alt-I

By pressing Alt-I, an iteration is performed changing the forces so that the stress reduction is closer to the required reduction. Table III.2 of the spreadsheet now takes this form:

TABLE III.2.

		Force (kips)	Sec. No.	Stress Reduction Required [Sr] (ksi)	Stress Reduction Achieved [Sa] (ksi)	Diff. [Sa-Sr] (ksi)	Is stress reduction achieved ?
PT EX END	F1 =	30.66	[1]	-3.56	-2.16	1.40	NO
PT EX CEN	F2 =	36.88	[2]	-3.02	-1.61	1.41	NO
TRUSS EX	F3 =	6.29	[3]	6.36	4.07	-2.29	NO
PT IN END	F4 =	36.51	[4]	-4.48	-2.33	2.15	NO
PT IN CEN	F5 =	39.72	[5]	-3.42	-1.76	1.66	NO
			[6]	2.23	2.11	-0.12	NO

PT: Post-tensioning EX: Exterior Stringer END: End-spans
TRUSS: Superimposed trusses IN: Interior stringers CEN: Center-spans

□ REPEAT THE ITERATION PROCESS BY PRESSING ALT-I

The user should repeat pressing ALT-I until all cells desired in the last column of Table III.2 indicate the desired stress reduction is achieved, i.e., a "YES" in all cells of the last column. If the engineer decides values in the [Sa-Sr] column are sufficiently small, one may proceed with one or more "NO's" in the last column. In this example, a total of 24 iterations were required to achieve the required stress reduction at all six critical sections. Table III.2 now takes this form:

TABLE III.2.

		Force (kips)	Sec. No.	Stress Reduction Required [Sr] (ksi)	Stress Reduction Achieved [Sa] (ksi)	Diff. [Sa-Sr] (ksi)	Is stress reduction achieved ?
PT EX END	F1 =	41.54	[1]	-3.56	-3.56	-0.00	YES
PT EX CEN	F2 =	67.48	[2]	-3.02	-3.02	-0.00	YES
TRUSS EX	F3 =	8.64	[3]	6.36	6.36	-0.00	YES
PT IN END	F4 =	81.55	[4]	-4.48	-4.48	0.00	YES
PT IN CEN	F5 =	82.22	[5]	-3.42	-3.42	0.00	YES
			[6]	2.23	3.91	1.68	YES

PT: Post-tensioning EX: Exterior Stringer END: End-spans
TRUSS: Superimposed trusses IN: Interior stringers CEN: Center-spans

Note, the stress difference value, $[S_a-S_r]$, at Sec. [6] is 1.68 ksi. This indicates that the achieved stress reduction is more than required.

5.8.3. Final design forces

- **PRESS ALT-W**

By running this macro, the design forces in the "Force" column in Table III.2 are transferred into the "Force" column of Table III.3, which consequently takes the following form:

TABLE III.3

Final design:

		Force (kips)	Sec. No.	Stress Reduction Required [Sr] (ksi)	Stress Reduction Achieved [Sa] (ksi)	Diff. [Sa-Sr] (ksi)	Is stress reduction achieved ?
PT EX END	F1 =	41.54	[1]	-3.56	-3.56	-0.00	YES
PT EX CEN	F2 =	67.48	[2]	-3.02	-3.02	-0.00	YES
TRUSS EX	F3 =	8.64	[3]	6.36	6.36	-0.00	YES
PT IN END	F4 =	81.55	[4]	-4.48	-4.48	0.00	YES
PT IN CEN	F5 =	82.22	[5]	-3.42	-3.42	0.00	YES
			[6]	2.23	3.91	1.68	YES

PT: Post-tensioning EX: Exterior Stringer END: End-spans
TRUSS: Superimposed trusses IN: Interior stringers CEN: Center-spans

- **REVIEW THE DESIGN FORCE VALUES FOR PRACTICALITY, AND INPUT THE FINAL FORCE VALUES INTO THE "FORCE" COLUMN OF TABLE III.3.**

The user has the option to override the previously determined values to meet practical design considerations. Some of these considerations have been outlined in Sec. 4.3. In this example, the strengthening forces were considered suitable, and were only rounded to the nearest integer value (F1 = 42 kips, F2 = 68 kips, F3 = 9 kips, F4 = 82 kips, F5 =

83 kips). This rounding process resulted in the desired stress reductions not being achieved at some of the critical sections. In such cases, the user should adjust the five forces to restore the "YES" in all cells of the last column. After a few minor changes, Table III.3 takes this form:

TABLE III.3.

Final design:

		Force (kips)	Sec. No.	Stress Reduction Required [Sr] (ksi)	Stress Reduction Achieved [Sa] (ksi)	Diff. [Sa-Sr] (ksi)	Is stress reduction achieved ?
PT EX END	F1 =	41.00	[1]	-3.56	-3.57	-0.01	YES
PT EX CEN	F2 =	67.00	[2]	-3.02	-3.03	-0.01	YES
TRUSS EX	F3 =	9.50	[3]	6.36	6.62	0.26	YES
PT IN END	F4 =	82.00	[4]	-4.48	-4.50	-0.02	YES
PT IN CEN	F5 =	82.00	[5]	-3.42	-3.44	-0.02	YES
			[6]	2.23	3.99	1.76	YES

PT: Post-tensioning EX: Exterior Stringer END: End-spans
TRUSS: Superimposed trusses IN: Interior stringers CEN: Center-spans

☐ COMPUTE THE TRUSS TENDON FORCES

The horizontal force in the truss tendons is computed based on the truss angle of inclination and the required truss vertical force (F3 in Table III.3) as follows:

From the truss detailed drawings, assuming the truss members are 6 in. x 6 in. square tubes, the angle between truss tube centerline and the horizontal is determined to be 4.45°. The horizontal tension force = 9.50 / tan(4.45°) = 122 kips. (Note, that this force is to be divided between the two trusses on both sides of the web of the exterior stringer).

☐ COMPUTE THE REQUIRED CROSS-SECTIONAL AREA OF THE TENDONS

High-strength steel should be used for the post-tensioning and truss tendons. In strengthening simple-span

and continuous-span bridges, the authors have used DYWIDAG threadbars [28]. The ultimate strength of these tendons is 150 ksi.

5.9. Check of stresses

In the previous section, the design forces were determined. These forces achieved the desired stress reduction in the bottom flange of the stringers at the six critical sections. Other critical locations in the stringers, however, must be checked also. Examples of these critical locations are: (1) the coverplate cutoff points, (2) the bracket locations, and (3) the truss bearing points. The stresses in the top flanges or coverplates of the steel stringers and in the concrete deck will be addressed in this section as well.

5.9.1. Stresses in the bottom flanges of the steel stringers

Part IV of the spreadsheet computes the bottom flange stresses at various locations along the length of the stringers.

- **CHECK THE VALUES IN TABLE IV.1, AND ADJUST VALUES IN THE "INPUT CELLS" IF NECESSARY**

The values in the "input cells" of Table IV.1 are transferred from Parts I and II of the spreadsheet. The user has the option to override the values in the "input cells" of this table to match those used for computation of stresses due to vertical loads. Table IV.1 appears on the screen as follows:

TABLE IV.1.

(A) Section Properties for computation of stresses in the different ranges of the EXTERIOR STRINGER due to maximum POSITIVE MOMENTS:

Range From (ft)	Range To (ft)	Area (in.^2)	Inertia (in.^4)	Dist. of bottom flange to NA (in.)	Stringer NA elev. (in.)	Elev. diff. (stringer NA -bridge NA) (in.)
0.00	36.75	71.65	5467.71	22.06	22.06	0.39
36.75	54.75	82.65	7736.72	23.15	20.65	1.80
54.75	75.00	71.65	5467.71	22.06	22.06	0.39
75.00						

(B) Section Properties for computation of stresses in the different ranges of the EXTERIOR STRINGER due to maximum NEGATIVE MOMENTS:

Range From (ft)	Range To (ft)	Area (in.^2)	Inertia (in.^4)	Dist. of bottom flange to NA (in.)	Stringer NA elev. (in.)	Elev. diff. (stringer NA -bridge NA) (in.)
0.00	36.75	18.30	1330.00	10.50	10.50	11.95
36.75	54.75	28.30	2485.83	11.00	10.50	11.95
54.75	75.00	18.30	1330.00	10.50	10.50	11.95
75.00						

(C) Section Properties for computation of stresses in the different ranges of the INTERIOR STRINGER due to maximum POSITIVE MOMENTS:

Range From (ft)	Range To (ft)	Area (in.^2)	Inertia (in.^4)	Dist. of bottom flange to NA (in.)	Stringer NA elev. (in.)	Elev. diff. (stringer NA -bridge NA) (in.)
0.00	36.25	80.48	6094.99	23.04	22.79	-0.34
36.25	55.25	95.61	9952.41	21.29	23.04	1.40
55.25	75.00	80.48	6094.99	23.04	22.79	-0.34
75.00						

(D) Section Properties for computation of stresses in the different ranges of the INTERIOR STRINGER due to maximum NEGATIVE MOMENTS:

Range From (ft)	Range To (ft)	Area (in.^2)	Inertia (in.^4)	Dist. of bottom flange to NA (in.)	Stringer NA elev. (in.)	Elev. diff. (stringer NA -bridge NA) (in.)
0.00	36.25	22.40	2100.00	12.00	11.75	10.70
36.25	55.25	17.51	4405.16	12.69	11.75	10.70
55.25	75.00	22.40	2100.00	12.00	11.75	10.70
75.00						

It should be noted that in most of the spreadsheet tables, there are cells designated as input cells (shown here underlined). The spreadsheet, in most instances, automatically computes values and inputs them into these cells. However, the user should change these values depending on his/her assumptions. To demonstrate the flexibility of the design spreadsheet, an example in which some of the values in Table IV.1 of the spreadsheet are changed is given here.

In Sec. 5.6, the coverplate lengths input into Table II.1 of the spreadsheet are the actual coverplate lengths (i.e., 18.0 ft and 19.0 ft for the exterior and interior stringers, respectively). These lengths were used in the spreadsheet to compute section properties used in the three moment equations. They were also used automatically to create the first two columns of Table IV.1.[A,B,C, and D]. When the stresses due to vertical loads were computed, theoretical coverplate lengths (i.e., 15.50 ft and 16.25 ft for the exterior and interior stringers, respectively) were used (See Sec. 5.4). The user therefore needs to change the limits of the different section properties in Table IV.1 of the spreadsheet (i.e., values in column 2 of the table). By making this modification, the range limits used for computing the stresses induced by the strengthening system match those used for computing the vertical load stresses.

In Sec. 5.4, the limits of the regions of different section properties along the stringers were computed as follows:

On the exterior stringers:

First range:	from	00.00 ft	to	38.00 ft
Second range:	from	38.00 ft	to	53.50 ft
Third range:	from	53.50 ft	to	75.00 ft

On the interior stringers:

First range:	from	00.00 ft	to	37.62 ft
Second range:	from	37.62 ft	to	53.88 ft
Third range:	from	53.88 ft	to	75.00 ft

Since the stresses are computed at intervals of one ft, stresses are computed at one section which is exactly 38.00 ft from the support. When computing stresses due to vertical loads, this section was considered to be in the first range. It is important to adjust the limits of the different ranges in Table IV.1 to ensure that the stresses at this section due to the strengthening system are computed based on the same section properties that were used to compute vertical load stresses. Therefore, a value of 38.02 ft (slightly higher than 38.00 ft) was substituted for 38.00 ft as the limit of the first range.

- **INPUT THE VALUES [38.02, 53.50, AND 75.00] INTO THE FIRST THREE CELLS OF THE SECOND COLUMN OF TABLE IV.1.[A,B] AND INPUT [37.62, 53.88, AND 75.00] INTO THE FIRST THREE CELLS OF THE SECOND COLUMN OF TABLE IV.1.[C,D].**

Table IV.1 now takes the following form:

TABLE IV.1.

[A] Section Properties for computation of stresses in the different ranges of the EXTERIOR STRINGER due to maximum POSITIVE MOMENTS:

Range From (ft)	Range To (ft)	Area (in.^2)	Inertia (in.^4)	Dist. of bottom flange to NA (in.)	Stringer NA elev. (in.)	Elev. diff. (stringer NA -bridge NA) (in.)
0.00	38.02	73.65	5467.71	22.06	22.06	0.39
38.02	53.50	81.65	7796.73	21.15	20.65	1.80
53.50	75.00	73.65	5467.71	22.06	22.06	0.39
75.00						

[B] Section Properties for computation of stresses in the different ranges of the EXTERIOR STRINGER due to maximum NEGATIVE MOMENTS:

Range From (ft)	Range To (ft)	Area (in.^2)	Inertia (in.^4)	Dist. of bottom flange to NA (in.)	Stringer NA elev. (in.)	Elev. diff. (stringer NA -bridge NA) (in.)
0.00	38.02	18.30	1330.00	10.50	10.50	11.95
38.02	53.50	28.30	2485.81	11.00	10.50	11.95
53.50	75.00	18.30	1330.00	10.50	10.50	11.95
75.00						

[C] Section Properties for computation of stresses in the different ranges of the INTERIOR STRINGER due to maximum POSITIVE MOMENTS:

Range From (ft)	Range To (ft)	Area (in.^2)	Inertia (in.^4)	Dist. of bottom flange to NA (in.)	Stringer NA elev. (in.)	Elev. diff. (stringer NA -bridge NA) (in.)
0.00	37.62	80.48	6094.99	23.04	22.79	-0.34
37.62	53.88	95.61	9952.41	21.29	21.04	1.40
53.88	75.00	80.48	6094.99	23.04	22.79	-0.34
75.00						

[D] Section Properties for computation of stresses in the different ranges of the INTERIOR STRINGER due to maximum NEGATIVE MOMENTS:

Range From (ft)	Range To (ft)	Area (in.^2)	Inertia (in.^4)	Dist. of bottom flange to NA (in.)	Stringer NA elev. (in.)	Elev. diff. (stringer NA -bridge NA) (in.)
0.00	37.62	22.40	2100.00	12.00	11.75	10.70
37.62	53.88	37.53	4405.26	12.68	11.75	10.70
53.88	75.00	22.40	2100.00	12.00	11.75	10.70
75.00						

- **DETERMINE THE NUMBER OF DIVISIONS ALONG THE STRINGER LENGTHS AT WHICH STRESSES ARE TO BE COMPUTED FOR PLOTTING.**

The sections used for stress computation in the spreadsheet should be the same as those used in the computation of the vertical load stresses. This is particularly important since the stresses will be added to give the final stress diagrams along the stringers in Table IV.3. Therefore, the spacing used here is the same as that which was used in the vertical load stress computations (i.e., one ft).

Half-bridge length = 150/2 = 75.00 ft
Number of divisions = 75.00 / 1.00 = 75 divisions

- **INPUT THE NUMBER OF DIVISIONS INTO THE SPREADSHEET**

In this example, it was determined that 75 divisions would be used. The maximum number of divisions permitted in the spreadsheet is 80.

- **PRESS ALT-E**

This macro uses the number of divisions specified to create the first column of Table IV.2. The user can override these values to input other values for the location of the sections at which stresses are to be computed (unequal spacing of the sections is allowed). These sections positions do not have to be equally spaced, but should match those used for computation of vertical load stresses.

- **PRESS ALT-Y**

This macro uses the section properties in Table IV.1 to create a table containing the section properties for each section along the stringer length. It is usually unnecessary for the user to review this table, however, the table is given in spreadsheet area [S490..AI580].

- **PRESS ALT-R**

This macro uses the final design force values in Table III.3, together with the force and moment fractions computed for the bridge, to compute the axial force and moment values due to the strengthening system at the stringer sections previously identified. The stress values are placed in columns [2 through 5] of Table IV.2. A portion of Table IV.2 is shown here for illustration, and a full printout of the table is given in Appendix B.

TABLE IV.2.

Axial forces and moments due to the strengthening system:

Distance (ft)	Axial Force (kips)		Moment at standard neutral axis (in.k)	
	Exterior Stringer	Interior Stringer	Exterior Stringer	Interior Stringer
0.00	0.00	0.00	0.00	0.00
1.00	0.52	-0.52	-2.79	-32.70
2.00	1.04	-1.04	-5.59	-65.41
3.00	1.56	-1.56	-8.38	-98.11
...				
72.00	67.28	81.72	533.77	627.41
73.00	67.31	81.69	528.76	632.41
74.00	67.33	81.67	523.75	637.42
75.00	67.36	81.64	518.75	642.42

□ IMPORT FILE "STRESS.VRT" INTO THE SPREADSHEET TABLE IV.3.

The file "STRESS.VRT" contains the stresses due to the applied vertical loads as explained in Sec. 5.4. Since the file will be imported into columns [B through E] of Table IV.3 of the spreadsheet, it is important to check that the number of rows in the file does not exceed 80. Also, one should check that the computed stresses are placed in the file in the correct order as was explained in Sec. 5.4.

To import the file, move the cursor to the cell in the first row and the second column of numbers of Table IV.3. Use " / FILE IMPORT NUMBERS A:\STRESS.VRT ", and press RETURN. The file is imported into columns [B through E] of Table IV.3. The table now takes this form:

TABLE IV.3.

Distance (ft)	Bottom flange stress envelopes due to vertical loads (dead + live + impact) (ksi)				Bottom flange stress envelopes due to vertical loads and the strengthening system (ksi)			
	Exterior Stringer		Interior Stringer		Exterior Stringer		Interior Stringer	
	Maximum Tension	Maximum Compres.	Maximum Tension	Maximum Compres.	Maximum Tension	Maximum Compres.	Maximum Tension	Maximum Compres
0.00	0.00	0.00	0.00	0.00	0.00	0.00	0.00	0.00
1.00	2.39	0.25	2.50	0.35	2.39	0.29	2.63	0.53
2.00	4.59	0.45	4.82	0.65	4.60	0.54	5.08	1.00
3.00	6.65	0.61	6.98	0.90	6.67	0.74	7.37	1.43
. .								
. .								
. .								
. .								
. .								
72.00	20.70	-0.68	21.09	0.03	17.71	-2.22	17.59	-2.21
73.00	20.90	-0.21	21.31	0.47	17.93	-1.72	17.80	-1.80
74.00	21.00	0.20	21.42	0.85	18.06	-1.26	17.89	-1.44
75.00	21.00	0.58	21.42	1.19	18.07	-0.85	17.87	-1.13
MAX.	21.56		22.48		18.15		18.03	
MIN.		-24.36		-20.23		-17.67		-16.35

- **CHECK THE MAXIMUM STRESSES IN THE LAST TWO ROWS OF TABLE IV.3.**

The last two rows of Table IV.3 entitled "MAX & MIN" give the maximum positive and negative stresses in the bottom flanges of the stringers, respectively. The values in the last four columns of these rows indicate the maximum and minimum stresses after strengthening and should not exceed the allowable stress limits.

In this example, the maximum tension stress on the interior stringer was found to be 18.03 ksi on the exterior stringer and 18.15 ksi on the interior stringer, which are slightly larger than the allowable stress limit of 18 ksi. The reason for this is that in this design procedure, the maximum stress section was assumed to be at a distance of 40% of the end-span length from the support. Checking the stress values in Table IV.3, the actual maximum stress section is shifted slightly towards the midspan. To account for this slight overstress, one possibility is to increase the overstress value at sec. [4] and repeat the spreadsheet design steps starting from Table II.2.

Overstress at sec. [1] = 3.56 + (18.03 - 18.0) = 3.59 ksi.
Overstress at sec. [4] = 4.48 + (18.15 - 18.0) = 4.63 ksi.
Details of the repeated design steps are not shown here.

- **DISPLAY GRAPHS OF THE FINAL STRESSES ON THE EXTERIOR AND INTERIOR STRINGERS ON THE SCREEN. CHECK THAT STRINGER STRESSES AFTER STRENGTHENING ARE BELOW THE ALLOWABLE LIMIT AT ALL LOCATIONS**

Reviewing the graphs of the final stresses is particularly important due to the several locations along the stringers at which the stresses could exceed the allowable limits.

To view the graphs use " / GRAPH NAME USE ", use the arrow keys to choose the desired graph, and press RETURN.

After viewing, the user can leave the graphics screen by pressing RETURN. Four named graphs are available for the engineer to review:

EXTINITL: Exterior stringer stress envelopes before strengthening: See Fig. 5.3a.

INTINITL: Interior stringer stress envelopes before strengthening: See Fig. 5.3b.

EXTFINAL: Exterior stringer stress envelopes after strengthening: See Fig. 5.7a

INTFINAL: Interior stringer stress envelopes after strengthening: See Fig. 5.7b

5.9.2. Stresses in the top flanges of the steel stringers

□ CHECK THE STRESSES IN THE STRINGER TOP FLANGES

In positive moment regions, the stresses in the top fibers of the steel stringers are relatively small. In this example, the maximum stresses in the top fibers before strengthening are equal to:

- 5.17 ksi at Sec. [1]
- 6.93 ksi at Sec. [4]

Since the stresses are below the allowable stress level, and the effect of the strengthening system is to produce a reduction in stresses at these sections, there is no need to check the stresses after strengthening.

In the negative moment regions, all stresses are computed based on the "bare" steel sections. Due to the symmetry of the section and the top and bottom coverplates, the stresses in the top flange are equal to those in the bottom flange. Also, since the axial forces resulting from the post-tensioning system are small at the piers, the stress reduction is achieved solely by the moments imposed

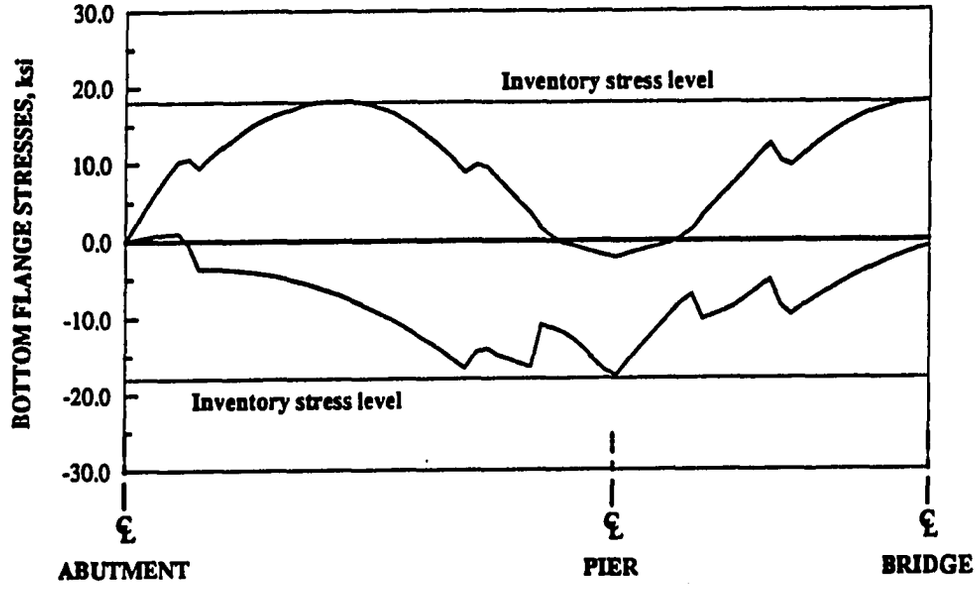

a. EXTERIOR STRINGER

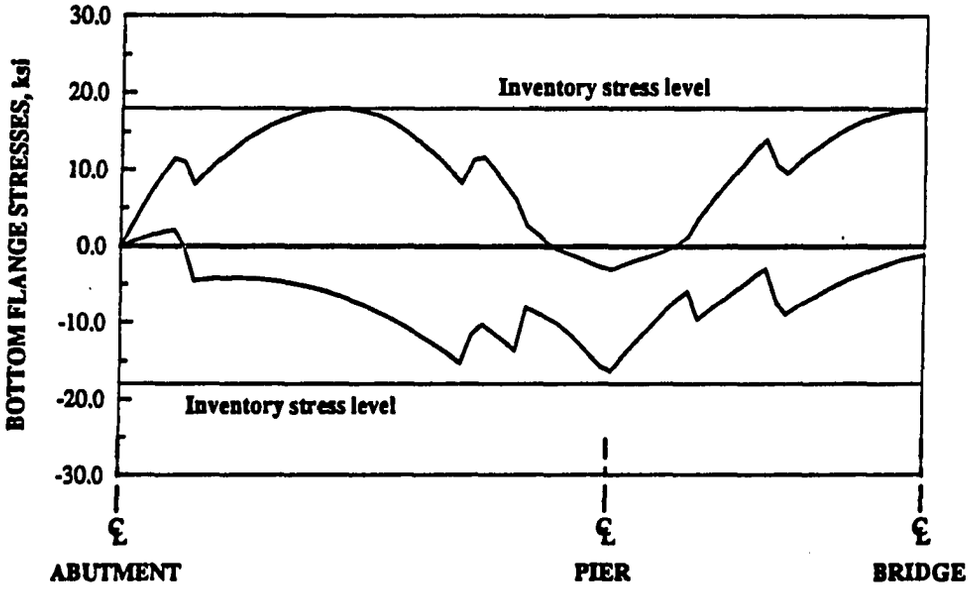

b. INTERIOR STRINGER

Fig. 5.7. Stress envelopes due to vertical loads and strengthening system.

by the strengthening system. Therefore, the stress reduction is the same at the top and bottom fibers, and there is no need for an additional stress check.

5.9.3. Stresses in the concrete deck

□ CHECK THE STRESSES IN THE CONCRETE DECK

The allowable compression stress in the concrete is given by:

$$f_{call} = 0.4\ f'_c = 0.4 \times 3.00 = 1.2 \text{ ksi comp.}$$

In this example, the maximum compression stresses in the concrete deck are equal to:

0.44 ksi comp.	< 1.20 ksi comp.	at Sec. [1]
0.59 ksi comp.	< 1.20 ksi comp.	at Sec. [4]

The effect of the strengthening system is to reduce the concrete stresses at these sections. However, one must check to determine if there are excessive tension stresses at these sections which would cause excessive deck cracking.

5.10. Accounting for post-tensioning losses and approximations in the design methodology

As explained in Sec. 4.1.2, several assumptions have been made in developing the design methodology which may result in some small errors in the computed strengthening forces. In addition, the post-tensioning losses which occur in the tendons with time need to be taken into account.

In the force and moment fraction formulas, the error range varies from one formula to another, which makes it difficult to account for the errors using the error ranges given in Appendix A. An easier approach to account for the errors and losses is outlined in Sec. 4.1.2. The approach is based on increasing the design force values by 8% and

checking the stringer stresses for the design forces with and without the increase.

- **INCREASE ALL DESIGN FORCE VALUES BY 8%**

F1 = 41.00 x 1.08 = 44.28 kips
F2 = 67.00 x 1.08 = 72.36 kips
F3 = 9.50 x 1.08 = 10.26 kips
F4 = 82.00 x 1.08 = 88.56 kips
F5 = 82.00 x 1.08 = 88.56 kips

- **CHECK STRINGER STRESSES FOR THE REVISED DESIGN FORCES**

Although the revised Table III.3 with F1= 44.28 kips, F2= 72.36 kips, etc. has not been included, all stresses were within allowable limits. The user should input the new design force values into the "Force" column in Table III.3 and repeat the stress check procedure.

6. SUMMARY AND CONCLUSIONS

6.1. Summary

Two methods of strengthening continuous-span composite bridges have been described in this study. The first is the post-tensioning of the positive moment regions of the bridge stringers, the second is the addition of superimposed trusses to the exterior stringers at the piers.

The use of post-tensioning and superimposed trusses is an efficient method of correcting flexural overstresses in undercapacity bridges. However, if the bridge has other deficiencies such as inadequate shear connection, fatigue problems, or extensive corrosion, correction or elimination of these problems must be considered in the decision to strengthen or replace a given bridge.

Transverse and longitudinal distribution of axial forces and moments induced by the strengthening system occur since the bridge is an indeterminant structural unit. The force and moment distribution fraction formulas developed in this study (valid for standard Iowa DOT V12 and V14, three-span, four-stringer bridges) provide the practicing engineer with a tool for determining the distribution of forces and moments induced by the strengthening system throughout the bridge. These formulas are valid within the limits of the variables stated in this thesis. Use of the distribution fraction formulas beyond these limits is not recommended.

Post-tensioning (and the superimposed trusses) will reduce elastic, flexural-tension stresses in bridge stringers, will induce a small amount of camber, and will increase the strength of the bridge. Post-tensioning of the positive moment regions and the application of superimposed trusses both increase the redundancy of the original structure and thus increase its strength.

For long-term preservation of the strengthening system, components (such as the tendons, brackets, truss tubes, etc.) must be protected against corrosion. It also should be noted that removal of portions of the bridge deck or integral curbs after strengthening will cause losses in the tendon forces. Also, reduction of the cross-section (due to removal of a portion of the deck or integral curbs) while the bridge is post-tensioned will result in undesired (and possibly damaging) large upward deflections of the bridge. Thus, in most instances, it is advisable to completely remove or significantly reduce the post-tensioning forces before removing portions of deck and/or integral curbs.

A finite element model for the analysis of continuous span bridges was developed using the finite element analysis package ANSYS. The model was verified using experimental data from previous research projects. The theoretically predicted results showed good agreement with the experimental results.

A design methodology was developed to provide the practicing engineer with a method for designing a strengthening system for continuous-span composite bridges. The design methodology is extremely complex due to the fact that both transverse and longitudinal distribution of the strengthening forces must be taken into account. To simplify the procedure, a spreadsheet has been developed for use by practicing engineers. This design aid greatly simplifies the design of a strengthening system for a given bridge in that it eliminates numerous tedious hand calculations, computes the different force and moment fractions, and performs the necessary iterations for determining the required strengthening forces.

As part of this research project, one continuous-span composite bridge was strengthened by post-tensioning the positive moment regions of all stringers and by adding

superimposed trusses at the piers of exterior stringers. The bridge was instrumented and field-tested before and after strengthening.

With the help of the Office of Bridge Design at the Iowa DOT, the bridge to be strengthened was selected. This bridge is a three-span, continuous, steel-stringer, concrete-deck bridge from the V12 series. The bridge is located in Cerro Gordo County approximately 12 miles south of Mason City, Iowa. The total length of the bridge is 150 ft. Exterior stringers are W21x62 and the interior stringers are W24x76.

The bridge was analyzed for overstresses considering Iowa legal loads using AASHTO standard procedures. A strengthening system composed of post-tensioning in the positive moment regions of the stringers and superimposed trusses at the intermediate supports of the exterior stringers was designed to reduce the overstresses in the bridge stringers.

The field work included application of the post-tensioning brackets and tendons in the positive moment regions and the truss tubes, brackets, and tendons at the piers. Shear connectors were added in the positive moment regions to satisfy the current AASHTO design specification [23].

Field tests were performed to evaluate the structural behavior of the strengthened bridge when subjected to the strengthening forces as well as live loads. Load tests with heavily loaded trucks were performed before and after strengthening. Strain gages and direct current displacement transducers were used to measure the effect of the applied loads.

6.2. Conclusions

Based on the research performed and presented in this thesis the following conclusions have been made:

1. Iowa continuous span composite bridges with exterior stringers slightly smaller than the interior stringers can be strengthened to meet AASHTO and Iowa legal load standards by post-tensioning the positive moment regions of the stringer spans. Sometimes the addition of superimposed trusses at the piers of the exterior stringers is needed.
2. Using superimposed trusses at the piers of the exterior stringers together with the post-tensioning, considerably reduces the required post-tensioning forces required to achieve the stress reduction. In this case, the resulting stresses along the stringers are generally less, and the potential of slab cracking is less.
3. The fabrication and installation of a post-tensioning system on the bridge stringers is easier and less costly than using superimposed trusses. It is therefore recommended to use only post-tensioning for strengthening if there was no strong need for the superimposed trusses.
4. A finite element model was developed which accurately predicted the behavior of a composite bridge due to the effect of post-tensioning and superimposed trusses. The model was verified using test results from previous work done in the Iowa State University Laboratory and in the field.
5. The finite element model developed was used to design a strengthening system for a 3-span, 4-stringer, composite bridge near in Cerro Gordo county, Iowa. Comparison of the finite element analysis results and

the field results showed good agreement. The differences between theoretical and field-measured values were more for the superimposed trusses than for the post-tensioning system.

6. There is considerable end-restraint on the abutment-ends of the end-span stringers, which causes some difference between the field and analytical results.
7. The resulting strains in the guardrails were significant which caused the strains induced by the superimposed trusses to be generally less than expected.
8. The post-tensioning system and the superimposed trusses produced beneficial strains in the bridge stringers both in the positive and negative moment regions.
9. The axial forces resulting from the post-tensioning of stringers in one span have a small effect on the other spans, whereas the resulting moments in the other spans are significant. Longitudinal distribution should therefore be considered.
10. The design methodology developed in this thesis and presented in the associated design manual is an effective means of designing a strengthening system for continuous-span, composite, steel-stringer bridges.
11. In the design methodology developed, force and moment distribution fractions were developed at several locations along the bridge length. Linear interpolation for the axial forces and moments between these locations accurately represents the actual force and moment diagrams on the stringers.
12. The force and moment fractions at the different locations in typical Iowa three-span four-beam composite bridges can be determined accurately from the formulas developed in this investigation.

13. In this study, it was determined that most the deck thickness, beam spacing, bridge length, span lengths, and the lengths of the post-tensioning and the superimposed truss tendons have the most significant effect on the force and moment distribution fractions.
14. The spreadsheet developed in this research study provides a useful tool for the practicing engineer to use in designing a strengthening system for Iowa typical continuous-span composite bridges.

7. RECOMMENDED FURTHER RESEARCH

On the basis of the literature reviewed and the work completed in the area of bridge strengthening (for this project as well as for previous projects), it would be logical to consider continuing related research as follows:

1. Data from the investigation as well as from other investigations have determined that the guardrails are supporting a significant portion of the live load. The various guardrail configurations, connections, etc. should be reviewed and analyzed so that their structural contribution to the capacity of the bridge can be taken into account in the rating process. Modifications that could increase the structural contribution of the guardrail to the capacity of the bridge should also be investigated.
2. Although approximate procedures have been developed for determining the ultimate strength of the two strengthening procedures, these procedures should be extended and possibly modified to be consistent with the AASHTO LRFD Specifications.
3. With consideration of the new AASHTO Manual for Maintenance Inspection of Bridges, a practical method for evaluating the strength provided by the strengthening system should be developed for use by bridge rating engineers.
4. The combination of post-tensioning the positive moment regions and superimposed trusses was successful in eliminating the overstresses in the positive and

negative moment regions of the bridge investigated in this project.

5. To date, all post-tension strengthening research has been tested and implemented on steel stringers. The post-tension strengthening procedures developed should be tested on reinforced concrete and prestressed concrete beams. Such a strengthening scheme could also be used for repairing damaged beams. A preliminary study to determine the current state-of-the-art and the feasibility of the strengthening procedures is appropriate.
6. The use of prestressing should be reviewed for use in new designs. Based on preliminary analysis, it appears post-tensioning of steel stringers in new bridges can result in considerable weight savings. A theoretical as well as laboratory investigation of this concept should be initiated.

REFERENCES

1. American Association of State Highway Officials, *Standard Specifications for Highway Bridges, 7th Edition,* Washington, D.C., 1957.

2. Klaiber, F. W., T. J. Wipf, F. S. Fanous, T.E. Bosch, H. El-Arabaty. *Strengthening of an Existing Continuous-Span, Steel-Beam, Concrete Deck Bridge,* Final Report, Iowa DOT Project HR-333, ISU-ERI-Ames-94403. Ames: Engineering Research Institute, Iowa State University, Ames, IA, 1993.

3. Klaiber, F. W., F. S. Fanous, T. J. Wipf, H. El-Arabaty. *Design Manual for Strengthening of a Continuous-Span Composite Bridge,* ISU-ERI-Ames-94404. Ames: Engineering Research Institute, Iowa State University, Ames, IA, 1993.

4. Klaiber, F. W., , K. F., Dunker, S. M. Planck, W. W. Sanders, Jr. *Strengthening of an Existing Continuous-Span, Steel-Beam, Concrete Deck Bridge by Post-Tensioning,* Final report, Iowa DOT Project HR-308, ISU-ERI-Ames-90210. Ames: Engineering Research Institute, Iowa State University, Ames, IA, 1990.

5. Dunker, K. F., F. W. Klaiber, F. K. Daoud, W. E. Wiley, W. W. Sanders, Jr. *Strengthening of Existing Continuous Composite Bridges,* Final Report, ISU-ERI-Ames-88007, Ames: Engineering Research Institute, Iowa State University, Ames, IA, 1987.

6. Dunker, K. F., F. W. Klaiber, W. W. Sanders, Jr. *Design Manual for Strengthening Single-Span Composite Bridges by Post-Tensioning,* Final Report-Part III. ISU-ERI-Ames-85229. Ames: Engineering Research Institute, Iowa State University, Ames, IA, 1985.

7. Klaiber, F. W., D. J. Dedic, K. F. Dunker, W. W. Sanders, Jr. *Strengthening of Existing Single Span Steel Beam and Concrete Deck Bridges,* Final Report-Part I. ISU-ERI-Ames-83185. Ames: Engineering Research Institute, Iowa State University, Ames, IA, 1983.

8. Dunker, K. F., F. W. Klaiber, B. L. Beck, W. W. Sanders, Jr. *Strengthening of Existing Single-Span Steel-Beam and Concrete Deck Bridges,* Final Report-Part

II. ISU-ERI-Ames-85231. Ames: Engineering Research Institute, Iowa State University, Ames, IA, 1985.

9. Klaiber, F. W., K. F. Dunker, W. W. Sanders, Jr. *Feasibility Study of Strengthening Existing Single Span Steel Beam Concrete Deck Bridges,* Final Report. ISU-ERI-Ames-81251. Ames: Engineering Research Institute, Iowa State University, Ames, IA, 1981.

10. Klaiber, F. W., Wipf, T. J., Dunker, K. F., Abu-Kishk, R. B., Planck, S. M. *Alternate Methods of Bridge Strengthening,* Final Report. ISU-ERI-Ames-89262. Ames: Engineering Research Institute, Iowa State University, Ames, IA, 1989.

11. Klaiber, F. W., K. F. Dunker, T. J. Wipf, W. W. Sanders, Jr. *Methods of Strengthening Existing Highway Bridges,* National Cooperative Highway Research Program Report 293, Transportation Research Board, 1987, pp. 114.

12. Klaiber, F. W., K. F. Dunker, T. J. Wipf, Fanous, F. S. *Strengthening of Existing Bridges by Post-Tensioning,* Symposium on Practical Solutions for Bridge Strengthening & Rehabilitation, Proceedings. Bridge Engineering Center, Iowa State University, 1993, pp. 143-152.

13. Saadatmanesh, H., P. Albrecht, B. M. Ayyub. *Guidelines for Flexural Design of Prestressed Composite Beams,* Journal of Structural Engineering, ASCE, 115, No. 11, November, 1989, pp. 2944-2961.

14. Ayyub, B. M., Y. G. Sohn, H. Saadatmanesh. *Prestressed Composite Girders. I: Experimental Study for Negative Moment,* Journal of Structural Engineering, ASCE, 118, No. 10, October, 1992, pp. 2743-2762.

15. Ayyub, B. M., Y. G. Sohn, H. Saadatmanesh. *Prestressed Composite Girders. II: Analytical Study for Negative Moment,* Journal of Structural Engineering, ASCE, 118, No. 10, October, 1992, pp. 2763-2782.

16. Ayyub, B. M., Y. G. Sohn, H. Saadatmanesh. *Prestressed Composite Girders Under Positive Moment,* Journal of Structural Engineering, ASCE, 116, No. 11, November, 1990, pp. 2931-2951.

17. Tong, W., H. Saadatmanesh. *Parametric Study of Continuous Prestressed Composite Beams,* Journal of

Structural Engineering, ASCE, 118, No. 1, January, 1992, pp. 186-206.

18. Mancarti, G. D. *Strengthening Short Span Bridges for Increased Live Loads,* Proceedings of the Third International Conference on Short and Medium Span Bridges, Canadian Society of Civil Engineers, Volume II, 1990, pp. 169-180.

19. Albrecht, P., W. Li. *Fatigue Strength of Prestressed Composite Beams,* Final Report. NSF Project ECE-85-13684, University of Maryland, College Park, MD 1990.

20. Saadatmanesh, H., M. R. Ehsani. *RC Beams Strengthened with GFRP Plates. I: Experimental Study. Journal of Structural Engineering,* ASCE, 117, No. 11, November, 1991, pp. 3417-3433.

21. An, W., H. Saadatmanesh. *RC Beams Strengthened with FRP Plates. II: Analysis and Parametric Study,* Journal of Structural Engineering, ASCE, 117, No. 11, November, 1991, pp. 3434-3455.

22. Seible, F., Priestley, M. J. N., and Krishnan, K., *Bridge Superstructure Rehabilitation and Strengthening,* Transportation Research Record, No. 1290, Volume 1, 1991, pp. 59-67.

23. American Association of State Highway and Transportation Officials. *Standard Specifications for Highway Bridges, 14th Edition,* Washington, D.C., 1989.

24. Dedic, D. J. *Push-out and Composite Beam Tests of Shear Connectors.* M. S. Thesis, Iowa State University, Ames, Iowa, 1983.

25. Klaiber, F. W., T. J. Wipf, K. F. Dunker, R. B. Abu-Kishk, and S. M. Plank. *Alternate Methods of Bridge Strengthening,* Final Report, ERI Project 1961, ISU-ERI-Ames-892677. Ames: Engineering Research Institute, Iowa State University, Ames, Iowa, 1989.

26. Standard Design, Continuous 3-Span I-Beam Bridges, 24 ft Roadway, Concrete Floor, Steel Rail, H-15 Loading. Ames: Iowa State Highway Commission, 1957.

27. Standard Design, 28 ft Roadway, Continuous I-Beam Bridges, Concrete Floor, Steel Rail, H-20 Loading. Ames: Iowa State Highway Commission, 1960.

28. DYWIDAG Systems International, USA, Inc. *DYWIDAG Threadbar Post-tensioning System,* Lemont, IL : DYWIDAG Systems International, USA, Inc., 1983.

29. Enerpac. *Hydraulic Tools for General Construction,* CS 653 Catalog. Butler: Enerpac, 1980.

ACKNOWLEDGEMENTS

All praise belongs to God. Only through His help and guidance was this work accomplished. He is the Most Gracious, Most Merciful.

My deepest gratitude is due to my major professors Dr. F. Wayne Klaiber, Dr. Fouad S. Fanous, and Dr. Terry J. Wipf for their continuous guidance and encouragement throughout the course of this work.

I would like to express my thanks to Dr. Loren W. Zachary and Dr. Thomas J. Rudolphi for their valuable advice and comments as members of my graduate committee.

This study is sponsored by the Iowa Department of Transportation Highway Division and the Iowa Highway Research Board under Research Project HR 333. Sincere appreciation is accorded to the engineers of the Iowa DOT for their support, cooperation and counseling.

APPENDIX A

FORMULAS FOR FORCE AND MOMENT FRACTIONS

Definition of terms

R^2 = Coefficient of Determination.

ERROR = Predicted value (using formula)

– Actual value (from finite element analysis).

Strengthening schemes:

Case A : Post-tensioning of all end-span exterior stringers.

Case B : Post-tensioning of all end-span interior stringers.

Case C : Post-tensioning of all center-span exterior stringers.

Case D : Post-tensioning of all center-span interior stringers.

Case E : Superimposed trusses on exterior stringers at all pier locations.

For cases A, C, and E:

$$FF_i = \text{Force Fraction at Sec (i)} = \frac{\text{Axial force in exterior stringer at Sec (i)}}{\text{Total axial force on the bridge at Sec (i)}}$$

$$MF_i = \text{Moment Fraction at Sec (i)} = \frac{\text{Moment in exterior stringer at Sec (i)}}{\text{Total moment on the bridge at Sec (i)}}$$

For cases B and D:

$$FF_i = \text{Force Fraction at Sec (i)} = \frac{\text{Axial force in interior stringer at Sec (i)}}{\text{Total axial force on the bridge at Sec (i)}}$$

$$MF_i = \text{Moment Fraction at Sec (i)} = \frac{\text{Moment in interior stringer at Sec (i)}}{\text{Total moment on the bridge at Sec (i)}}$$

Definition of parameters

$$X_L = 0.0167 \times \frac{\text{TOTAL BRIDGE LENGTH}}{\text{STRINGER SPACING}} + 0.3$$

$$0.50 < X_L < 1.00$$

$$X_S = 9.0 \times \frac{\text{DECK THICKNESS}}{\text{STRINGER SPACING}}$$

$$0.50 < X_S < 1.00$$

$$X_{P1} = 1.5 \times \frac{\text{LENGTH OF POST} - \text{TENSIONED PORTION OF END SPAN}}{\text{LENGTH OF END SPAN}}$$

$$0.60 < X_{P1} < 1.00$$

$$X_{P2} = 1.5 \times \frac{\text{LENGTH OF POST} - \text{TENSIONED PORTION OF CENTER SPAN}}{\text{LENGTH OF CENTER SPAN}}$$

$$0.60 < X_{P2} < 1.00$$

$$X_{P3} = 1.5 \times \frac{\text{LENGTH OF SUPERIMPOSED TRUSS TENDON}}{\text{LENGTH OF END SPAN}}$$

$$0.60 < X_{P3} < 1.00$$

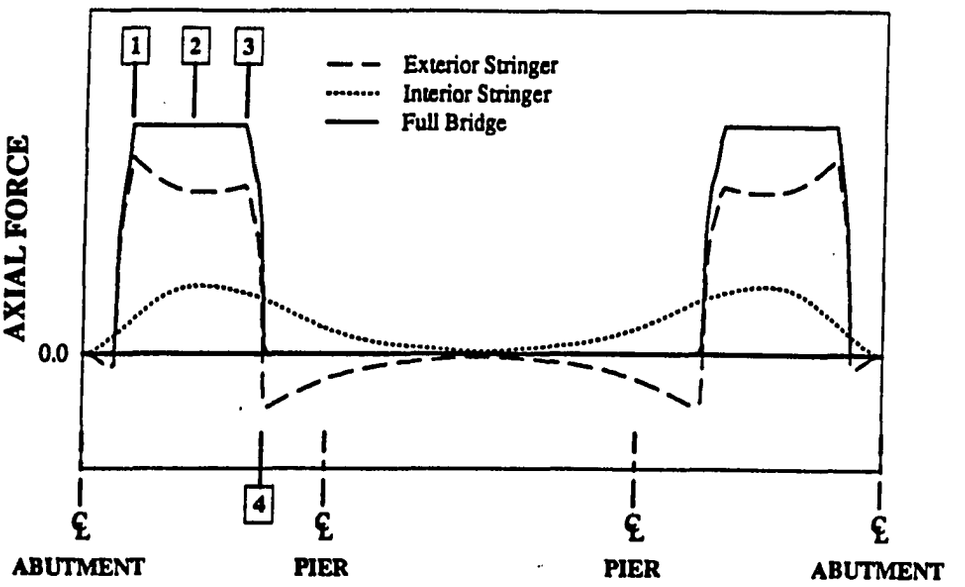

a. AXIAL FORCE

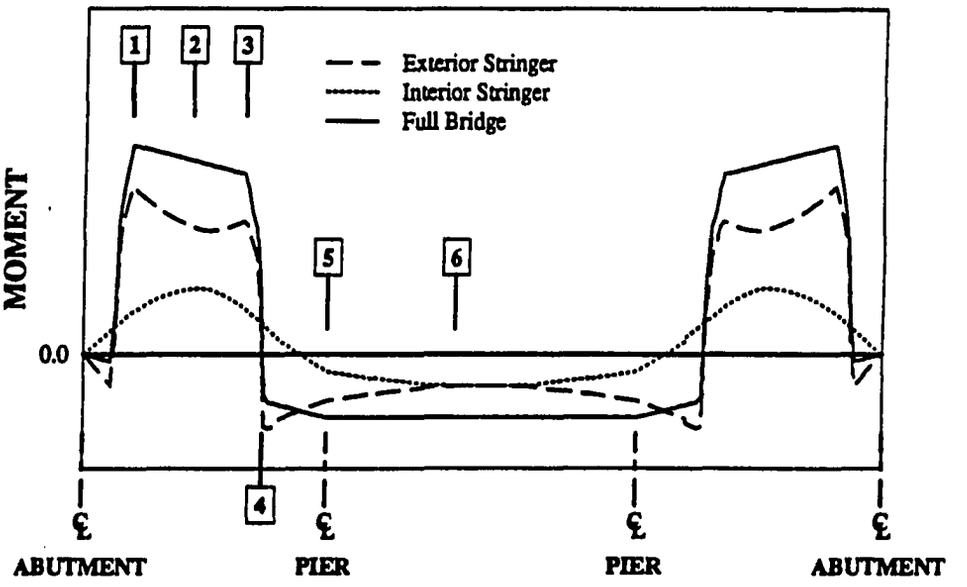

b. MOMENT

Fig. A.1. Locations of distribution fractions: Strengthening scheme [A].

Table. A.1. Force Fractions for strengthening scheme [A].

$$FF_1 = 0.1659 + \frac{0.4171}{X_S} + \frac{0.0490}{X_L} - 0.1035\ X_{P1}$$

$0.76 < FF_1 < 0.92$; $R^2 = 0.98$; $-0.010 < ERROR < +0.015$

$$FF_2 = -0.1460 + \frac{0.6331}{X_S} + \frac{0.0465}{X_L} - 0.2650\ X_{P1}$$

$0.62 < FF_2 < 0.84$; $R^2 = 0.97$; $-0.020 < ERROR < +0.020$

$$FF_3 = -0.1928 + \frac{0.4057}{X_S} + \frac{0.0234}{X_L} + \frac{0.2099}{X_{P1}}$$

$0.66 < FF_3 < 0.82$; $R^2 = 0.97$; $-0.015 < ERROR < +0.015$

$$FF_4 = -0.1254 + 0.4852\ X_S - 0.0181\ X_L + \frac{0.0377}{X_L} + 0.0763\ X_{P1} - \frac{0.0417}{X_L\ X_{P1}}$$

$0.17 < FF_4 < 0.25$; $R^2 = 0.96$; $-0.008 < ERROR < +0.010$

Table. A.2. Moment Fractions for strengthening scheme [A].

$$MF_1 = 1.4444 - 1.0496\,X_S - 0.1532\,X_L + \frac{0.0724}{X_{P1}}$$

$0.68 < MF_1 < 0.86$; $R^2 = 0.98$; $-0.010 < ERROR < +0.013$

$$MF_2 = 1.6750 - 1.4748\,X_S + \frac{0.0782}{X_L} - \frac{0.2663}{X_{P1}}$$

$0.53 < MF_2 < 0.82$; $R^2 = 0.99$; $-0.015 < ERROR < +0.020$

$$MF_3 = 0.0084 + \frac{0.3657}{X_S} + \frac{0.0525}{X_L} + 0.0503\,X_{P1}$$

$0.66 < MF_3 < 0.82$; $R^2 = 0.98$; $-0.015 < ERROR < +0.020$

$$MF_4 = -5.8310 + 0.8482\,X_S - 0.6426\,X_L + \frac{0.6780}{X_L} + 1.7923\,X_{P1} + \frac{4.7586}{X_{P1}} + 0.5884\,X_L\,X_{P1} - \frac{0.6578}{X_L\,X_{P1}}$$

$1.20 < MF_4 < 2.00$; $R^2 = 0.99$; $-0.030 < ERROR < +0.040$

$$MF_5 = +2.8190 - 2.3043\,X_S - 0.2371\,X_L + \frac{0.1034}{X_L} - \frac{0.6381}{X_{P1}}$$

$0.35 < MF_5 < 1.00$; $R^2 = 0.98$; $-0.040 < ERROR < 0.060$

$$MF_6 = +0.8804 - 0.8078\,X_S + 0.0570\,X_L + \frac{0.0547}{X_L}$$

$0.47 < MF_6 < 0.57$; $R^2 = 0.96$; $-0.015 < ERROR < +0.025$

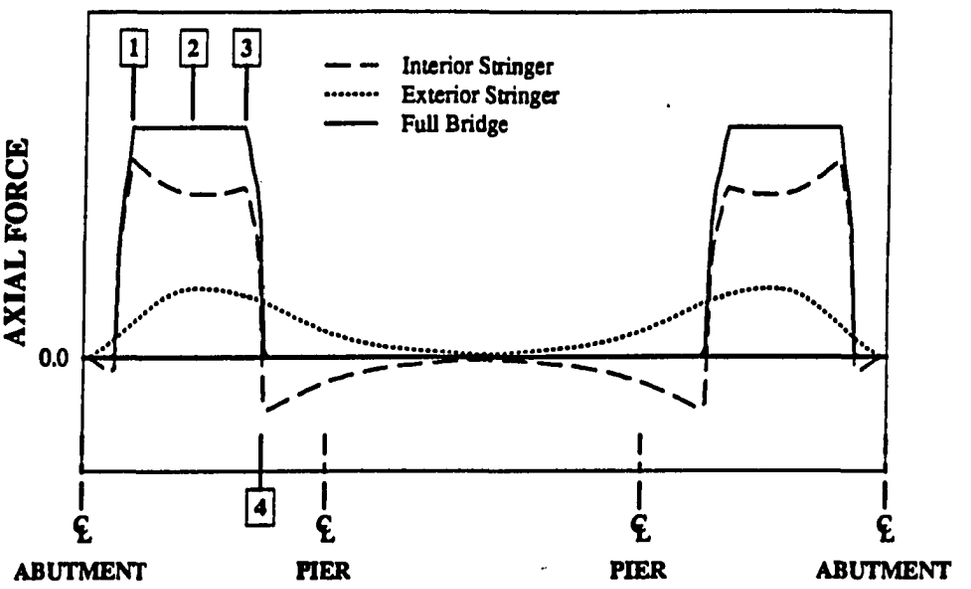

a. AXIAL FORCE

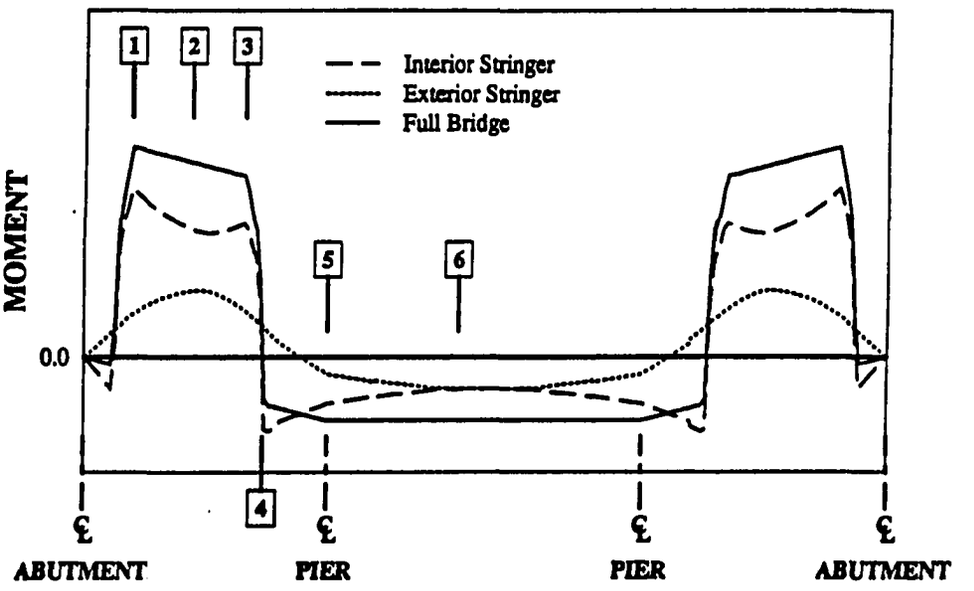

b. MOMENT

Fig. A.2. Locations of distribution fractions: Strengthening scheme [B].

Table. A.3. Force Fractions for strengthening scheme [B].

$$FF_1 = 1.4847 - 1.1178\ X_S + 0.1157\ X_L + \frac{0.0419}{X_L} - 0.0576\ X_{P1} - 0.0464\ X_L\ X_{P1}$$

$$0.81 < FF_1 < 0.92\ ;\ R^2 = 0.96\ ;\ -0.015 < ERROR < +0.015$$

$$FF_2 = 1.7760 - 1.6438\ X_S + 0.1516\ X_L + \frac{0.0617}{X_L} - 0.2043\ X_{P1}$$

$$0.70 < FF_2 < 0.86\ ;\ R^2 = 0.96\ ;\ -0.020 < ERROR < +0.015$$

$$FF_3 = 1.4215 - 1.0827\ X_S - 0.0356\ X_L + \frac{0.0395}{X_L} - 0.2193\ X_{P1} + \frac{0.0828}{X_{P1}} + 0.1636\ X_L\ X_{P1}$$

$$0.72 < FF_3 < 0.86\ ;\ R^2 = 0.96\ ;\ -0.015 < ERROR < +0.015$$

$$FF_4 = -0.2683 + 0.5053\ X_S + 0.0411\ X_L - \frac{0.0219}{X_L} + 0.2395\ X_{P1} - 0.1342\ X_L\ X_{P1}$$

$$0.13 < FF4 < 0.21\ ;\ R^2 = 0.97\ ;\ -0.006 < ERROR < +0.008$$

Table. A.4. Moment Fractions for strengthening scheme [B].

$$MF_1 = 1.1697 - 0.9576\,X_S + \frac{0.0405}{X_L} + \frac{0.1008}{X_{P1}} + 0.0849\,X_L\,X_{P1}$$

$0.77 < MF_1 < 0.87$; $R^2 = 0.96$; $-0.020 < ERROR < +0.010$

$$MF_2 = 1.0494 - 1.3421\,X_S + \frac{0.0652}{X_L} + \frac{0.2531}{X_{P1}} + 0.1488\,X_L\,X_{P1}$$

$0.62 < MF_2 < 0.80$; $R^2 = 0.96$; $-0.030 < ERROR < +0.015$

$$MF_3 = 1.4142 - 0.9255\,X_S - 0.3347\,X_L + 0.2518\,X_L^2 + 0.0305\,X_{P1}$$

$0.72 < MF_3 < 0.80$; $R^2 = 0.93$; $-0.015 < ERROR < +0.015$

$$MF_4 = -4.6041 + 1.1642\,X_S - 1.9754\,X_L + \frac{0.6102}{X_L} + 0.8588\,X_{P1} + \frac{4.3578}{X_{P1}} + 1.7884\,X_L\,X_{P1} - \frac{0.5963}{X_L\,X_{P1}}$$

$1.20 < MF_4 < 1.85$; $R^2 = 0.99$; $-0.030 < ERROR < +0.030$

$$MF_5 = 0.9533 - 1.8118\,X_S + \frac{0.1361}{X_L} + 0.7762\,X_{P1}$$

$0.50 < MF_5 < 1.05$; $R^2 = 0.98$; $-0.040 < ERROR < +0.030$

$$MF_6 = 0.9568 - 0.9214\,X_S + 0.1971\,X_L + \frac{0.0268}{X_L}$$

$0.50 < MF_6 < 0.59$; $R^2 = 0.95$; $-0.020 < ERROR < +0.010$

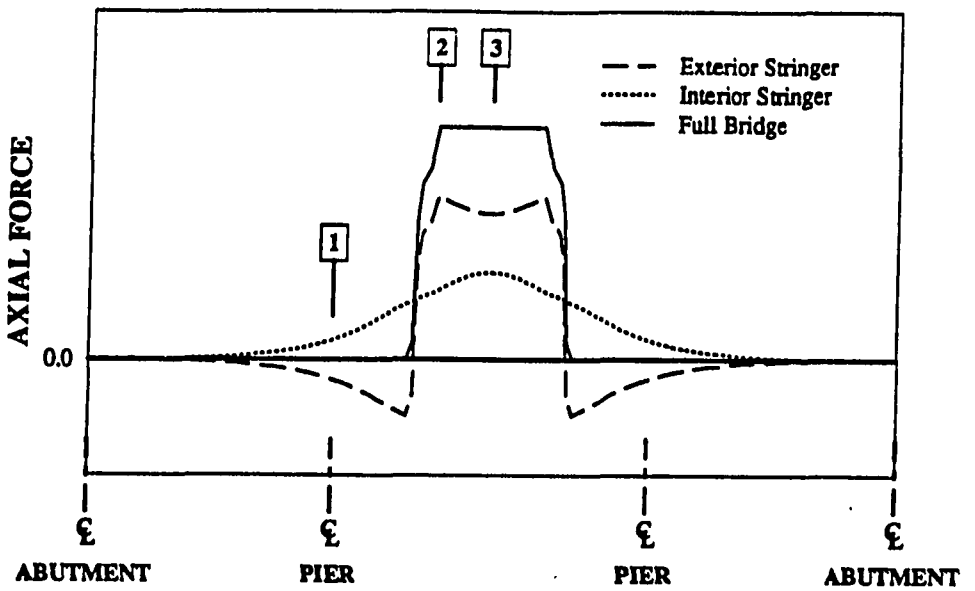

a. AXIAL FORCE

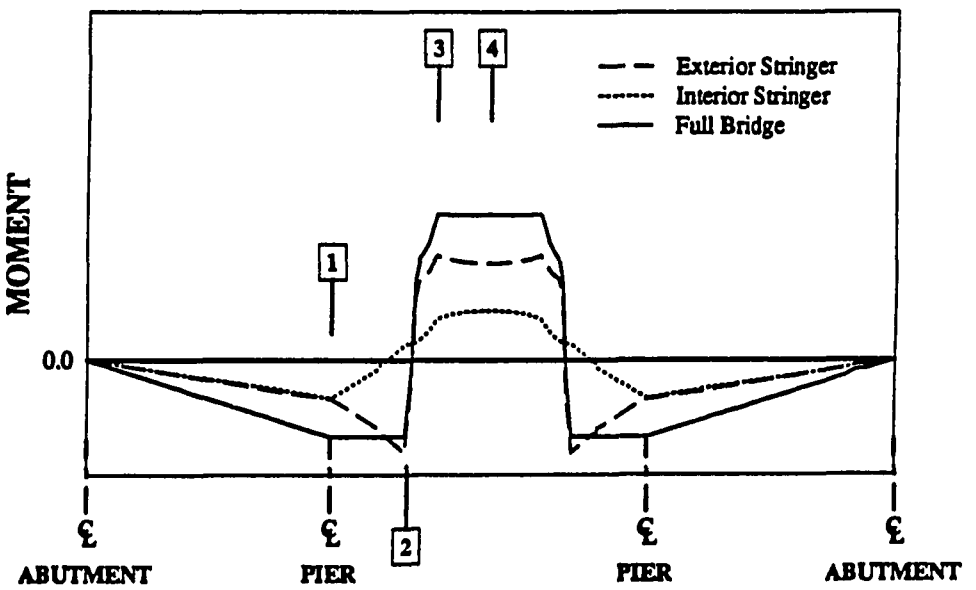

b. MOMENT

Fig. A.3. Locations of distribution fractions: Strengthening scheme [C].

Table. A.5. Force Fractions for strengthening scheme [C].

$$FF_1 = 0.1305 + 0.2323\,X_S + \frac{0.0104}{X_L} + 0.0363\,X_L\,X_{P2} - \frac{0.0527}{X_{P2}}$$

$0.21 < FF_1 < 0.27$; $R^2 = 0.84$; $-0.015 < \text{ERROR} < +0.020$

$$FF_2 = 1.1259 - 0.7558\,X_S - \frac{0.0042}{X_L} - 0.0719\,X_L\,X_{P2} + \frac{0.0604}{X_{P2}}$$

$0.63 < FF_2 < 0.75$; $R^2 = 0.93$; $-0.020 < \text{ERROR} < +0.015$

$$FF_3 = 1.4098 - 1.2269\,X_S + \frac{0.0744}{X_L} - 0.2491\,X_{P2} + \frac{0.1110}{X_{P2}} - \frac{0.0464}{X_L\,X_{P2}}$$

$0.51 < FF_3 < 0.73$; $R^2 = 0.93$; $-0.030 < \text{ERROR} < +0.030$

Table. A.6. Moment Fractions for strengthening scheme [C].

$$MF_1 = 0.9832 - 1.7646\,X_S + 0.5882\,X_{P2} + \frac{0.0831}{X_L\,X_{P2}}$$

$0.32 < MF_1 < 0.74$; $R^2 = 0.99$; $-0.025 < ERROR < +0.010$

$$MF_2 = 0.7190 - 0.6419\,X_L + \frac{0.4874}{X_L} - 1.0113\,X_{P2} + \frac{0.7383}{X_{P2}} + 0.9387 X_L\,X_{P2} - \frac{0.3317}{X_L\,X_{P2}}$$

$0.90 < MF_2 < 1.25$; $R^2 = 0.93$; $-0.060 < ERROR < +0.060$

$$MF_3 = 0.1070 - 1.060\,X_S - 0.6953\,X_L + \frac{0.2683}{X_L} + 0.2219\,X_{P2} + \frac{0.7311}{X_{P2}} + 0.9839\,X_L\,X_{P2} - \frac{0.1566}{X_L\,X_{P2}}$$

$0.65 < MF_3 < 0.83$; $R^2 = 0.98$; $-0.020 < ERROR < +0.015$

$$MF_4 = 1.7184 - 1.5195\,X_S - 0.3942\,X_L + \frac{0.2319}{X_L} - 0.6210\,X_{P2} + \frac{0.2605}{X_{P2}} + 0.4269\,X_L\,X_{P2} - \frac{0.1500}{X_L\,X_{P2}}$$

$0.50 < MF_4 < 0.77$; $R^2 = 0.98$; $-0.020 < ERROR < +0.025$

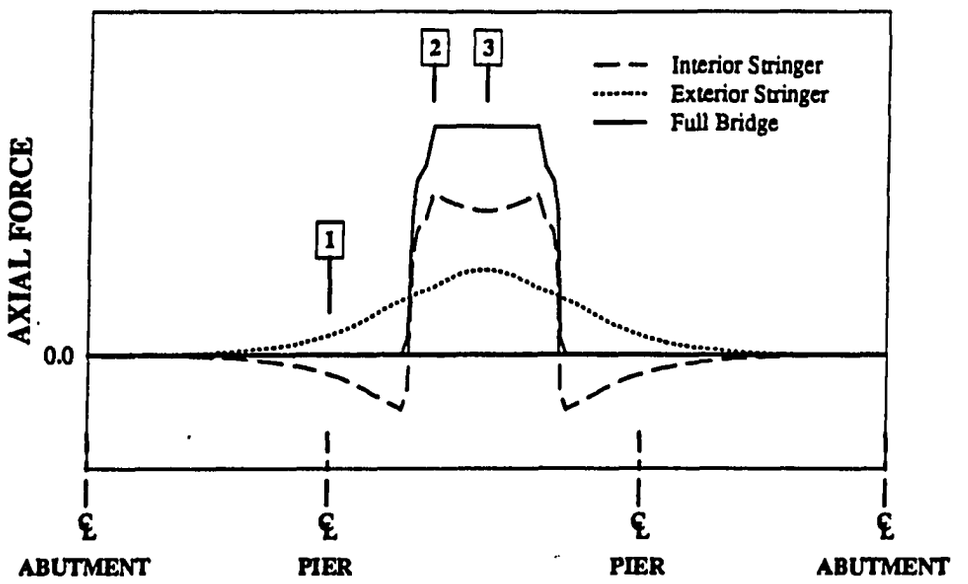

a. AXIAL FORCE

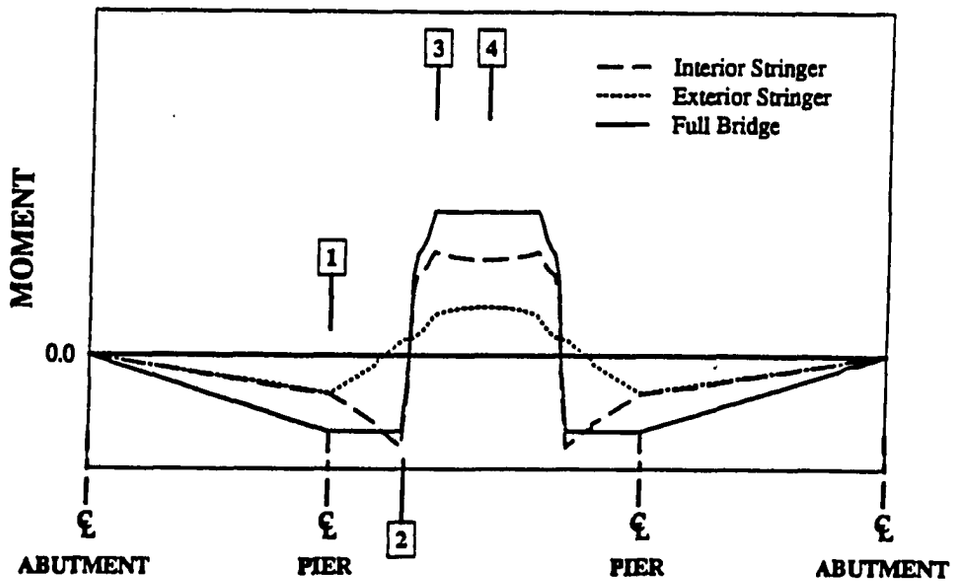

b. MOMENT

Fig. A.4. Locations of distribution fractions: Strengthening scheme [D].

Table. A.7. Force Fractions for strengthening scheme [D].

$$FF_1 = -0.0081 + 0.3222\,X_S - 0.0240\,X_L + 0.0639\,X_{P2} - \frac{0.0238}{X_{P2}}$$

$0.16 < FF_1 < 0.23$; $R^2 = 0.88$; $-0.010 < \text{ERROR} < +0.020$

$$FF_2 = 1.3411 - 0.8362\,X_S + 0.0653\,X_L - 0.1033\,X_{P2} - 0.0589\,X_L\,X_{P2}$$

$0.71 < FF_2 < 0.80$; $R^2 = 0.91$; $-0.015 < \text{ERROR} < +0.015$

$$FF_3 = 1.6851 - 1.3404\,X_S + 0.0500\,X_L - 0.2444\,X_{P2}$$

$0.60 < FF_3 < 0.78$; $R^2 = 0.90$; $-0.030 < \text{ERROR} < +0.030$

Table. A.8. Moment Fractions for strengthening scheme [D].

$$MF_1 = 0.4763 - 1.3346\ X_S + 0.1545\ X_L + \frac{0.1003}{X_L} + 0.5963\ X_{P2} + \frac{0.1720}{X_{P2}}$$

$0.50 < MF_1 < 0.75$; $R^2 = 0.96$; $-0.030 < ERROR < +0.030$

$$MF_2 = 0.7626 + 0.1591\ X_S - 1.5176\ X_L + \frac{0.5503}{X_L} - 1.2904\ X_{P2} + \frac{1.0697}{X_{P2}} + 1.7569\ X_L\ X_{P2} - \frac{0.4462}{X_L\ X_{P2}}$$

$1.00 < MF_2 < 1.30$; $R^2 = 0.95$; $-0.035 < ERROR < +0.040$

$$MF_3 = 0.2304 - 0.8381\ X_S + 0.0655\ X_L + \frac{0.0405}{X_L} + 0.6248\ X_{P2} + \frac{0.3385}{X_{P2}} + 0.0760\ X_L\ X_{P2}$$

$0.75 < MF_3 < 0.84$; $R^2 = 0.93$; $-0.020 < ERROR < +0.010$

$$MF_4 = 1.5390 - 1.4148\ X_S - 0.5483\ X_L + \frac{0.3146}{X_L} - 0.8432\ X_{P2} + \frac{0.3868}{X_{P2}} + 0.9180\ X_L\ X_{P2} - \frac{0.2036}{X_L\ X_{P2}}$$

$0.60 < MF_4 < 0.78$; $R^2 = 0.94$; $-0.040 < ERROR < +0.025$

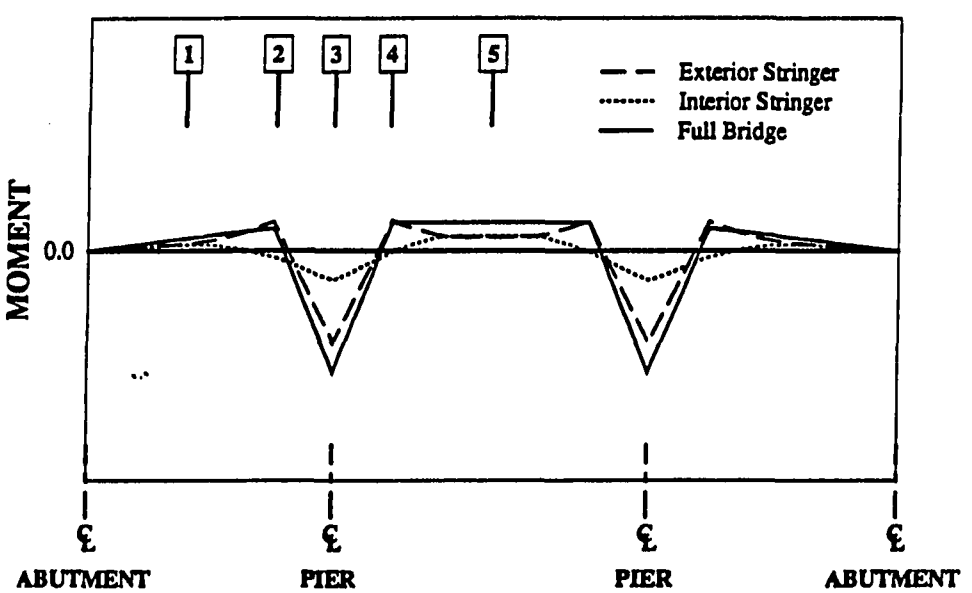

Fig. A.5. Locations of distribution fractions: Strengthening scheme [E].

Table. A.9. Moment Fractions for strengthening scheme [E].

$$MF_1 = 0.8058 - 0.9633\,X_S - 0.4868\,X_L + 0.1297\,X_{P3} + 0.4863\,X_{P3}\,X_L + \frac{0.2024}{X_L}$$

$0.15 < MF_1 < 0.85$; $R^2 = 0.99$; $-0.020 < ERROR < +0.015$

$$MF_2 = 1.0614 - 0.8774\,X_S + \frac{0.1419}{X_L} - 0.1127\,X_{P3} + \frac{0.5645}{X_{P3}} - 0.3796\,X_L\,X_{P3} - \frac{0.1302}{X_L\,X_{P3}}$$

$1.00 < MF_2 < 1.45$; $R^2 = 0.97$; $-0.050 < ERROR < +0.030$

$$MF_3 = 1.4033 - 0.9035\,X_S + 0.0520\,X_L - 0.2553\,X_{P3} - 0.1892\,X_L\,X_{P3}$$

$0.55 < MF_3 < 0.90$; $R^2 = 0.99$; $-0.008 < ERROR < +0.013$

$$MF_4 = 0.8143 - 0.4088\,X_S + 0.7628\,X_L + \frac{0.3008}{X_{P3}} - 1.5101\,X_L\,X_{P3} - \frac{0.0262}{X_L X_{P3}}$$

$0.80 < MF_4 < 1.30$; $R^2 = 0.99$; $-0.020 < ERROR < +0.025$

$$MF_5 = 0.2333 - 0.3800\,X_S + 0.3370\,X_{P3} + \frac{0.1548}{X_L}$$

$0.25 < MF_5 < 0.70$; $R^2 = 0.99$; $-0.015 < ERROR < +0.015$

APPENDIX B

DESIGN METHODOLOGY SPREADSHEET TABLES

NOTE: This appendix contains two tables which are printouts from the spreadsheet (STRCONBR.WK1). The tables are TABLE.IV.2 and TABLE.IV.3. Due to their large size only portions of these tables were given in Chp.5. The printout given in this appendix have been reduced in size.

TABLE.IV.2.

Axial forces and bending moments due to the strengthening system:

Distance (ft)	Axial Force (kips)		Bending Moment at standard neutral axis (in.k)	
	Exterior Stringer	Interior Stringer	Exterior Stringer	Interior Stringer
0.00	0.00	0.00	0.00	0.00
1.00	0.52	-0.52	-2.79	-32.70
2.00	1.04	-1.04	-5.59	-65.41
3.00	1.56	-1.56	-8.38	-98.11
4.00	2.07	-2.07	-11.18	-130.81
5.00	2.59	-2.59	-13.97	-163.52
6.00	17.61	23.39	258.28	299.47
7.00	47.13	75.87	805.59	1258.14
8.00	47.40	75.60	797.19	1231.04
9.00	47.67	75.33	788.80	1203.93
10.00	47.95	75.05	780.41	1176.83
11.00	48.22	74.78	772.02	1149.72
12.00	48.49	74.51	763.62	1122.62
13.00	48.76	74.24	755.23	1095.51
14.00	49.03	73.97	746.84	1068.40
15.00	49.30	73.70	738.45	1041.30
16.00	49.58	73.42	730.05	1014.19
17.00	49.85	73.15	721.66	987.09
18.00	50.12	72.88	713.27	959.98
19.00	50.17	72.83	702.11	935.64
20.00	50.12	72.88	689.76	912.49
21.00	50.08	72.92	677.41	889.34
22.00	50.03	72.97	665.06	866.19
23.00	49.99	73.01	652.71	843.05
24.00	49.94	73.06	640.36	819.90
25.00	49.90	73.10	628.01	796.75
26.00	49.85	73.15	615.66	773.60
27.00	49.81	73.19	603.31	750.45
28.00	49.76	73.24	590.97	727.30
29.00	49.72	73.28	578.62	704.15
30.00	49.67	73.33	566.27	681.00
31.00	49.63	73.37	553.92	657.85
32.00	49.58	73.42	541.57	634.70
33.00	20.60	20.40	-14.30	-386.41
34.00	5.98	-5.98	-301.43	-905.52
35.00	5.74	-5.74	-342.65	-928.30
36.00	5.50	-5.50	-452.35	-968.09
37.00	5.25	-5.25	-562.06	-1007.89
38.00	5.01	-5.01	-671.76	-1047.68
39.00	4.77	-4.77	-781.46	-1087.48
40.00	4.53	-4.53	-891.17	-1127.27
41.00	4.28	-4.28	-1000.87	-1167.07
42.00	4.04	-4.04	-1110.57	-1206.86
43.00	3.80	-3.80	-1220.28	-1246.66
44.00	3.55	-3.55	-1329.98	-1286.45
45.00	3.31	-3.31	-1439.69	-1326.25
46.00	3.07	-3.07	-1500.21	-1349.35
47.00	2.82	-2.82	-1413.19	-1322.37
48.00	2.58	-2.58	-1326.17	-1295.39
49.00	2.34	-2.34	-1239.15	-1268.41
50.00	2.10	-2.10	-1152.13	-1241.43
51.00	1.85	-1.85	-1065.11	-1214.45

52.00	1.61	-1.61	-978.09	-1187.47
53.00	1.37	-1.37	-891.07	-1160.49
54.00	1.12	-1.12	-804.05	-1133.51
55.00	0.88	-0.88	-717.03	-1106.53
56.00	0.64	-0.64	-630.01	-1079.55
57.00	0.39	-0.39	-565.47	-1058.59
58.00	0.15	-0.15	-568.35	-1055.70
59.00	0.16	-0.16	-571.24	-1052.81
60.00	0.16	-0.16	-574.13	-1049.92
61.00	44.74	54.60	199.51	33.25
62.00	67.03	81.97	583.83	577.34
63.00	67.06	81.94	578.82	582.35
64.00	67.08	81.92	573.81	587.36
65.00	67.11	81.89	568.81	592.36
66.00	67.13	81.87	563.80	597.37
67.00	67.16	81.84	558.80	602.38
68.00	67.18	81.82	553.79	607.38
69.00	67.21	81.79	548.78	612.39
70.00	67.23	81.77	543.78	617.39
71.00	67.26	81.74	538.77	622.40
72.00	67.28	81.72	533.77	627.41
73.00	67.31	81.69	528.76	632.41
74.00	67.33	81.67	523.75	637.42
75.00	67.36	81.64	518.75	642.42

TABLE.IV.3.

Distance (ft)	Bottom flange stress envelopes due to vertical loads (dead + live + impact) (ksi)				Bottom flange stress envelopes due to vertical loads and the strengthening system (ksi)			
	Exterior Stringer		Interior Stringer		Exterior Stringer		Interior Stringer	
	Maximum Tension	Maximum Compres.	Maximum Tension	Maximum Compres.	Maximum Tension	Maximum Compres.	Maximum Tension	Maximum Compres
0.00	0.00	0.00	0.00	0.00	0.00	0.00	0.00	0.00
1.00	2.39	0.25	2.50	0.35	2.39	0.29	2.63	0.53
2.00	4.59	0.45	4.82	0.65	4.60	0.54	5.08	1.00
3.00	6.65	0.61	6.98	0.90	6.67	0.74	7.37	1.43
4.00	8.55	0.73	8.97	1.10	8.57	0.90	9.50	1.82
5.00	10.30	0.80	10.80	1.26	10.32	1.01	11.45	2.15
6.00	11.89	0.82	12.46	1.36	10.63	-0.52	11.01	0.04
7.00	13.33	0.80	13.96	1.42	9.49	-3.69	8.16	-4.52
8.00	14.61	0.74	15.30	1.43	10.81	-3.68	9.61	-4.36
9.00	15.75	0.63	16.49	1.39	11.98	-3.71	10.90	-4.24
10.00	16.74	0.47	17.51	1.31	13.00	-3.79	12.03	-4.18
11.00	17.74	0.27	18.56	1.17	14.03	-3.91	13.18	-4.17
12.00	18.63	0.03	19.47	0.99	14.94	-4.08	14.21	-4.20
13.00	19.37	-0.26	20.23	0.75	15.72	-4.29	15.07	-4.28
14.00	19.96	-0.60	20.84	0.47	16.34	-4.55	15.79	-4.41
15.00	20.42	-0.97	21.36	0.14	16.83	-4.85	16.41	-4.59
16.00	20.93	-1.40	21.88	-0.23	17.37	-5.19	17.04	-4.82
17.00	21.29	-1.87	22.24	-0.66	17.76	-5.58	17.50	-5.09
18.00	21.50	-2.38	22.44	-1.13	18.00	-6.02	17.81	-5.42
19.00	21.56	-2.94	22.48	-1.66	18.10	-6.49	17.94	-5.80
20.00	21.54	-3.54	22.45	-2.23	18.13	-6.99	18.00	-6.24
21.00	21.51	-4.19	22.39	-2.85	18.15	-7.55	18.03	-6.73
22.00	21.32	-4.88	22.17	-3.52	18.02	-8.14	17.90	-7.26
23.00	20.99	-5.61	21.79	-4.23	17.73	-8.78	17.60	-7.84
24.00	20.50	-6.40	21.25	-5.00	17.30	-9.47	17.15	-8.48
25.00	19.86	-7.22	20.55	-5.81	16.71	-10.20	16.54	-9.16
26.00	19.07	-8.09	19.69	-6.67	15.97	-10.97	15.76	-9.88
27.00	18.13	-9.01	18.67	-7.58	15.08	-11.79	14.83	-10.66
28.00	17.04	-9.97	17.49	-8.54	14.03	-12.66	13.73	-11.49
29.00	15.88	-10.97	16.25	-9.54	12.93	-13.57	12.58	-12.36
30.00	14.62	-12.02	14.89	-10.60	11.71	-14.52	11.31	-13.28
31.00	13.21	-13.12	13.38	-11.70	10.35	-15.52	9.88	-14.25
32.00	11.65	-14.26	11.71	-12.85	8.85	-16.57	8.31	-15.27
33.00	10.06	-15.44	10.01	-14.05	9.86	-14.51	11.19	-11.51
34.00	8.39	-16.67	8.22	-15.30	9.53	-14.06	11.72	-10.23
35.00	6.61	-17.95	6.34	-16.60	7.92	-15.01	9.93	-11.39
36.00	4.73	-19.27	4.33	-17.95	6.48	-15.48	8.06	-12.50
37.00	2.85	-20.63	2.33	-19.34	5.05	-15.98	6.21	-13.67
38.00	0.89	-22.04	0.42	-11.06	3.54	-16.54	2.69	-8.06
39.00	-0.45	-14.52	-0.79	-11.85	1.63	-10.98	1.57	-8.74
40.00	-1.85	-15.45	-2.07	-12.67	0.54	-11.43	0.38	-9.44
41.00	-3.06	-16.41	-3.00	-13.52	-0.38	-11.90	-0.47	-10.17
42.00	-3.72	-17.80	-3.61	-14.79	-0.73	-12.82	-1.00	-11.33
43.00	-4.40	-19.63	-4.25	-16.31	-1.12	-14.17	-1.56	-12.73
44.00	-5.11	-21.51	-4.92	-17.86	-1.53	-15.56	-2.14	-14.17
45.00	-5.85	-23.43	-5.61	-19.45	-1.97	-17.00	-2.75	-15.64
46.00	-6.26	-24.36	-5.99	-20.23	-2.21	-17.67	-3.08	-16.35
47.00	-5.60	-22.26	-5.38	-18.50	-1.79	-15.96	-2.53	-14.71
48.00	-4.98	-20.21	-4.80	-16.82	-1.40	-14.30	-2.01	-13.10
49.00	-4.38	-18.21	-4.25	-15.19	-1.03	-12.69	-1.51	-11.54
50.00	-3.81	-16.26	-3.72	-13.59	-0.70	-11.12	-1.05	-10.02

51.00	-3.26	-14.37	-3.21	-12.04	-0.39	-9.62	-0.60	-8.55
52.00	-2.27	-12.52	-2.48	-10.53	0.37	-8.17	0.07	-7.12
53.00	-0.96	-11.10	-1.29	-9.28	1.45	-7.13	1.21	-5.94
54.00	0.10	-16.64	-0.67	-16.08	3.33	-10.25	3.63	-9.62
55.00	1.99	-15.38	1.32	-14.77	4.87	-9.68	5.51	-8.46
56.00	3.80	-14.15	3.23	-13.51	6.33	-9.15	7.32	-7.35
57.00	5.53	-12.98	5.06	-12.30	7.81	-8.50	9.06	-6.26
58.00	7.19	-11.84	6.80	-11.14	9.48	-7.35	10.79	-5.11
59.00	8.76	-10.75	8.46	-10.03	11.06	-6.24	12.44	-4.02
60.00	10.25	-9.71	10.03	-8.97	12.56	-5.17	14.00	-2.97
61.00	11.65	-8.71	11.51	-7.95	10.29	-8.51	10.63	-7.24
62.00	12.96	-7.76	12.89	-6.98	9.77	-9.70	9.58	-8.93
63.00	14.18	-6.85	14.18	-6.06	11.01	-8.75	10.85	-8.04
64.00	15.30	-5.98	15.37	-5.19	12.16	-7.85	12.03	-7.20
65.00	16.33	-5.16	16.46	-4.37	13.20	-6.99	13.09	-6.40
66.00	17.26	-4.39	17.44	-3.60	14.15	-6.17	14.06	-5.66
67.00	18.09	-3.66	18.32	-2.87	15.00	-5.40	14.92	-4.96
68.00	18.82	-2.97	19.09	-2.19	15.75	-4.68	15.67	-4.31
69.00	19.44	-2.33	19.76	-1.57	16.40	-3.99	16.32	-3.72
70.00	19.97	-1.73	20.31	-0.98	16.94	-3.36	16.85	-3.16
71.00	20.38	-1.18	20.75	-0.45	17.37	-2.77	17.28	-2.66
72.00	20.70	-0.68	21.09	0.03	17.71	-2.22	17.59	-2.21
73.00	20.90	-0.21	21.31	0.47	17.93	-1.72	17.80	-1.80
74.00	21.00	0.20	21.42	0.85	18.06	-1.26	17.89	-1.44
75.00	21.00	0.58	21.42	1.19	18.07	-0.85	17.87	-1.13

MAX.	21.56		22.48		18.15		18.03	
MIN.		-24.36		-20.23		-17.67		-16.35

APPENDIX C

AXLE LOADS FOR 1980 IOWA DOT RATING TRUCKS

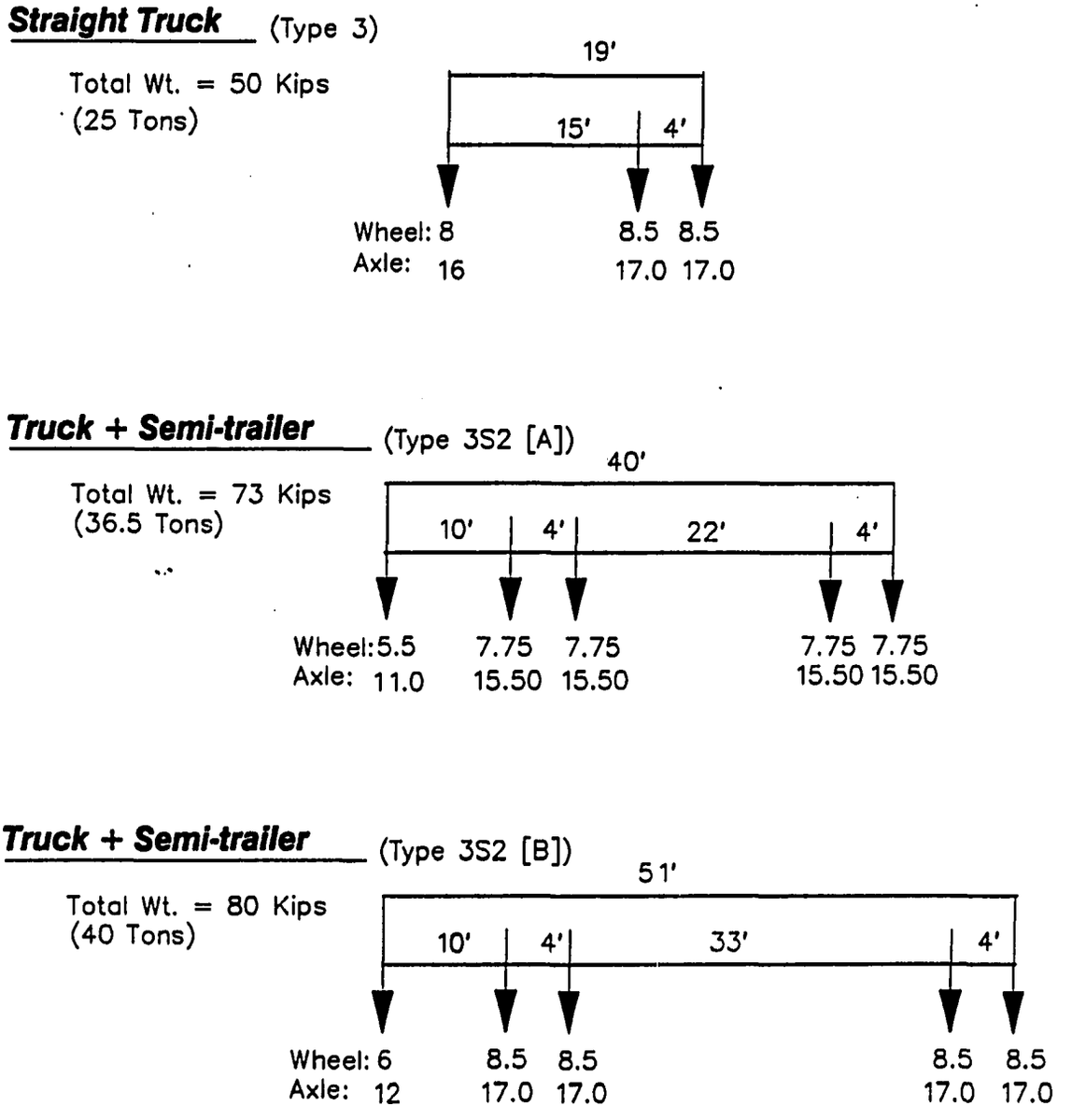

Fig. C.1. Iowa Department of Transportation legal dual axle truck loads

Straight Truck (Type 3)

Total Wt. = 54.5 Kips
(27.25 Tons)

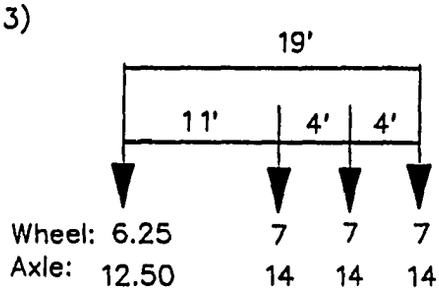

Truck + Semi-trailer (Type 3S3)

Total Wt. = 80 Kips
(40 Tons)

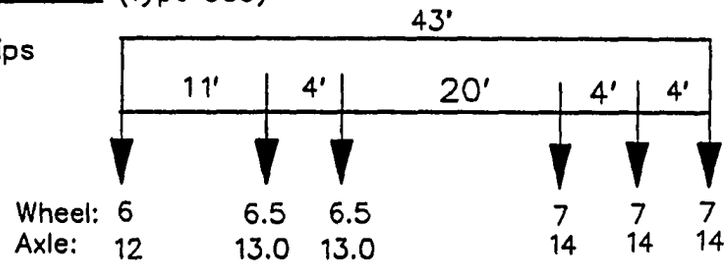

Truck + Semi-trailer (Type 3-3)

Total Wt. = 80 Kips
(40 Tons)

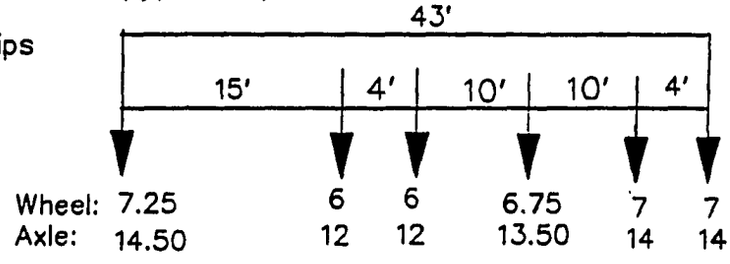

Fig. C-1. Continued.